Relationship between the physical parameters of musical wind instruments and the psychoacoustic attributes of the produced sound

Sandra Carral Robles León

A thesis submitted in fulfilment of the requirements
for the degree of Doctor of Philosophy
to the
University of Edinburgh
2005

Abstract

Musical wind instrument building techniques have been developed by trial and error throughout history. The modern shapes of musical wind instruments are the result of empirical modifications that have produced instruments with an acceptable sound, ease of play, and response. Despite the technological advance of our era, there is still little understanding on what makes a good quality instrument, or how small changes in the shape of the bore or the characteristics of the reed affect the produced sound of the instrument, and in turn the perceived psychoacoustic attributes of pitch, loudness and timbre.

This work attempts to correlate small changes in the physical parameters of a wind instrument with how humans perceive the pitch and timbre of the produced sound, with a view of helping in the design and quality assessment of musical instruments. The perceptual significance of small changes in the sound of a trombone played with mouthpieces of different shapes is investigated by synthesising the sound recordings with additive synthesis, and performing psychoacoustic tests asking people to state whether they can hear a difference or not, using a two alternative forced choice (2AFC) test. The just noticeable difference in the timbre of the trombone is also found.

The psychoacoustic parameters of pitch and timbre of a Scottish Border bagpipe chanter and reed sound played with an artificial blowing machine were measured after having stored the reed under different relative humidity conditions. It was found that the pitch and spectral centroid are inversely correlated with the moisture content of the reed, which depends on the relative humidity of the air around it. The physical parameters of stiffness, resonance frequency and damp-

ing factor of the reed were measured. These parameters were used to predict the playing frequency and spectrum of the sound that the chanter and reed system would produce using a physical model based on the Harmonic Balance Method.

Declaration

I do hereby declare that this thesis was composed by myself and that the work described within is my own, except where explicitly stated otherwise.

Sandra Carral Robles León
November 2005

Acknowledgements

First of all, I would like to acknowledge and present my greatest gratitude to my first supervisor Prof. Murray Campbell, who provided me with endless support, both academically and personally, all throughout my PhD, without which the completion of this work would not have been possible.

My husband Jürgen made a significant contribution by offering his love, patience and support, especially throughout the final stages of my PhD. Also, I would like to thank our baby for having filled our lives with joy in this critical stage of my PhD.

I would also like to remark on the unconditional support that I received from my parents and family in this journey of self discovery that started five years ago. I recognise that it has not been easy for any of us, and nevertheless I have never ceased to receive a word of encouragement.

Nigel Richards was very generous with us in donating the chanter and reeds that were used for some of the experiments described in this work.

I had the priceless opportunity to work with Tom Rossing during his short visit to Edinburgh in Spring 2003. Not only was his academic advice and guidance greatly beneficial, but also his kindness that lead to the development of a dear friendship.

Joël Gilbert came every spring to Edinburgh, and was always keen on having highly valuable and rewarding discussions about various aspects of the physics of wind instruments. All his comments have been and will always be enormously appreciated. I would like to remark on the particularly useful comments that I received about the usage of `harmbal`.

I would also like to thank Maarten van Walstijn for the fruitful discussions that lead to the idea of the synthesis method used in Chapter 4.

Tim Mills and his wife Deena provided me, through their friendship, with invaluable moral support. Particularly, I would like to thank Tim for helping me with some important issues on the logistic transformation used for calculating the JND presented in Chapter 4.

Snorre Farner and Claudia Fritz helped me significantly with the various problems I encountered while using `harmbal`. I thank both for their patience and support.

I would also like to express my deepest gratitude to James Beauchamp for providing the program SNDAN, for all his support, and for his fruitful comments.

This work was supported by CONACYT scholarship number 146702.

Contents

List of Figures

List of Tables

Chapter 1

Introduction

1.1 Introduction

Musical reed wind instruments are, from the physical point of view, self-sustained oscillating systems consisting of a constant supply of pressure provided by the player, a valve, and a resonator. From the listeners point of view, they generate sound with certain attributes: pitch, loudness and timbre. From the musical point of view, a particular instrument must provide with sounds of different pitch and dynamic level that are combined into a musical context.

Musical wind instrument manufacturers are faced with the problem of building a system that provides the following requirements: they must be able to produce a wide range of notes that are tuned to a particular scale system; they must be capable of playing in a wide range of environmental conditions; they must be relatively easy to play; and finally they must produce a beautiful sound. This is a difficult problem that has been solved throughout centuries by trial and error. Nowadays modern instrument design is the result of traditional techniques which have been developed empirically, making it a handcraft activity. This is the main reason why musical instruments are expensive.

Instrument quality is assessed by the instrument maker, the musician and the listener. The main characteristics that musicians test when choosing an instrument are: dynamic range; tuning; tone quality; consistency of tone throughout the whole range of the instrument; how easy it is to produce a note; and stability. Most of these attributes are subjective, but those characteristics related to the

sound of the instrument can be measured or quantified in some way, and these characteristics are also judged by makers, players and listeners alike. Is there such a thing as an ideal sound for a particular instrument? If there is, there should also be a way of measuring its characteristics.

When an instrument maker seeks to improve an existing instrument, he/she usually makes a small change in a parameter thought to make the difference he/she is looking for. How big does this change have to be for people to perceive a difference? Does that affect other aspects of the instrument, or how the musician feels it? Finding the answer to such questions could give instrument makers a guideline on how to go about doing these changes, and a tolerance range to the different variables available to them. This would in turn make the whole process of instrument making easier, and in the long run the building costs would go down, making musical instruments more accessible to everyone.

1.2 Aims and contents

The aim of this work is to correlate the physical characteristics of a wind instrument with the psychoacoustic attributes of the sound it produces. The physical characteristics that are taken into account throughout this work are: the shape and size of the mouthpiece (in case of brass instruments); the stiffness, resonance frequency and damping factor of the reed (in case of woodwind instruments); and the input impedance of the air column. The psychoacoustic attributes of the sound are obtained by measuring the radiated sound and its spectrum, and deriving quantitative measures of the pitch and timbre.

The first two Chapters of this work present the relevant theoretical background. Chapter 2 presents a review of the current state of knowledge about the physics of wind instruments, including the air column, the reed, and how the pressure and volume flow are coupled together. Chapter 3 reviews how sounds are perceived by the human ear, defining three main attributes: pitch, loudness and timbre.

A preliminary study on how the sound of a given trombone changes when played with a different mouthpiece is presented in Chapter 4. Several analysis/synthesis techniques are attempted to include the relevant attributes of the sound that enable a listener to distinguish between similar sounds. How small a

difference in the trombone mouthpiece is necessary for the human ear to perceive a difference in the produced sound of the trombone is investigated.

Chapter 5 describes experiments playing a bagpipe chanter and reed with an artificial blowing machine. The effect of mouth pressure in the estimated psychoacoustic attributes of pitch and timbre is investigated.

From a hypothesis drawn in Chapter 5, an experiment that studies the effect of the moisture content of the reed on the physical characteristics of the reed (stiffness, resonance frequency and damping factor) and the psychoacoustic attributes of the sound the chanter and reed produce (pitch and timbre) is described in Chapter 6.

In Chapter 7, the physical characteristics of the reed measured in Chapter 6 are used in a physical model of the chanter and reed, to see if the psychoacoustic attributes of pitch and timbre found in Chapter 6 could be mimicked.

A summary of the findings presented throughout his work, together with some suggestions for improving some of the experiments, as well as for future work are presented in Chapter 8.

Chapter 2

The Physics of wind instruments

2.1 Introduction

Wind instruments are self-sustained oscillatory systems, as they only need a steady, external supply of energy to generate self-sustained oscillations [34]. A block diagram of a typical wind instrument is shown in Figure 2.1 [33]. This diagram shows that the steady supply of energy comes from the player's mouth, which acts on the of the instrument, making it vibrate and become an active generator. When the generator is coupled to the air column, the resonances of the air column are excited, generating a standing wave inside the instrument. Some of the energy from the standing wave will be reflected back into the instrument to reinforce the standing wave, some will be radiated as sound waves, and some will be lost due to viscous and thermal effects.

The coupling between generator and resonator is so close, that they cannot be considered separately [32]. Furthermore, the frequency at which the instrument sounds cannot be predicted by studying the vibrational properties of the generator or the resonator as isolated systems [13]. The player also provides a feedback loop, as he/she can in turn modify dynamically certain parameters to influence the sound of the instrument.

Another version of this block diagram is shown in Figure 2.2 [19]. It emphasises the feedback loop that exists between the exciter or valve and the resonator: The pressure difference across the generator depends on the standing wave, and the standing wave depends on the motion of the generator, which is regulated by

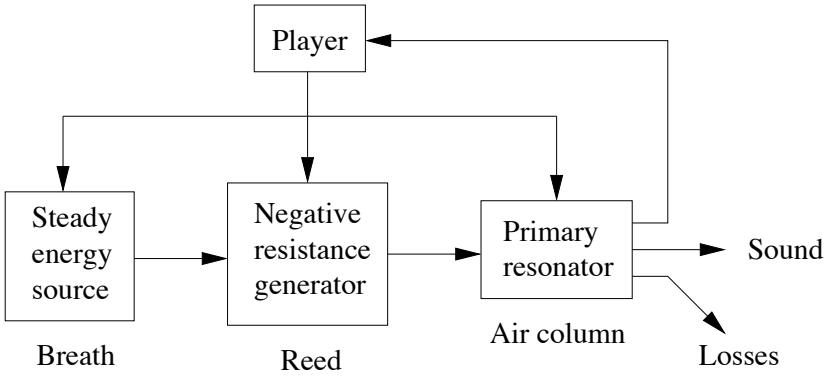

Figure 2.1: Block diagram of a wind instrument. The player provides the supply of energy through his/her breath, the acts as a generator, and the air column as a resonator (taken from [33])

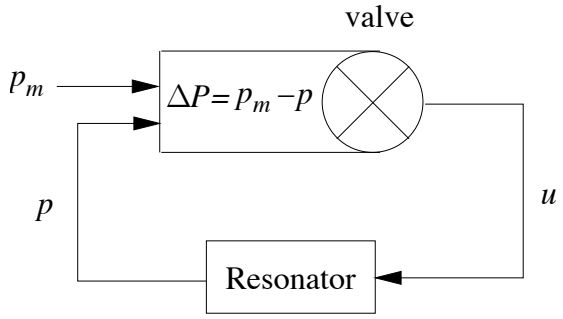

Figure 2.2: Block diagram of a wind instrument. The acts like a valve that modulates the flow of air u into the air column. The valve opening depends on the difference between the mouth pressure p_m and the mouthpiece pressure p. $\Delta P = p_m - p$ (taken from [19])

the pressure difference across it.

The wind instruments that are relevant in this study are those driven by a reed mechanism, this being either a piece or pieces of flexible material or the lips of the player. Depending on how the instrument is excited, or in other words, on the nature of the reed, wind instruments are classified as woodwind or brass. Within the woodwinds, the exciter can be a single reed (a strip of flexible material attached to the lay of the mouthpiece) or a double reed (two strips of flexible material bound together around a staple that is introduced at the top of the instrument). Brass instruments are excited by pressing the player's lips against a mouthpiece, and blowing. As flute and flute-like instruments are excited

by means of an air jet, these have not been included in this study.

The problem of studying the physics of reed wind instruments can be separated in four different parts [13]:

1. The behaviour of the bore or air column as the resonator, including the effect of tone holes where present
2. The behaviour of the as an exciter or generator
3. The coupling between the resonator and the generator
4. The nonlinearities present in the system

This Chapter describes each of these topics, forming a review of the musical acoustic theory as given in standard textbooks such as [34], [20], [63], [17]. Section 2.2 presents the typical bores found in wind instruments, including a mathematical description of their behaviour. Section 2.3 describes the two main types of reeds present in wind instruments. The way the resonator and the generator are coupled together is presented in Section 2.4. Finally, Section 2.5 introduces the nonlinear effects due to the relationship between pressure and volume flow, as well as beating reeds.

2.2 Bore or air column: The resonator

All wind instruments of reed type are excited by a pressure controlled valve nearly closed at the top (where the mouthpiece is). This boundary condition implies that there is a pressure antinode, or a velocity node at the top of the instrument. In contrast, the bottom of the instrument is open, thus having at that point a pressure node.

As we have mentioned before, in order to play a wind instrument, a standing wave has to be set up in the air column. The waves that are excited in an air column are longitudinal, as they are the result of compressing or expanding the air at different points along its axis, thus generating points of increased or reduced pressure. In order to be able to set up a standing wave, there must be reflection. In the case of a wind instrument, the reflection comes from the points along the air column that present a change in conditions, e.g. the end of the tube, the presence of tone holes, change in bore diameter. At these points the

waves are diffracted. Some of the energy of the waves will be reflected back into the tube, reinforcing the standing wave, some will be transmitted to the open space, generating the sound of the instrument [20], and the rest will be lost due to viscous and thermal effects.

The different bores of real musical instruments have complicated shapes that are difficult to study in their own right, as they are normally not simple shapes like an ideal cone or cylinder. Sometimes they are a combination of cylindrical and conical sections of different taper, sometimes they include a bell that flares out quickly at the bottom of the instrument. However, these different shapes can often be approximated with small sections of cylinders of increasing diameter or even cones of varying taper [85]. This section presents the mathematical treatment of cylinders and cones.

The behaviour of standing waves inside a tube is described by the wave equation, which in its general form is:

$$\frac{\partial^2 p}{\partial t^2} = c^2 \nabla^2 p \tag{2.1}$$

where p is pressure and c is the speed of sound. The problem lies in solving the wave equation on a suitable coordinate system, depending on the shape of the bore, as the shape of the waves themselves will be affected by the bore in which they are enclosed. The coordinate surface must coincide with the walls of the bore in question, and in which equation 2.1 is separable. Moreover, the shape of the wavefronts must be orthogonal to the coordinate surfaces [34]. For cylindrical bores, the wave equation can be solved in a cylindrical coordinate system, where we get plane waves. For conical bores, the wavefronts are spherical, thus the wave equation is solved in a spherical coordinate system [85]. The mathematical treatment of the wave equation for finite length cylindrical and conical bores is described in the following Sections.

2.2.1 Cylindrical bore

The wave equation 2.1 in a one dimensional cylindrical coordinate system becomes:

$$\frac{\partial^2 p}{\partial t^2} = c^2 \frac{\partial^2 p}{\partial x^2} \tag{2.2}$$

where x is the position along the length of the tube.

The pressure is related to the volume velocity flow of a wave propagating into an aperture of area S as follows:

$$\frac{\rho}{S}\frac{\partial U}{\partial t} = -\frac{\partial p}{\partial x} \tag{2.3}$$

where ρ is the density of air and U is the volume velocity flow. The general solution of equation 2.2 can be written as follows:

$$p(x,t) = Ae^{j(\omega t - kx)} + Be^{j(\omega t + kx)} \tag{2.4}$$

where ω is the angular frequency, A is the amplitude of the forward travelling wave, B is the amplitude of the backward travelling wave, and $k = \frac{\omega}{c}$ is the wave number.

Inserting equation 2.4 into 2.3, differentiating the right hand side and integrating, the volume velocity flow becomes:

$$U(x,t) = \frac{S}{\rho c}\left(Ae^{j(\omega t - kx)} - Be^{j(\omega t + kx)}\right) \tag{2.5}$$

For an infinitely long tube, where there are no reflections, we take the forward travelling wave of equation 2.4, and substitute it in 2.1, obtaining the Helmholtz equation:

$$\nabla^2 p + k^2 p = 0 \tag{2.6}$$

The acoustic impedance of a wave travelling in the forward direction only (i.e. $B = 0$) is defined as:

$$Z_0^+ = \frac{p^+(x,t)}{U^+(x,t)} = \frac{\rho c}{S} \tag{2.7}$$

This is referred to as the characteristic impedance of the bore. Note that the impedance for the wave travelling in the backward direction (i.e. $A = 0$) is $Z_0^- = -Z_0^+$.

In a real musical instrument, we must allow for reflections to come from the end of the instrument, so that a standing wave regime can be set up inside the pipe. Assuming a tube of length L, the terminating impedance of the pipe Z_L

(at $x = L$) is defined as:

$$Z_L = \frac{p(L,t)}{U(L,t)} \tag{2.8}$$

Combining equations 2.4, 2.5, and 2.8, we obtain:

$$Z_L = Z_0 \frac{Ae^{-jkL} + Be^{jkL}}{Ae^{-jkL} - Be^{jkL}} \tag{2.9}$$

From this we can calculate the reflectance, which is the fraction of incident wave that is reflected back from the end of the pipe:

$$\frac{B}{A} = e^{-2jkL} \frac{Z_L - Z_0}{Z_L + Z_0} \tag{2.10}$$

The impedance at the bore entry is usually referred to as the input impedance, and is defined as:

$$Z_{in} = \frac{p(0,t)}{U(0,t)} \tag{2.11}$$

Combining equations 2.4, 2.5 and 2.11, the input impedance becomes:

$$Z_{in} = Z_0 \frac{A+B}{A-B} = Z_0 \frac{1 + \frac{B}{A}}{1 - \frac{B}{A}} \tag{2.12}$$

Inserting equation 2.10 in equation 2.12, expanding and rearranging, we get:

$$Z_{in} = Z_0 \frac{Z_L cos(kL) + jZ_0 sin(kL)}{jZ_L sin(kL) + Z_0 cos(kL)} \tag{2.13}$$

We are interested in instruments that are open at the bottom end. For an ideally open pipe, where radiation is neglected ($Z_L = 0$), the input impedance becomes:

$$Z_{in} = jZ_0 tan(kL) \tag{2.14}$$

We can deduce the modes of vibration of a standing wave inside a tube by looking at its input impedance. We are interested in the case where the input section of the tube is closed. In this case, there will be a pressure antinode or a velocity node at that point. To satisfy this boundary condition, the resonances will be at the frequencies in which the magnitude of the input impedance is at a

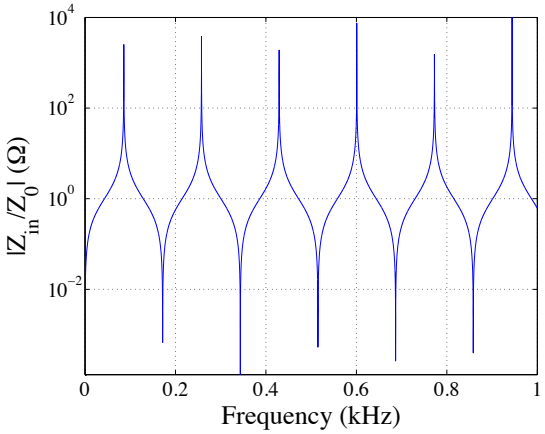

Figure 2.3: Normalised input impedance magnitude of an ideal cylinder with $L = 1$ m and $r = 2$ cm, open at $x = L$

maximum [34].

From equation 2.14 one can deduce that $Z_{in} = \infty$ when $k = \frac{\pi}{2}$, $k = \frac{3\pi}{2}$, $k = \frac{5\pi}{2}$, etc. Figure 2.3 shows the input impedance magnitude of a pipe open at $x = L$, where $Z_L = 0$. As expected, the impedance maxima of a tube closed at the top and open at the bottom lie at odd multiples of the fundamental: It has got only odd harmonics. The magnitude of the impedance in Figure 2.3 is never ∞, because of the digitisation of k. It is also worth noting that the minima of the input impedance occur in between the maxima, exactly at the middle. Also, as in this figure the magnitude is plotted logarithmically, the admittance $Y_{in} = \frac{1}{Z_{in}}$ can be obtained by simply placing the figure up side down [20].

Figure 2.4 (a) shows the first three modes of vibration of pressure for a cylinder closed at the top and open at the bottom. Note that the wavelengths correspond to $4L$, $\frac{4L}{3}$ and $\frac{4L}{5}$, or the odd harmonics of the series. It is worth noting at this point that the resonances of an open cylinder, which can be deduced by looking at the impedance minima of Figure 2.3, lie in integer relationship. This can also be deduced from equation 2.14, by looking at the points where $Z_{in} = -\infty$, which occur when $k = \pi$, $k = 2\pi$, $k = 3\pi$, etc. The first three modes of vibration of such a pipe are shown in Figure 2.4 (b), where the wavelengths correspond to $2L$, L and $\frac{2L}{3}$. Moreover, the frequency of the first mode of vibration in the open case is double as much compared to that of the closed case, for a particular length of cylinder L. This implies that a cylinder closed at one end will sound an octave

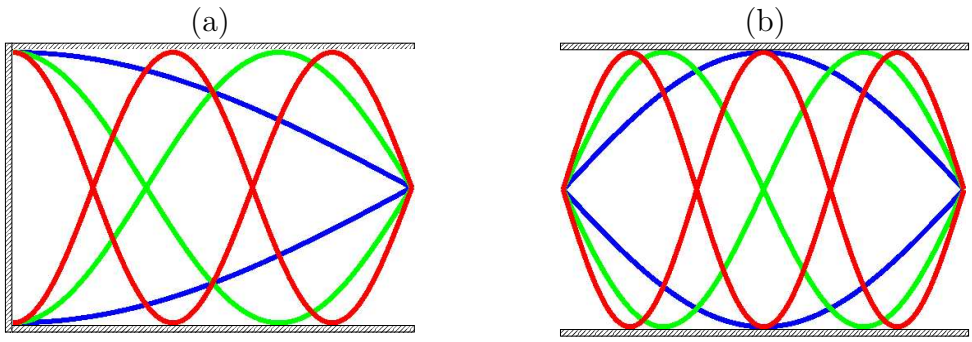

Figure 2.4: First three modes of vibration of pressure for a perfect cylinder (a) closed and (b) open at $x = 0$

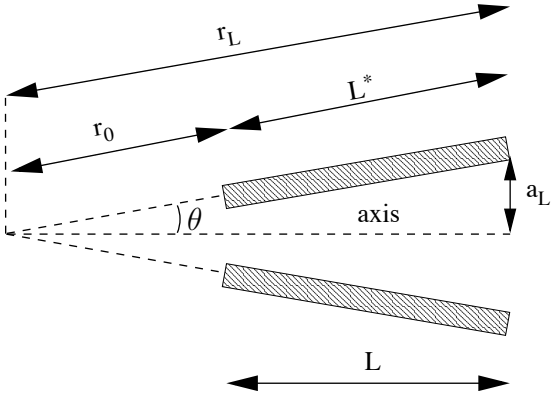

Figure 2.5: Conical bore and its geometrical parameters

lower than an open one, even when the length is the same.

2.2.2 Conical bore

For the treatment of a conical bore, as the one shown in Figure 2.5, it is necessary to solve equation 2.1 in spherical coordinates. In this case, the wave equation becomes:

$$\frac{\partial^2 p}{\partial r^2} + \frac{2}{r}\frac{\partial p}{\partial r} = \frac{1}{c^2}\frac{\partial^2 p}{\partial t^2} \tag{2.15}$$

where r is the local cone apex distance. The general solution becomes:

$$p(r,t) = \frac{1}{r}\left(Ae^{j(\omega t - kr)} + Be^{j(\omega t + kr)}\right) \tag{2.16}$$

Similarly, equation 2.3 in spherical coordinates becomes:

$$\frac{\rho}{S^*}\frac{\partial U}{\partial t} = -\frac{\partial p}{\partial r} \tag{2.17}$$

where S^* is the spherical wave surface [15]:

$$S^* = \pi a^2 F(\theta) \tag{2.18}$$

$$F(\theta) = 2\left[\frac{1 - cos\theta}{sin^2\theta}\right] \tag{2.19}$$

Inserting equation 2.16 into 2.17, differentiating the right hand side and integrating, the volume velocity becomes:

$$U(r,t) = \frac{S^*}{\rho c r}\left[A\left(1 + \frac{1}{jkr}\right)e^{j(\omega t - kr)} - B\left(1 - \frac{1}{jkr}\right)e^{j(\omega t + kr)}\right] \tag{2.20}$$

The characteristic impedance of the conical bore depends on the position along the bore and on the direction of the flow:

$$Z_0^+(r) = \frac{p^+(r,t)}{U^+(r,t)} = \frac{\rho c}{S^*}\frac{jkr}{jkr + 1} \tag{2.21}$$

$$Z_0^-(r) = \frac{p^-(r,t)}{U^-(r,t)} = \frac{\rho c}{S^*}\frac{jkr}{jkr - 1} \tag{2.22}$$

For a truncated cone of finite length as in Figure 2.5, we define the terminating impedance Z_{L^*}, where $L^* = r_L - r_0$ as:

$$Z_{L^*} = \frac{p(L^*,t)}{U(L^*,t)} = \frac{Ae^{-jkL^*} + Be^{jkL^*}}{A\frac{e^{-jkL^*}}{Z_0^+(L^*)} - B\frac{e^{jkL^*}}{Z_0^-(L^*)}} \tag{2.23}$$

From equation 2.23 we can calculate the reflectance:

$$\frac{B}{A} = \left[\frac{Z_0^-(L^*)}{Z_0^+(L^*)}\right]\left[\frac{Z_{L^*} - Z_0^+(L^*)}{Z_{L^*} + Z_0^-(L^*)}\right]e^{-2jkL^*} \tag{2.24}$$

The input impedance then becomes:

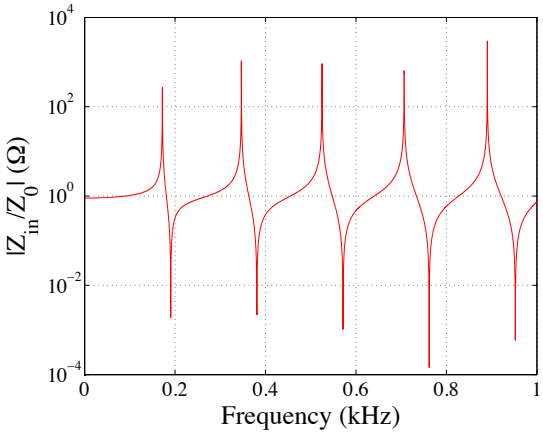

Figure 2.6: Normalised input impedance magnitude of an ideal truncated cone with $L = 1$ m, $r_0 = 10$ cm and $\theta = 3^o$, open at $r = L^*$

$$Z_{in} = \frac{p(r_0,t)}{U(r_0,t)} = \frac{e^{-2jkr_0} + \frac{B}{A}}{\frac{e^{-2jkr_0}}{Z_0^+ r_0} - \frac{\frac{B}{A}}{Z_0^- r_0}} \tag{2.25}$$

We are interested in a cone that is closed at the top, and open at the bottom. For an ideally open cone, where radiation is neglected ($Z_L^* = 0$), the reflectance becomes:

$$\frac{B}{A} = -e^{-2jkL^*} \tag{2.26}$$

Figure 2.6 shows the input impedance magnitude for the case of a truncated cone open at the bottom end. For the case of a cone closed at the top, the resonances lie at the impedance maxima. In this case, the resonances are at the same frequencies as those of a cylinder open at both ends. Note that the minima are not exactly at the middle in between the maxima, as was the case with the cylinder.

Ayers et al. [4] present an extensive analysis on how this apparent paradox, where a cone closed at the top has the same modes of vibration as a cylinder open at both ends, is possible. They explain how it is logical that a cone open at both ends will have the same resonances as a cylinder, given the fact that both have the same boundary conditions. However, the amplitude of the standing wave increases as the crosssectional area of the cone is reduced (it is possible to construct a hearing aid using a cone). As the small end of the cone is further reduced, the

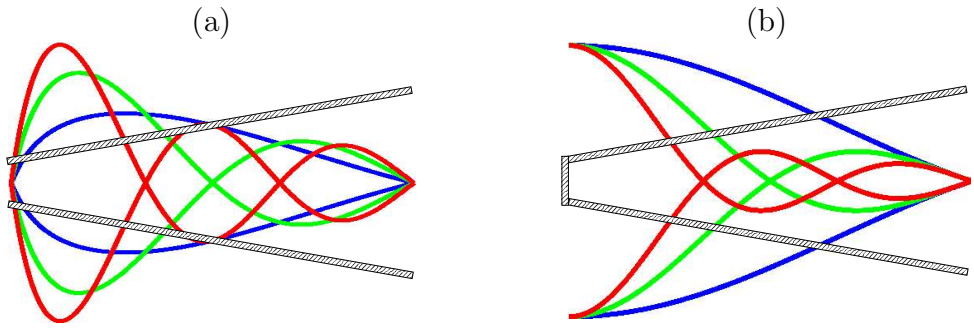

Figure 2.7: First three modes of vibration of pressure for a truncated cone (a) open and (b) closed at the top end

amplitude of the standing wave at that point increases, and is proportional to $1/r$. When the cone is complete, the boundary condition changes, so that there is a pressure antinode at that point, but the wavelength remains constant regardless of the taper, and whether the cone is open or closed. It can be better understood if one thinks of the standing wave of a closed cone as being $\frac{sin(r)}{r}$ where the frequency of oscillation is the same as that of $sin(r)$. Furthermore, for small truncations of cone, the modes of vibration are those of the complete cone. Figure 2.7 shows the first modes of vibration of pressure for an open cone and a closed cone. Note how at the limit, where the cone is closed, the pressure at the closed end is at an antinode, as is a $\frac{sin(r)}{r}$ function.

2.2.3 Wall losses

So far we have been dealing with perfect cylinders and cones. However, it is important to consider how viscous and thermal effects affect the waves inside the pipes. Given the viscosity η and a bore of radius a, the ratio of the tube radius to the viscous boundary layer is [34]:

$$r_v = a\sqrt{\frac{\omega\rho}{\eta}} \tag{2.27}$$

where ρ is the density of air. Also, the thermal exchange between the air and the walls adds resistance, which depends on the ratio of the tube radius a to the thermal boundary layer thickness [34]:

$$r_t = a\sqrt{\frac{\omega\rho C_p}{\kappa}} \tag{2.28}$$

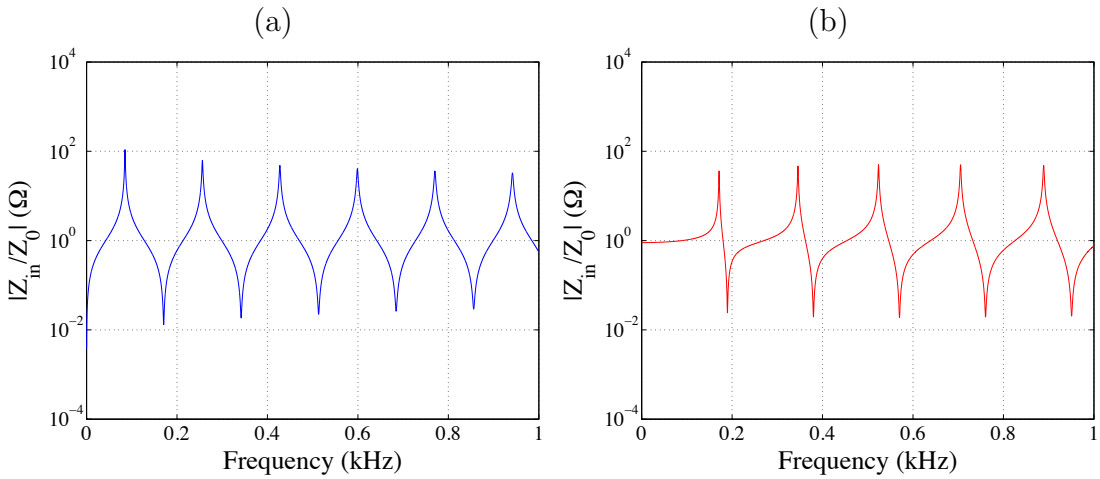

Figure 2.8: Normalised input impedance magnitude of (a) cylinder of $L = 1$ m and $r = 2$ cm open at $x = L$ and (b) truncated cone with $L = 1$ m, $r_0 = 10$ cm and $\theta = 3^o$, open at $r = L^*$, taking into account viscous and thermal drag

where C_p is the specific heat of air at constant pressure and κ is its thermal conductivity. The effect of these loss terms will be to make Z_0 complex, which in turn will make the wave number k complex. It is convenient then to rewrite $k = \frac{\omega}{v} - j\alpha$, where α is the attenuation coefficient per unit length of path and v is the phase velocity [34]:

$$v \approx c\left[1 - \frac{1.65 \times 10^{-3}}{a\sqrt{f}}\right] \tag{2.29}$$

$$\alpha \approx \frac{3 \times 10^{-5}\sqrt{f}}{a} \tag{2.30}$$

where c is the speed of sound, and $f = \frac{\omega}{2\pi}$ is the frequency in Hz. Inserting this new complex wave number in equations 2.13 directly will give the input impedance taking into account these viscous and thermal drags for a cylindrical pipe. Figure 2.8 (a) shows this effect. Note that the amplitude of the peaks is lower, and the shape of the peaks is also somewhat less "sharp" than in the ideal case (shown in Figure 2.3). For the conical case, the radius of the pipe varies with axial distance. However, in musical acoustics this is considered negligible, and usually the losses in a conical duct are calculated as for a cylindrical section with identical length and with a radius that equals the mean radius of the cone [85]. Figure 2.8 (b) shows this effect.

2.2.4 End correction

So far, we have been considering that for an open pipe, the terminating impedance $Z_L = 0$, which is not strictly correct, although $Z_L \ll Z_0$ [34]. Z_L will depend on the ratio of the wavelength to the radius of the pipe at $x = L$. For high frequencies, the wavelength is small compared to the radius. In this case, $Z_L \approx Z_0$. However, for low frequencies, the wavelength is large compared to the radius, in which case the change in impedance is more significant. Z_L of an unflanged cylindrical duct can be approximated for low frequencies as follows [85]:

$$Z_L = Z_0 \left[\frac{(ka)^2}{4} + 0.6jka \right] \tag{2.31}$$

For a conical duct, the cylindrical open-end model can be scaled by the spherical/plane wavefront surface ratio, giving:

$$Z_L^* = Z_L \frac{S}{S^*} \tag{2.32}$$

Figure 2.9 shows how the input impedance of (a) a cylinder and (b) a truncated cone is affected when viscous and thermal drag, as well as end correction effects are taken into account. In this figure, the green/cyan lines show where the original ideal resonant frequencies would be. Notice that the impedance maxima do not lie in integral relationship anymore.

2.2.5 Effect of tone holes

Wind instruments are capable of producing a range of notes. This is usually accomplished by drilling holes along the length of the tube at specific locations. This has the effect of shortening the sounding length of the instrument [20].

Consider a tube with one side hole near the bottom of the tube. Both the size and position of the hole will determine the acoustic length of the tube: If the diameter of the hole is comparable to that of the tube, it will act effectively as an open end. If, on the other hand, the diameter of the hole is smaller than that of the tube (which is commonly the case for the tone holes of woodwind instruments), the equivalent tube will be larger than if the tube was sawn off at that point. Very small holes (like the so-called "speaker holes" of woodwind instruments), will not have a significant effect on the original acoustical length of

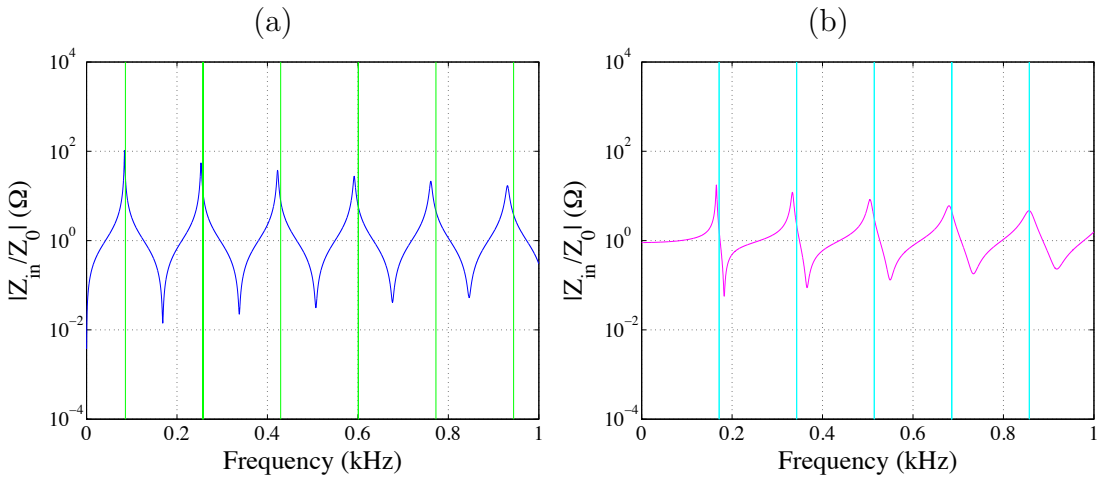

Figure 2.9: Normalised input impedance magnitude of (a) cylinder of $L = 1$ m and $r = 2$ cm open at $x = L$ and (b) truncated cone with $L = 1$ m, $r_0 = 10$ cm and $\theta = 3^o$, open at $r = L^*$, taking into account viscous and thermal drag, as well as end correction effects due to the change of impedance at $x = L$ and $r = L^*$ respectively. The green/cyan lines show where the resonant frequencies would lie, without taking into account wall losses and end correction effects

the tube. These holes are normally used to assist the player in the production of higher oscillation regimes (overblowing).

Real wind instruments need to have at least six tone holes in order to be able to produce a major scale. It is difficult to generalise the input impedance of a real wind instrument, because of the variation in bore diameter at different points, and of how the tone holes affect the resonances of the tube. Plitnik and Strong [69] showed that it is possible to calculate the input impedance of an oboe, by approximating the conical bore of the oboe with contiguous cylindrical sections of varying diameter, approximating in this way the shape of the bore. Careful measurements of the bore diameter at different parts along the length of the tube are necessary. They found good agreement with experimental measurements. This method is outlined in the rest of this Section.

Transmission line theory models an acoustical system by a two-port representation, like the one shown in Figure 2.10 (b). For such a system, the transfer matrix maps the input volume flow U_{in} and pressure p_{in} into the output volume flow U_{out} and pressure p_{out} as follows [52]:

$$\begin{bmatrix} p_{in} \\ U_{in} \end{bmatrix} = \begin{bmatrix} A & B \\ C & D \end{bmatrix} \begin{bmatrix} p_{out} \\ U_{out} \end{bmatrix} \tag{2.33}$$

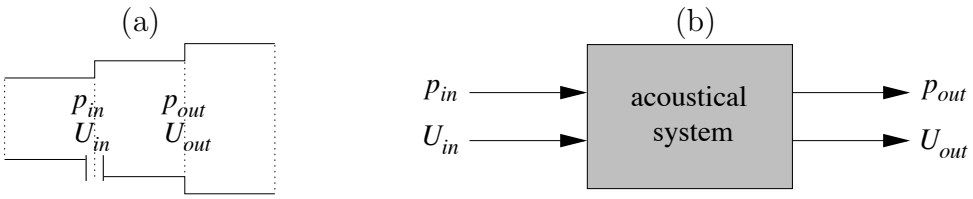

Figure 2.10: (a) Cylindrical section of an arbitrary bore shape and (b) two port representation of a transmission line model of an acoustical system

where A, B, C and D depend on the shape of the section. For a cylindrical section [85],

$$A = cos(kL) \tag{2.34}$$

$$B = jZ_0 sin(kL) \tag{2.35}$$

$$C = \frac{j}{Z_0} sin(kL) \tag{2.36}$$

$$D = cos(kL) \tag{2.37}$$

and for a conical section [15],

$$A = \frac{r_L}{r_0} cos(kL^*) - \frac{1}{kr_o} sin(kL^*) \tag{2.38}$$

$$B = \frac{r_0}{r_L} jZ_0^* sin(kL^*) \tag{2.39}$$

$$C = \frac{j}{Z_0^*} \left\{ \left[\frac{r_L}{r_0} + \left(\frac{1}{kr_0} \right)^2 \right] sin(kL^*) - \frac{L^*}{r_0} \frac{1}{kr_0} cos(kL^*) \right\} \tag{2.40}$$

$$D = \frac{r_0}{r_L} \left[cos(kL^*) + \frac{1}{kr_0} sin(kL^*) \right] \tag{2.41}$$

where Z_0^* is a locally defined characteristic impedance parameter:

$$Z_0^* = \frac{\rho c}{S^*} \tag{2.42}$$

If we consider a pipe of an arbitrary bore shape, it can be approximated by sections of cylinder, such as those shown in Figure 2.10 (a). Each section of cylinder can be modelled as a transmission line, and we can calculate the input impedance of the section as follows:

$$Z_{in} = \frac{p_{in}}{U_{in}} \tag{2.43}$$

where

$$p_{in} = Ap_{out} + BU_{out} \tag{2.44}$$

$$U_{in} = Cp_{out} + DU_{out} \tag{2.45}$$

and the output impedance will be:

$$Z_L = \frac{p_{out}}{U_{out}} \tag{2.46}$$

Given a transfer matrix, we can calculate the input impedance of each section by combining equations 2.33, 2.43, 2.44, 2.45 and 2.46. We obtain:

$$Z_{in} = \frac{AZ_L + B}{CZ_L + D} \tag{2.47}$$

To calculate the input impedance of the whole instrument, we proceed as follows: starting from the radiation impedance at the bottom of the tube (Z_L), we calculate the input impedance of the first section by using equation 2.47. This input impedance then becomes the output impedance of the next section, and this process is repeated until the last cylinder is reached at the top end of the bore. Whenever a tone hole is encountered (as shown in Figure 2.10 (a)), its impedance is added in parallel to Z_{in} before proceeding to the next section [69]. The input impedance of the tone holes is calculated using equation 2.13. For an open hole, Z_L is calculated using equation 2.31, and for a closed hole $Z_L = \infty$, so that equation 2.13 becomes:

$$Z_{in} = -jZ_0 cot(kL) \tag{2.48}$$

The wave number k can be set to $k = \frac{\omega}{v} - j\alpha$ as described in Section 2.2.3 to account for thermal and viscous losses.

Let us consider a cylindrical tube of length $L = 1$ m and radius $r = 2$ cm, closed at the top, whose impedance curve is shown in Figure 2.9. The first resonance lies at around 83 Hz. If this cylinder was cut off at $L = 70$ cm, its first resonance would be at around 120 Hz. If instead of cutting it we place a tone

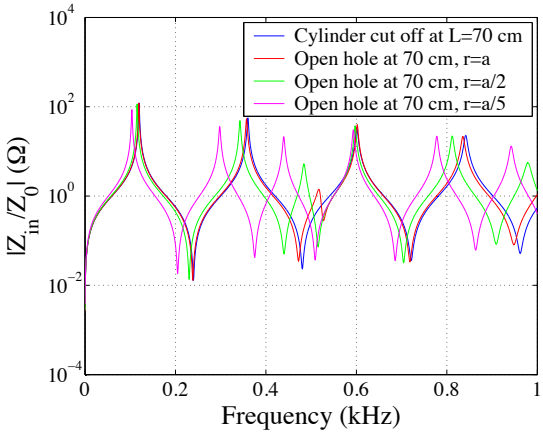

Figure 2.11: Normailsed input impedance magnitude of a cylindrical tube of length $L = 1$ m and $r = 2$ cm with a tone hole placed at L =70 cm of different radius

hole at $L = 70$ cm, each resonance peak will be shifted in frequency, depending on the diameter of the tone hole. Figure 2.11 shows the effect of having a tone hole drilled at L =70 cm of radius $r = a$ (first resonance at 119 Hz), $r = a/2$ (first resonance at 115 Hz) and $r = a/5$ (first resonance at 103 Hz), where a is the radius of the tube. When the tone hole radius is the same as that of the cylinder, the first resonance lies almost at the same place as if the tube had been cut off. However, if the tone hole radius is smaller, the first resonance is shifted to the left, i.e. the effective tube is longer. It is worth noting that each and every resonance peak will be shifted a different amount, depending on frequency. This makes the design of a musical instrument a difficult task, as the placement of one hole could shift the resonances of other notes. Also, when upper octaves are considered, the size of a tone hole could shift the second register, making it too flat.

The method described in this Section can be used to calculate the input impedance of real musical instruments, provided that their dimensions are known or can be measured, specifically the radius of the tone holes and of the bore. This method has been tested and found to be in good agreement with experimental measurements of real musical instruments [69].

It is also possible to replace the sections of cylinders by sections of cones, and calculate the input impedance of each section by using equations 2.38 to 2.41.

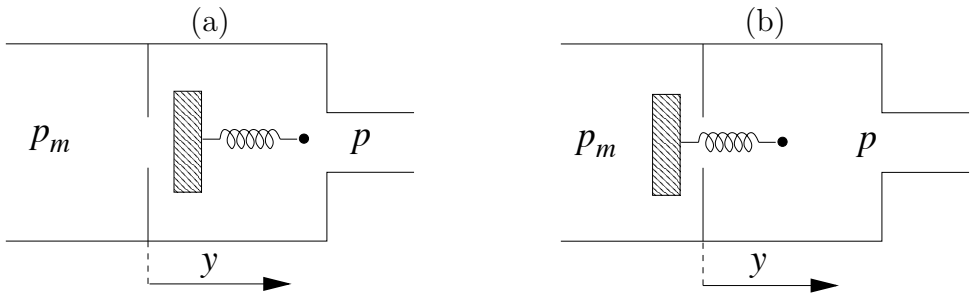

Figure 2.12: Two basic types of a pressured controlled valve: (a) outward striking, where an increase of pressure difference $\Delta P = p_m - p$ tends to open the valve; and (b) inward striking, where an increase in pressure difference $\Delta P = p_m - p$ tends to close the valve

2.3 Reed: The generator

The generators that are relevant to this study are reed generators, which act as pressure controlled valves, as the difference of pressure across them makes them vibrate. Instruments that have this type of excitation mechanism are the brass instruments, and the woodwind instruments of reed type, such as the clarinet, saxophone, the drones of a bagpipe (single reed instruments), oboe, bassoon, and the chanter of a bagpipe (double reed instruments).

Helmholtz [45] described two main types of generator: outward striking, where an increase in the pressure difference across it $\Delta P = p_m - p$ tends to open the valve, as shown in Figure 2.12 (a); and inward striking, where an increase in pressure difference $\Delta P = p_m - p$ tends to close the valve, as shown in Figure 2.12 (b) [34]. The woodwind type of reed is an inward striking reed. Although Helmholtz considered the brass instrument reed as being an outward striking reed, this is still under debate, since it is possible to play both above and below the resonance frequency of the air column. Experiments carried out by Richards [74] have provided evidence that the lips of a brass player can indeed act as both inward striking and outward striking, depending on the embouchure. Figure 2.13 shows an example of inward (a) and outward (b) striking reeds respectively, as explained by Helmholtz.

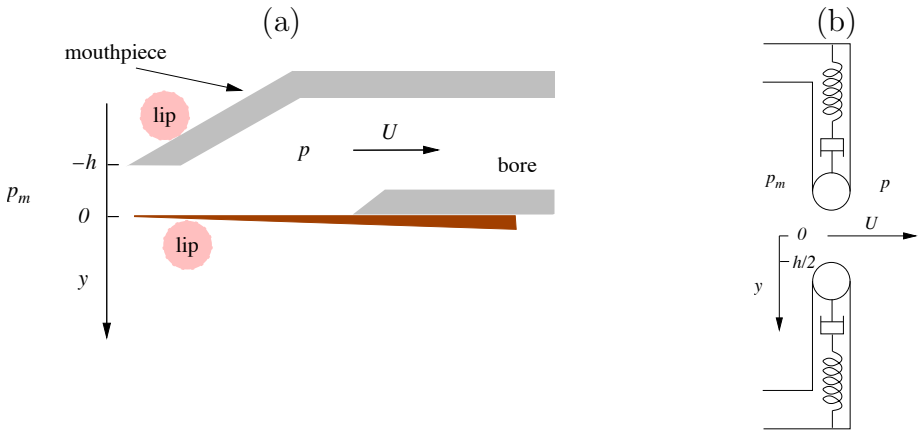

Figure 2.13: Two pressure controlled valves: (a) Clarinet mouthpiece and (b) lips of a brass player

2.3.1 Inward and Outward striking reeds

The motion of a pressure controlled valve such as those shown in Figure 2.13. can be represented by a damped linear oscillator driven by the pressure difference across it [84]:

$$\frac{\mathrm{d}^2 y}{\mathrm{d}t^2} + g_r \frac{\mathrm{d}y}{\mathrm{d}t} + \omega_r^2 y = \pm \frac{1}{\mu_r} \Delta P \tag{2.49}$$

where ω_r is the reed resonance frequency, g_r its half power bandwidth or reed damping factor, μ_r is the reed effective mass per unit area, p_m is the mouth pressure, p is the mouthpiece pressure, and $\Delta P = p_m - p$ is the pressure difference across the reed. As a positive pressure difference in an outward striking reed will tend open the reed, the sign of ΔP in equation 2.49 will be positive. In contrast, for an inward striking reed, a positive pressure difference will tend to close the reed, making it move in the negative direction, hence the sign of ΔP in equation 2.49 will be negative.

The relationship between the particle velocity in the reed channel and the pressure drop along it is described by the Bernoulli equation:

$$\frac{\rho u^2}{2} = \Delta P \tag{2.50}$$

where u is the particle velocity. u is related to the volume velocity flow U by:

$$U = w(h + y)u \tag{2.51}$$

where w is the width of the reed channel, and h is the equilibrium opening, as shown in Figure 2.13. Combining equations 2.50 and 2.51 we obtain the relationship between pressure difference ΔP and volume velocity U:

$$\Delta P = \frac{\rho \left(\frac{U}{w(h+y)}\right)^2}{2} \tag{2.52}$$

$$U = w(y+h)\sqrt{\frac{2\Delta P}{\rho}} \tag{2.53}$$

showing that the relationship between pressure difference and volume flow is nonlinear.

The reed can be excited to forced oscillation by applying a pressure difference $\Delta P = Pe^{j\omega t}$. The amplitude P can be set to be sufficiently small so that the nonlinear effects become negligible. Substituting ΔP and $y = Ae^{j\omega t}$ in equation 2.49, we obtain the displacement:

$$y = \pm \frac{\Delta P}{\mu_r(\omega_r^2 - \omega^2 + j\omega g_r)} \tag{2.54}$$

where the sign is positive for an outward striking reed, and negative for an inward striking reed. Figure 2.14 shows the magnitude and phase of this displacement versus frequency. At very low frequency ($\omega \ll \omega_r$), the oscillation is said to be stiffness dominated. As ω approaches ω_r, ($\omega \approx \omega_r$) this region is said to be resistance dominated, as the amplitude will depend mainly on the damping factor. At high frequencies ($\omega \gg \omega_r$), this region is said to be mass dominated.

Figure 2.14 shows that the displacement of an inward striking reed in forced oscillations has a $+90°$ phase difference with the supply pressure, while an outward striking reed has a $-90°$ phase difference with the supply pressure. Richards [74] used this information to find how artificial lips coupled to brass instruments can behave as both inward and outward striking reeds.

The acoustic admittance of the valve Y_r as seen from its output side is defined as [34]:

$$Y_r = \left(\frac{\partial U}{\partial(\Delta P)}\right)_{p=0} \tag{2.55}$$

Differentiating equation 2.53 with respect to ΔP, and evaluating at $p = 0$,

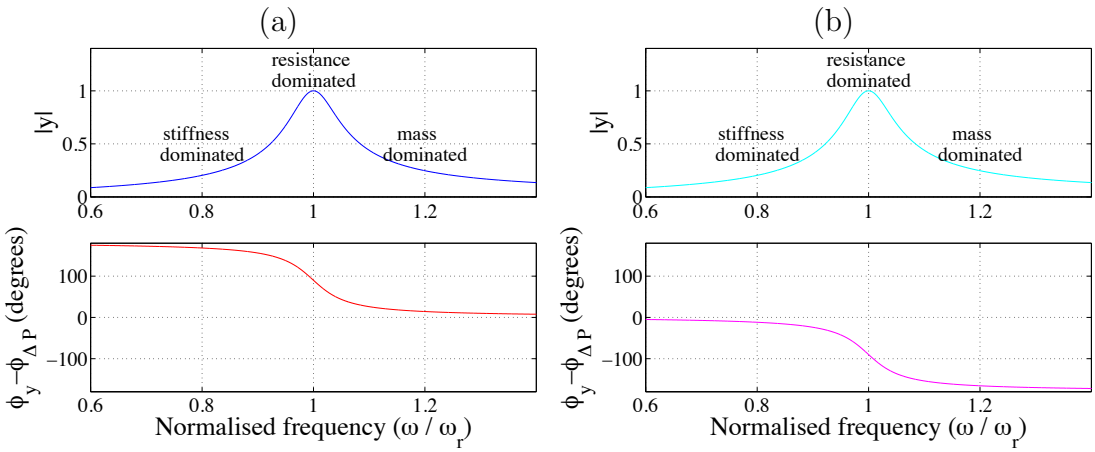

Figure 2.14: Magnitude and phase of displacement y as a function of frequency for (a) an inward striking reed and (b) an outward striking reed

the admittance Y_r becomes:

$$Y_r = \frac{w(h+y)}{2}\sqrt{\frac{2}{p_m \rho}} \tag{2.56}$$

Figure 2.15 shows the real and imaginary parts of the valve admittance for both reed configurations. Note that for the inward striking case, the real part of the admittance is negative just before resonance, and positive just after resonance, the opposite being for an outward striking reed.

Now we come to analyse the nonlinear relationship described in equations 2.52 and 2.53, where ΔP is no longer sinusoidal. It will be shown in section 2.4 that an inward striking reed must play below its resonance frequency ($\omega \ll \omega_r$), operating in the stiffness dominated regime, and than an outward striking reed must play close to its resonance frequency ($\omega \approx \omega_r$), operating in the resistance dominated regime. For the case of an inward striking reed, equation 2.54 becomes:

$$y = -\frac{\Delta P}{\mu_r \omega_r^2} \tag{2.57}$$

Inserting this in equation 2.53 we obtain:

$$U = S_r \left[1 - \frac{\Delta P}{h \mu_r \omega_r^2}\right] \sqrt{\frac{2\Delta P}{\rho}} \tag{2.58}$$

where $S_r = wh$ is the area of opening of the reed at equilibrium. It is clear that the volume flow will be zero when either $\Delta P = 0$ (there is no pressure difference

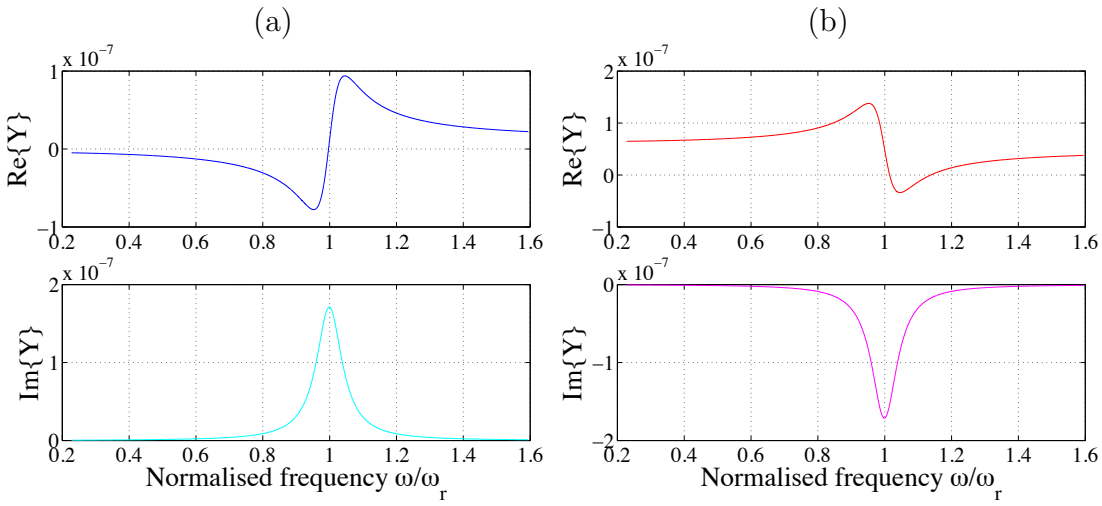

Figure 2.15: Real and imaginary parts of the reed admittance for (a) an inward striking reed, and (b) an outward striking reed

across the reed), or $\Delta P = h\mu_r\omega_r^2$, in which case the reed gap is completely closed. For $\Delta P < 0$ the volume flow would be negative, as the mouthpiece pressure p would be greater than the mouth pressure p_m. In order to avoid an imaginary volume flow for values of $\Delta P < 0$, equation 2.58 can be modified as follows:

$$U = S_r \left[1 - \frac{\Delta P}{h\mu_r\omega_r^2}\right] \sqrt{\frac{2|\Delta P|}{\rho}} sign(\Delta P) \tag{2.59}$$

For $\Delta P > h\mu_r\omega_r^2$, the reed would stay closed, and the flow would be zero thereafter. Figure 2.16 (a) shows this relationship. Note that for $\Delta P > h\mu_r\omega_r^2$ equation 2.59 no longer holds, as the volume flow becomes negative instead of being zero.

It is important to note that above certain value of ΔP (around 5 kPa in the case of Figure 2.16 (a)), the slope of the characteristic curve is negative, meaning that the valve is operating as a negative-resistance generator, or in other words, it is supplying energy to the system [34].

In contrast, an outward striking reed operates in the resistance dominated regime. As $\omega \approx \omega_r$, the displacement becomes:

$$y = +\frac{\Delta P}{\mu_r j\omega_r g_r} \tag{2.60}$$

Inserting this equation into equation 2.53, the volume flow becomes:

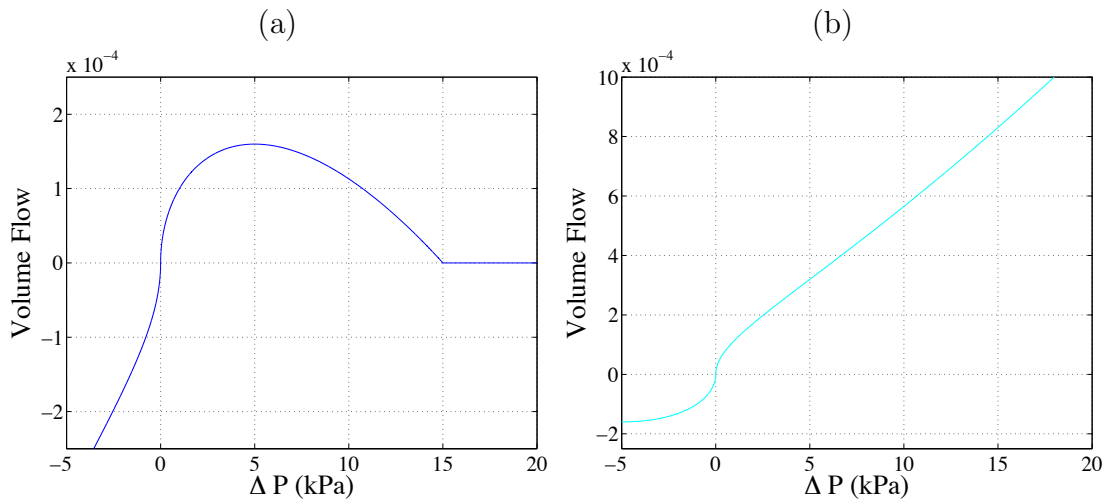

Figure 2.16: Steady volume flow characteristic curve of (a) an inward striking reed and (b) an outward striking reed

$$U = S_r \left[1 + \frac{\Delta P}{h\mu_r j\omega_r g_r}\right] \sqrt{\frac{2|\Delta P|}{\rho}} sign(\Delta P) \tag{2.61}$$

Figure 2.16 (b) shows the characteristic curve for this configuration. Note that there is no region where the slope is negative. In this case, as we will see in Section 2.4, the acoustic generation comes as a result of phase shifts that occur near resonance [34].

2.3.2 Double reed

We have mentioned that woodwind reeds, including double reeds are inward striking reeds. However, because of its particular geometry, it is possible that there is pressure recovery at the entrance of the reed (p_2) which contributes a flow resistance [33], [46]. In this case:

$$p_m - p_2 = \frac{1}{2}\rho u^2 \tag{2.62}$$

$$p_2 - p = RU^2 \tag{2.63}$$

The pressure difference $\Delta P = p_m - p$ from the mouthpiece to the entrance of the instrument is then:

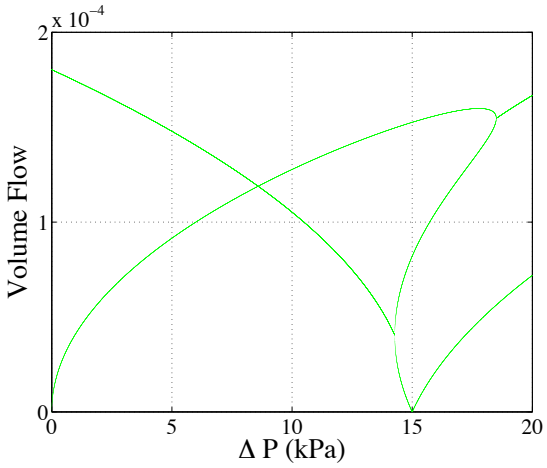

Figure 2.17: Volume flow characteristic curve of a double reed, taking into account the flow resistance R due to the geometry of the reed

$$\Delta P = \frac{1}{2}\rho u^2 + RU^2 \tag{2.64}$$

$$\Delta P - RU^2 = \frac{1}{2}\rho u^2 \tag{2.65}$$

This leads to the volume flow:

$$U = S_r \left(1 - \frac{\Delta P - RU^2}{hk}\right) \sqrt{\frac{2(\Delta P - RU^2)}{\rho}} \tag{2.66}$$

As the flow resistance R increases, the higher order terms of equation 2.66 start dominating the flow curve. The effect of having a resistance $R = 500 \times 10^9$ is shown in Figure 2.17. Note the strong hysteresis that takes place as ΔP increases. The pressure where the reed acts as an active generator is now around 18 kPa.

2.4 Coupling between air column and reed

The musical instruments we are interested in studying consist of a reed in conjunction with a pipe, where the reed acts as an active generator, and the air column as a passive resonator. It is important to study how these two elements

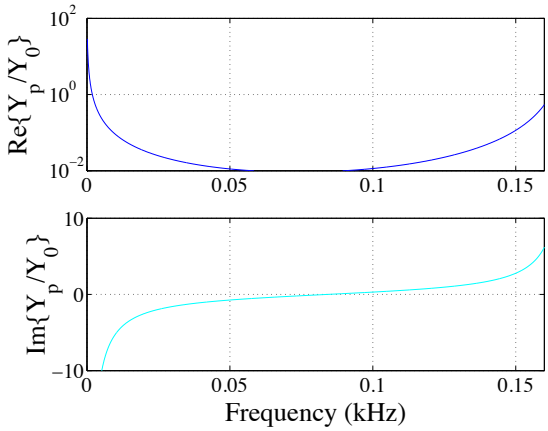

Figure 2.18: Real and imaginary parts of the normalised admittance for a cylindrical pipe, with $L = 1$ m and $r = 2$ cm

are coupled together.

Let us consider a perfect cylindrical pipe, with input impedance Z_p as in equation 2.13. As a first approximation, we can take the first resonance of the pipe, which corresponds to an impedance maximum, or admittance minimum. Figure 2.18 shows the real and imaginary parts of pipe $Y_p = \frac{1}{Z_p}$ first resonance peak (first admittance minimum). The real part is always positive, whereas the imaginary part is negative just before the impedance maxima, and positive just above. To get the coupled system in resonance, we require [34]:

$$\Im\{Y_r\} = -\Im\{Y_p\} \tag{2.67}$$

$$-\Re\{Y_r\} > \Re\{Y_p\} \tag{2.68}$$

Figure 2.15 shows the valve admittance Y_r. For an inward striking reed $\Im\{Y_r\} > 0$. To satisfy equation 2.67 we need $\Im\{Y_p\} < 0$, which implies that playing frequency ω lies slightly below a pipe resonance. For an outward striking reed, in contrast, $\Im\{Y_r\} < 0$ so in this case to satisfy equation 2.67 we require $\Im\{Y_p\} > 0$, and the playing frequency ω lies slightly above a pipe resonance.

It is worth remembering that we have only considered a single resonance in the linear approximation. Nonlinearities, as well as the presence of multiple resonances in the air column make real musical instruments behave in a much more complicated way.

The mode at which the pipe will sound will be the one for which the inequality of equation 2.68 is most strongly satisfied. This will depend on the specific behaviour of the generator.

For a woodwind reed, $\omega_r \gg \omega$, so the real part of the reed admittance is negative below the reed resonance (Figure 2.15 (a)). Figure 2.9 (a) shows the impedance curve of a cylindrical pipe considering losses and radiation impedance effects. The mode with the highest amplitude (impedance maximum) is the lowest one, thus the instrument will sound in the lowest mode. The real part of the impedance of an outward striking reed (Figure 2.15 (b)) is negative only for a narrow range just above ω_r. The reed resonance will dominate the behaviour of the system: It will drive a pipe resonance which is closest to the reed resonance [34].

2.5 Nonlinear effects

It is clear that the relationship between pressure and volume flow shown in equation 2.53 is nonlinear. If we assume a sinusoidal variation in pressure:

$$p = Psin(\omega t) \tag{2.69}$$

the volume flow U will have terms with frequencies $n\omega$, where $n = 1, 2, 3, ...$ All of these terms will interact with the air column, and each component of the flow $U_n sin(n\omega t)$ will generate in turn a pressure:

$$p_n = Z_p(n\omega)U_n sin(n\omega t) \tag{2.70}$$

which is rich in harmonics, each component rigorously locked in frequency and phase to the fundamental [34].

In Section 2.3 the reed was considered to be a damped linear oscillator. This approximation holds true for small oscillations [6]. However, for large amplitude oscillations, the reed starts beating, introducing other nonlinear effects.

Chapter 3

Psychoacoustics of musical sounds

3.1 Introduction

Music is made of sounds that are characterised by three distinct attributes, which are clearly specified in any given score: pitch (which note is played), loudness (dynamic markings), and timbre or tone quality (which instrument plays). The way humans perceive each of these mainly depends on the anatomy of the ear and the hearing health of the particular listener. Psychoacoustics is the study that links acoustic stimuli with auditory sensations [75].

If what we perceive is subjective and individually unique, is it possible to measure these attributes? For any given music signal, we can mainly measure its amplitude and its spectrum (frequency, amplitude and phase of its partials), and how these attributes change over time. Psychoacoustics links the acoustic stimuli with the auditory perception [75]. If we can correlate how each of the subjective attributes (pitch, loudness and timbre) is related to the objective physical attributes of a signal (amplitude and spectrum), we can obtain a measurable physical correlate that tells us how the sounds are perceived.

Psychoacoustics also studies the smallest change in a physical correlate that is just perceived. This is called just noticeable difference (JND), difference limen or differential threshold. It is defined as the smallest detectable change in a stimulus [59]. This quantity is statistical, and in order to be obtained, many

trials presenting various degrees of difference have to be presented in random order. It usually tells the amount of difference that a person can perceive 50% of the time.

This Chapter is organised as follows: Section 3.2 deals with our perception of pitch of simple and complex sounds, units of measurement, just noticeable difference, and measuring techniques. Section 3.3 deals with our perception of loudness, introduces equal loudness contours, masking effects, just noticeable difference, and measuring techniques. Finally, Section 3.4 deals with our perception of timbre of complex sounds, and presents different representations of timbre with emphasis in spectral centroid, just noticeable difference and measuring techniques.

3.2 Pitch

We saw in Chapter 2 that a sound produced by a wind instrument is generated by the nonlinear interaction between the generator and the resonator, which together produce a tone that is rich in harmonics. Since all the components of this complex tone are strictly locked in harmonic relationship, its waveform is periodic, except for the starting and finishing transients (attack and decay), and for the small random variations, deliberate or not, that the player introduces to make the instrument sound beautiful, such as vibrato effects.

In order to be able to understand how humans perceive the pitch of complex tones, we will start our discussion by analysing the pitch of pure tones.

3.2.1 Pitch of pure tones

According to the ANSI standard of Acoustical Terminology [82], pitch is defined as:

> That attribute of auditory sensation in terms of which sounds may be ordered on a scale extending from low to high...

When we listen to a pure tone of fixed amplitude, we hear its pitch changing as frequency varies. If the frequency of the tone increases, we hear the pitch rising, if the frequency decreases, we hear the pitch falling.

Pitch notation in western music names 7 main notes, which can be increased or reduced by a semitone by indicating a ♯ or a ♭ sign respectively. The chromatic

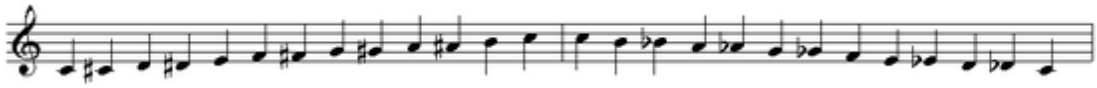

Figure 3.1: The western equally tempered chromatic scale, made of 12 equally spaced semitones (taken from [88])

scale in western music consists of the following notes: C, C$^\sharp$ or D$^\flat$, D, D$^\sharp$ or E$^\flat$, E, F, F$^\sharp$ or G$^\flat$, G, G$^\sharp$ or A$^\flat$, A, A$^\sharp$ or B$^\flat$, and B (see Figure 3.1). This gives 12 semitones in total, that are repeated every octave. In this way, we have for example the pitch A, that repeats at every octave, giving A_1, A_2, A_3, and so on, where the subscript indicates the octave number.

There is clearly a close correspondence between our subjective sensation of pitch and the frequency of a given tone, since the standard of pitch for note A_4 is defined as the pitch sensation evoked by a pure tone of 440 Hz. However, pitch sensation for pure tones also depends on the amplitude of the tone. Experiments performed by Snow [80] show that most people hear the pitch dropping as the amplitude of the tone is increased, for tones with frequencies between 75 Hz and 1 kHz. Musical notes are rarely composed of pure tones, so this effect has little musical relevance, except for the case of the tuning fork, as it gives a reasonably clean tone after the initial attack has died out [20].

The frequency of a note that is one octave above another in pitch is about twice as much as the frequency of the original note. This is illustrated in Figure 3.2. In order to understand why equal changes in pitch do not correspond to equal changes in frequency, we need to know what happens inside our ears when a pure tone reaches them.

The basilar membrane is located in the inner ear, inside the cochlea, dividing it roughly in half, where the top is the scala vestibuli and the bottom the scala Tympani. The basilar membrane is about 34 mm long from the base (input or oval window) to the apex (helicotrema), and exhibits a gradual change in width and thickness, both of which determine its stiffness at any point along it [75]. When a pure tone reaches the ear, the pressure disturbances of the air travel along the ear canal until they reach the basilar membrane. The pressure differences across the cochlear partition between the two scalae bend the basilar membrane up and down, generating a travelling wave. As this travelling wave

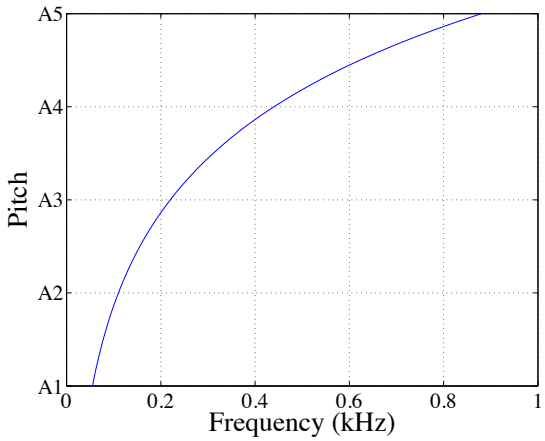

Figure 3.2: Relationship between pitch and frequency

moves along the basilar membrane towards the apex, its amplitude increases to a maximum at a given place depending on the frequency of the tone, and then dies out quickly towards the apex. An example of such a travelling wave is illustrated in Figure 3.3. Hair cells that are located along the basilar membrane send the motion information to the brain via the auditory nerve fibres in the form of electric signals [92].

As we double the frequency of a tone, this area of increased amplitude is shifted by a roughly constant amount (between 3.5 to 4 mm). Regardless of the frequency of the initial tone, if we double that frequency, the area of increased amplitude will always be shifted by the same amount. In general when we multiply a given frequency by a given factor, the area of increased amplitude in the basilar membrane will be shifted by a particular amount [75].

3.2.2 Unit of measurement

The standard unit to calculate the pitch interval between two notes is called the cent, and it takes into account this "shifting" property of the basilar membrane. We have seen that an octave corresponds to approximately doubling the frequency of a tone. So if we multiply a given frequency by two, the resulting tone will be one octave above the first one. If we multiply this new tone again by two (or the original tone by four), the resulting tone will be one octave above the previous tone, or two octaves above the first one. In order to get that pitch interval (PI),

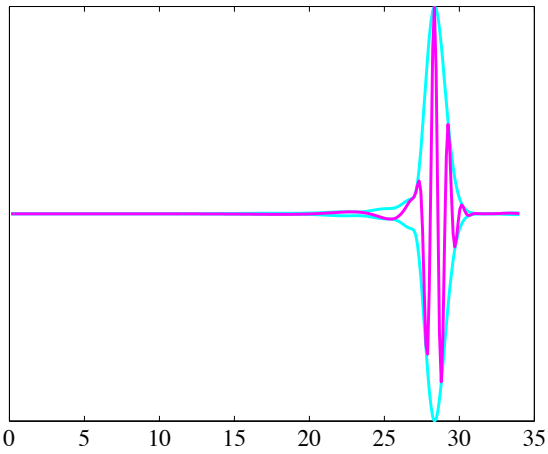

Figure 3.3: Travelling wave motion (magenta) and amplitude envelope (cyan) of the basilar membrane in response to a tone with frequency 1 kHz. Numbers from left to right indicate distance from base to apex in the basilar membrane in mm. Calculated using a MATLAB routine written by Renato Nobili, based on [56] and [64]

we find the following relationship:

$$PI[\text{octaves}] = log_2\left(\frac{f_2}{f_1}\right) \tag{3.1}$$

This equation will give us the number of octaves that the tone of frequency f_2 is above the tone of frequency f_1. Most modern instruments are tuned in what is called the equally tempered scale, which subdivides the octave in 12 equal semitones, so that one can calculate the frequency of a tone f_2 which is an equally tempered semitone above a tone with frequency f_1 by:

$$f_2 = 2^{\frac{1}{12}} \cdot f_1 \tag{3.2}$$

Similarly we can also calculate the number of semitones a tone of frequency f_2 is above a tone of frequency f_1 by:

$$PI[\text{semitones}] = 12 \cdot log_2\left(\frac{f_2}{f_1}\right) \tag{3.3}$$

Since we can distinguish changes in pitch that are much smaller than one semitone, we can further subdivide a semitone into 100 cents:

$$PI[\text{cents}] = 100 \cdot 12 \cdot log_2 \left(\frac{f_2}{f_1} \right) \tag{3.4}$$

3.2.3 Just noticeable difference in pitch of simple tones

Experiments have shown that the ability to discriminate simple tones of different frequency depends strongly on the frequency, intensity and duration of the tone, as well as the suddenness of the frequency change, and on the method of measurement employed. For example, if the frequency of a tone of constant intensity level (80 dB) is slowly and continuously modulated up and down, a change of 0.5% (approximately 9 cents) at 2 kHz can be detected. However, if the change in frequency is sudden, the JND is 30 times smaller than that. Also, frequency resolution is poorer at low frequencies (3% or approximately 50 cents at 100 Hz), and decreases with tone duration for durations below 100 ms [75].

3.2.4 Critical band

As most musical tones are the result of many simple tones sounding at the same time, let us analyse what happens when we listen to two pure tones simultaneously. As we mentioned in Section 3.2.1, whenever a pure tone arrives to the ear, a travelling wave will generate vibrations in the basilar membrane. The amplitude of this travelling wave will reach a peak at a particular place on the basilar membrane, depending on the frequency of the tone. When we apply two tones of two different frequencies, there will be two travelling waves, and thus two places on the basilar membrane with increased amplitude (see Figure 3.4). If the difference in frequency between the two tones is large, then the two areas of increased amplitude have little overlap, and the hair cells excited by one tone vibrate independently from the hair cells excited by the other tone, that is, they do not affect one another. However, if the difference in frequency is small, then the two areas of increased amplitude in the basilar membrane overlap, which means that there is strong interaction between the two sounds, as they fire almost the same set of hair cells. When there is a large overlap, the two frequencies lie within one critical band. Figure 3.4 shows the travelling wave amplitude envelope for two tones that lie well above one critical band, as well as within one critical band.

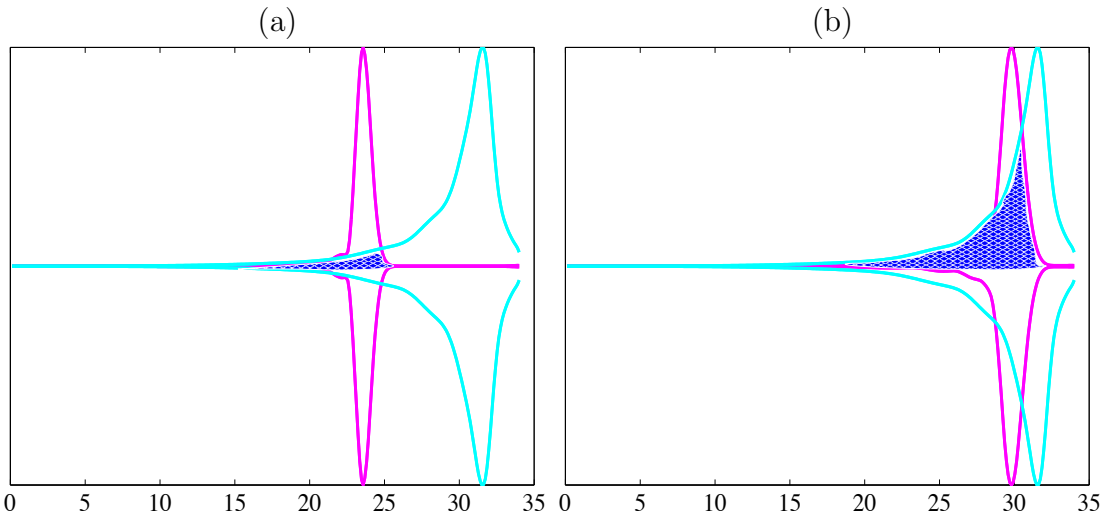

Figure 3.4: Amplitude envelope of travelling waves generated in the basilar membrane as a result of two tones of frequencies of (a) 500 Hz and 2 kHz and (b) 500 Hz and 800 Hz. Numbers from left to right indicate distance from base to apex in basilar membrane in mm. Blue shades indicate amount of overlap. Calculated using a MATLAB routine written by Renato Nobili, based on [56] and [64]

When two sounds of the same frequency are heard together, they reach the basilar membrane and excite one set of hair cells, sounding in unison. If we hear two sounds whose frequencies differ by less than the tone discrimination threshold, we hear a tone of one pitch, but with beating loudness. If we instead hear two sounds whose frequencies differ by more than the tone discrimination threshold, but less than a critical band, we hear two tones of different pitch, but since the regions in the basilar membrane that are being excited overlap, there is a sensation of "roughness" or "unpleasantness". If the frequency difference of the two tones is such that they do not lie within a critical band, we will hear two different tones with two distinct pitches, and the sensation of roughness will disappear. The size of the critical band varies with frequency, being almost an octave at 100 Hz. Above 1 kHz it remains fairly constant at about one third of an octave, or 400 cents [75].

3.2.5 Pitch of complex tones

When we listen to a note produced by a musical wind instrument, we are actually hearing many pure tones that are harmonically related. The basilar membrane detects each of these as being separate vibrations, as long as they are separated

by more than a critical band. Clearly, the first 5 harmonics of a sound will be separated by more than a critical band. However, we only hear one pitch. This ability to assign a single pitch to a series of tones is called fusion. Fusion only occurs however, if the frequencies of the tones are approximately or completely harmonic. If they are not at least approximately harmonically related, then they are heard separately, and there is no sensation of definite pitch [20].

In the case of a complex tone such as that generated by a wind instrument, the pitch will be closely related to the frequency of the fundamental of the harmonic series. In fact, when we remove the upper harmonics of a complex tone one by one, we still hear the same pitch, although the timbre or tone quality changes. But we can also remove gradually the lower harmonics, starting with the fundamental. In this case, we would also hear the same pitch, as though the fundamental was present. The pitch of a signal could in principle be estimated by tracking the periodicity of such a signal, as the periodicity of it would be equal to the difference in frequency between each harmonic component. This works well for tone complexes whose partials are the components of a harmonic series. However, if the components do not form an exact harmonic series, but are approximately harmonic, the perceived pitch is no longer related to the difference in frequency between each component. In this case, the brain assigns a pitch that corresponds to a sound with a harmonic series that resembles as close as possible the components of the heard sound. However, experiments have shown that there is a dominance region, roughly between 500 Hz and 2 kHz, so that the pitch of a tone is determined mainly by the harmonics that lie within this region [20]. For low frequency notes (up to around 200 Hz) the 5^{th} harmonic dominates, and for high frequency notes (higher than 2 kHz) the dominant harmonic is the 1^{st} [70].

3.2.6 Just noticeable difference in pitch of complex tones

We saw in section 3.2.3 that the pitch discrimination of low frequency sounds is rather poor (around 50 cents). In the case of complex tones, the pitch will be determined by those harmonics that lie within the dominance region. For a complex tone of low frequency, we find that several of its higher harmonics will lie within the dominance region. Although the fundamental of such a tone would have to be shifted by at least 50 cents to be detected, a much smaller change in the 5^{th} harmonic will be readily detected. Thus, the discrimination threshold for

complex tones is around 9 cents, regardless of pitch [20], which is the JND for a pure tone of 2 kHz.

3.2.7 Techniques for measuring the pitch of complex tones

There are two main types of pitch detection algorithms: [72]:

- Time domain based pitch detection, such as the Autocorrelation Method
- Frequency domain based pitch detection, such as the Harmonic Product Spectrum Method

The Autocorrelation Method calculates the Autocorrelation Function (ACF) by the following equation [27]:

$$\phi(\tau) = \frac{1}{N}\sum_{n=0}^{N-1} x(n)x(n+\tau) \tag{3.5}$$

where $x(n)$ is the sampled time signal, τ is a time offset, and $x(n+\tau)$ is a time offset version of $x(n)$. The Autocorrelation Function will present a peak at the value $\tau = T$, where T is the period of the signal. This method will succeed in finding the correct pitch when the fundamental is missing, as $\frac{1}{T}$ will approximately correspond to the difference in frequency between harmonics.

The Harmonic Product Spectrum Method converts the input signal $x(n)$ from the time domain to the frequency domain $X(\omega)$ by calculating its Short Time Fourier Transform (STFT). It then downsamples the STFT by $2, 3, ..., N$, N being the number of harmonics to be considered. It then calculates the product $Y(\omega)$ of the original STFT times the downsampled versions of it, and searches for a peak. The resulting peak gives the first harmonic of the original signal [27]:

$$Y(\omega) = \prod_{r=1}^{N} |X(\omega r)| \tag{3.6}$$

$$\hat{Y} = max\{Y(\omega)\} \tag{3.7}$$

The main drawback of this method is that it will give an octave mistake if the fundamental is missing. Also, the time signal $x(n)$ has to be zeropadded in order

to increase the frequency resolution, which will result in a slower computation [27].

Beauchamp [12] has developed a computer program (SNDAN, or Sound Analysis) to analyse quasi-periodic musical sounds. This program performs a pitch-synchronous phase vocoder analysis, so it tracks frequency deviations of the harmonics of the signal relative to integer multiples of the analysis frequency f_a provided by the user. Although this method is frequency domain based, it does not have the problem of making octave mistakes, as it takes the analysis frequency f_a as a parameter from the user, which should be close enough to the actual playing frequency of the sound to be analysed (within 1% to 2% [12]).

The pitch deviation f_c relative to the analysis frequency f_a is:

$$\Delta P(t) = 1200 \cdot log_2 \left(\frac{f_a + \Delta f_c(t)}{f_a} \right) \tag{3.8}$$

where

$$f_c = f_a + \Delta f_c \tag{3.9}$$

and

$$\Delta f_c(t) = \frac{\sum_{k=1}^{5} \frac{A_k(t) \cdot \Delta f_k(t)}{k}}{\sum_{k=1}^{5} A_k(t)} \tag{3.10}$$

k is the harmonic number, $A_k(t)$ is the amplitude of the k^{th} harmonic, and $\Delta f_k(t)$ is the frequency deviation of the k^{th} harmonic relative to f_a. The frequency deviation of each harmonic is weighted according to its instantaneous amplitude. This estimate of pitch uses the first 5 harmonics of the signal. Beauchamp [12] noted that, as sometimes the fundamental of a signal is weak, the composite frequency, which takes into account the first five harmonics, is a better measurement of frequency than the fundamental alone. Moreover, as we have seen in Section 3.2.5, the harmonics that are dominant in the sensation of low pitch (up to 200 Hz) are the first 5 harmonics, decreasing gradually as the frequency of the stimulus increases.

3.3 Loudness

The loudness of a note is usually specified in a music score by the dynamic markings. These typically range from ff (fortissimo) to pp (pianissimo), and are much more vague than the pitch specifications given to each note.

According to the ANSI standard of Acoustical Terminology [82], loudness is defined as:

> That attribute of auditory sensation in terms of which sounds may be ordered on a scale extending from soft to loud...

3.3.1 Dynamic level and intensity

The perceived loudness of a pure tone of fixed frequency increases as its amplitude increases. However, if the frequency of the tone changes, while keeping its amplitude constant, the loudness is found to depend on frequency. Also the loudness of a tone is often dependent on other simultaneous sounds, or sounds that occur shortly before the tone in question.

We can measure the pressure fluctuations of a sound wave. The intensity of the plane wave in the far field is the energy transfer rate through an area of 1 m^2:

$$I = \frac{p_{rms}^2}{z} \left[\frac{\mathrm{W}}{\mathrm{m}^2}\right] \tag{3.11}$$

where p_{rms} is the effective pressure, and z is the specific acoustic impedance of a wall of air of 1 m^2 (415 $\frac{\mathrm{Pa{\cdot}s}}{\mathrm{m}}$).

In order to specify which dynamic marking corresponds to a certain intensity, we can ask musicians to rate the dynamic level of a standard 1 kHz pure tone of varying intensity. The fact that the loudness sensation is different for every person will be reflected in the discrepancy of the results. A rough correspondence between intensity and dynamic marking is shown in Table 3.1.

As is the case with the pitch, where doubling the frequency corresponds to increasing one octave, multiplying the intensity by 10 corresponds to a one step increase in dynamic level (e.g. from p to mp or from mf to f). The intensity ratio (IR) between two sounds of intensities I_1 and I_2 can be expressed in bels as:

$$IR[\mathrm{bel}] = log_{10}\left(\frac{I_1}{I_2}\right) \tag{3.12}$$

Musical Dynamic Level	**Intensity** $\left(\frac{\mathbf{W}}{\mathbf{m}^2}\right)$	**Intensity Level (dB)**
fff	10^{-2}	100
ff	10^{-3}	90
f	10^{-4}	80
mf	10^{-5}	70
mp	10^{-6}	60
p	10^{-7}	50
pp	10^{-8}	40
ppp	10^{-9}	30

Table 3.1: Correspondence of dynamic markings with intensity (column 2) and intensity level relative to an intensity of $10^{-12}\frac{\mathrm{W}}{\mathrm{m}^2}$ (column 3)

This unit is normally subdivided into 10 decibels or dB, giving:

$$IR[\mathrm{dB}] = 10 \cdot log_{10}\left(\frac{I_1}{I_2}\right) \tag{3.13}$$

In this case, one step on the musical dynamic scale corresponds to a ratio of 10 dB. It is useful to have a standard intensity I_0 to which all other sounds are compared, making the dB scale absolute. This intensity is frequently chosen to be $I_0 = 10^{-12}\frac{\mathrm{W}}{\mathrm{m}^2}$, which is approximately the lowest intensity of a 1 kHz tone which can be heard by someone with acute hearing. The intensity level of a sound (IL) is defined as:

$$IL = 10 \cdot log_{10}\left(\frac{I}{I_0}\right) \tag{3.14}$$

At the standard intensity I_0 the effective pressure for a plane sound wave is $p_0 = 2 \times 10^{-5}$ Pa. As most microphones are sensitive to pressure, the sound pressure level is defined as:

$$SPL = 10 \cdot log_{10}\left(\frac{p_{rms}^2}{p_0^2}\right) = 20 \cdot log_{10}\left(\frac{p_{rms}}{p_0}\right) \tag{3.15}$$

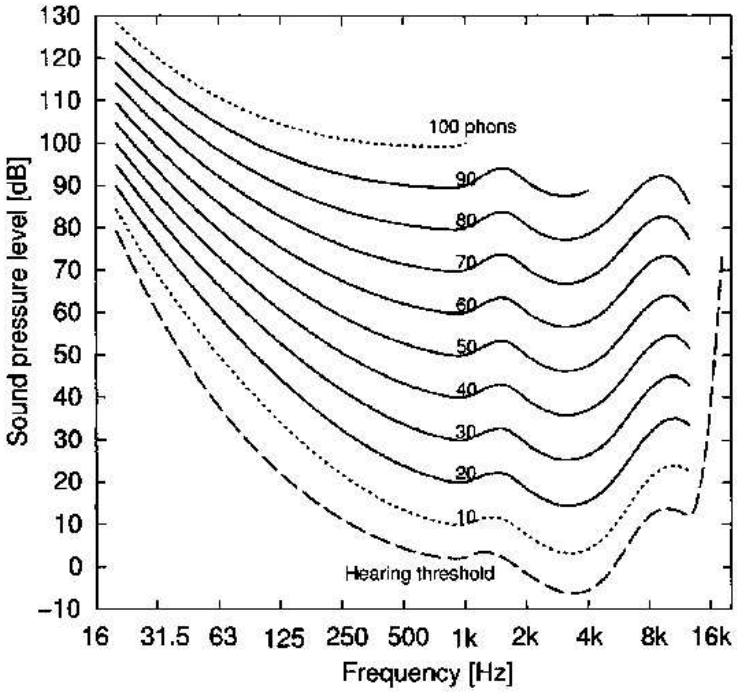

Figure 3.5: Equal loudness contours (taken from [83])

3.3.2 Equal loudness contours

Tones that have the same SPL but different frequency will not necessarily have the same loudness. Experiments have been made to establish what is called equal loudness contours (see Figure 3.5), which show the IL that a tone of a given frequency must have to be judged as loud as a 1 kHz tone of a fixed IL. Similarly, the threshold of audibility (the lowest IL at which a pure tone can be heard by a listener with acute hearing) varies with frequency. This threshold is also raised by background noise.

To account for these differences in loudness with frequency, a loudness level scale has been developed, with the phon as unit. The loudness level of a tone of frequency f is given by the SPL of a 1 kHz tone that is judged to be equally loud. The equal loudness contours are in fact curves of constant loudness levels.

The loudness of a tone is not proportional to the loudness level in phons; that is to say, a sound whose loudness level is twice as large does not sound twice as loud. In fact, experiments show that an increase of approximately 10 phons corresponds to doubling the loudness. The sone unit overcomes this problem:

1 sone is defined as the loudness of a 40 phon pure tone. Similarly, 2 sones corresponds to 50 phons, 4 sones to 60 phons, and so on. Loudness level in phons is approximately related to loudness in sones by the following equation [82], [92]:

$$LL[\text{phons}] = 10 \cdot log_2(L[\text{sones}]) + 40 \tag{3.16}$$

3.3.3 Masking

When two sounds are being played simultaneously, the apparent loudness of each of the sounds in general depends on the loudness of the other sound, i.e. it is not possible to obtain the total loudness of two sounds by just adding their individual loudnesses, as the loudness of each depends on the other. A sound is said to be masked by a second sound if it is audible in the absence of the second, but inaudible when the second is present.

Let us recall that when two pure tones of different frequencies reach the ear, each will set the basilar membrane in motion, creating an area of increased amplitude. If the amplitude of one of the two tones is much smaller than the other one, the brain will only be aware of the soft sound if the hair cells that are excited by it are separate from the ones excited by the loud sound. Figure 3.6 illustrates this effect. In Figure 3.6 (a) the two sounds are exciting a different set of hair cells. In Figure 3.6 (b) the soft tone is exciting a set of hair cells that is already being excited by the loud tone, and the soft tone is being masked.

3.3.4 Loudness of complex tones

As we have mentioned in Section 3.3.3, when calculating the loudness of two simultaneous sounds, we have to take into account the contribution of each component. If a sound that is composed of tones whose frequencies are well separated (i.e. by several critical bands), then the total loudness of the sound will be simply the sum of loudness (in sones) of the individual components, as each of the components will not influence the others significantly. However, if the components are within one critical band of each other, we can add their intensities together. For example, for a sound that is composed of two simple tones with loudness level of 60 phons each, its total loudness will be 4+4=8 sones if they are well

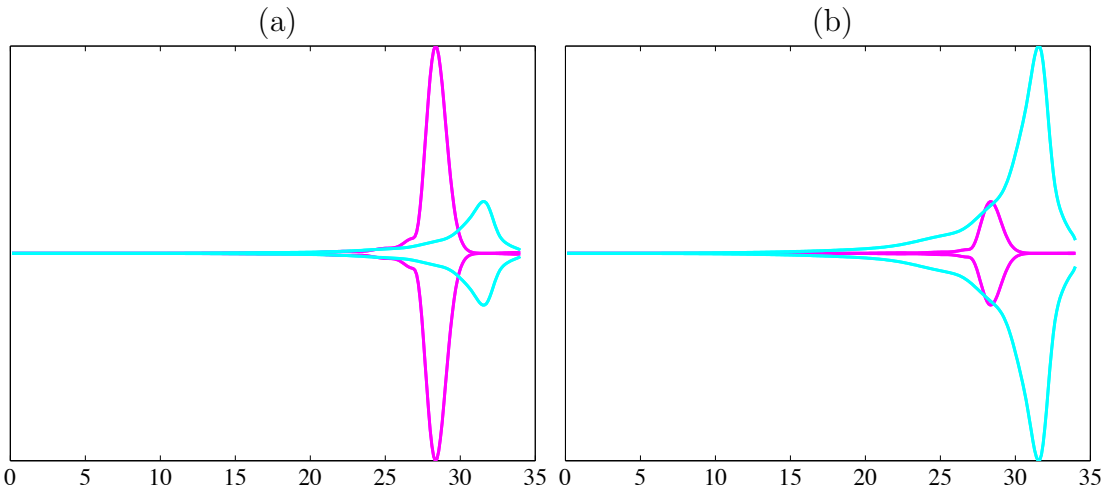

Figure 3.6: Amplitude envelope of travelling waves generated in the basilar membrane corresponding to (a) a soft tone of 500 Hz and a loud tone of 1 kHz, and (b) a loud tone of 500 Hz and a soft tone of 1 kHz. In (b) the 1 kHz tone (soft) is said to be masked by the 500 Hz tone (loud). Calculated using a MATLAB routine written by Renato Nobili, based on [56] and [64]

separated (LL of 70 phons), or 4.9 sones (LL of 63 phons) if they lie within one critical band.

3.3.5 Just noticeable difference in intensity level

It is important to know what minimum change in intensity level is necessary for the ear to detect. Experiments performed by Jesteadt et al. [49] show that the just noticeable difference in intensity level depends on the intensity of the tone. For very quiet sounds (pp), an increase of 1.5 dB IL is detected, whereas for loud sounds (ff) an increase of 0.5 dB IL is sufficient to be detected.

3.3.6 Sound pressure level meters

Sound pressure level meters take into account the complex dependency of frequency with loudness by incorporating a weighting network whose transfer function resembles the equal loudness contours. As the shape of the equal loudness contours varies with intensity, there are three scales available: dB(A) for quiet sounds, where the weighting network corresponds to the 40 phons equal loudness contour, dB(B) for moderate sounds, where the weighing network corresponds to the 70 phons equal loudness contour, and dB(C) for loud sounds, with an almost

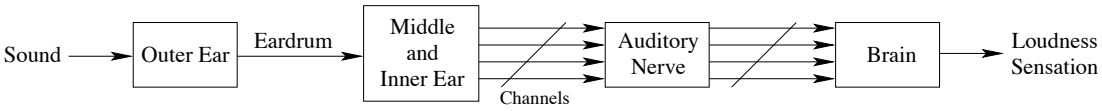

Figure 3.7: Block diagram of the basic auditory system (taken from [47])

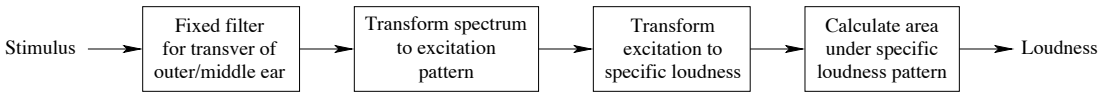

Figure 3.8: Block diagram of Zwicker's model for calculating loudness (taken from [60])

flat response across frequency. For most practical purposes, the dB(A) scale provides a good approximation to perceived loudness, even for loud sounds. This might be due to the fact that the effect of undervaluing low frequency components is compensated by overvaluing (masked) high frequency components [20].

3.3.7 Techniques for estimating loudness

More sophisticated techniques for measuring loudness have been developed [47], [58], [60]. They are based in the model developed by Zwicker [92]. A block diagram of the basic auditory system is shown in Figure 3.7. Zwicker's model is shown in Figure 3.8.

The model developed by Zwicker [92] calculates the loudness of a sound from its spectrum. The first stage in Zwicker's model accounts for the transmission of sound through the outer and middle ear. It is usually represented by a filter whose transfer function is the inverse of the absolute threshold curve [58]. The second stage of the model calculates the excitation pattern, which is the magnitude of the output of each filter in a band-pass filter bank, each filter having a bandwidth of $\frac{1}{3}$ octave, to account for the effect of critical bands and masking in the basilar membrane. The shape of these auditory filters has been derived from masking patterns, obtained experimentally. The third stage of the model transforms the excitation pattern of the sound into specific loudness of each critical band. The last stage is a summation of the specific loudnesses calculated

for each critical band, giving an expression of overall loudness.

Zwicker's original model has been modified to account for time varying sounds [93], [38]. A computer MATLAB program written by Marek Dziubinski, from the Technical University of Gdansk, Poland, which was based on the model presented by Glasberg and Moore [38], was used to calculate the loudness of sounds in the following Chapters.

The model developed by Glasberg and Moore [38] uses as input the time waveform of a sound. This makes it suitable for calculating the loudness of pre-recorded sounds. The model combines the effect of the outer and middle ear in one single filter. The cochlea is characterised as being a bank of bandpass filters. Instead of fixing the bandwidth of each filter to $\frac{1}{3}$ octave, the bandwidth of each filter increases with increasing centre frequency, as the size of the loudness critical band increases with frequency [91]. It then calculates the instantaneous loudness, which is defined as the summation of specific loudness of each critical band over 1 ms [60], [38]. It proceeds to calculate the short-term and long-term loudness, where short-term and long-term loudness are defined as the instantaneous loudness averaged over a period of 20 ms and 100 ms respectively. This model can be used for both steady and time-varying sounds. They found that the maximum value of the short-term loudness is a good estimate of loudness of brief sounds.

3.4 Timbre

In a music score, the timbre (also called tone colour) of a particular note is specified by the instrument that will play it. It is clear that different instruments generate different timbre sensations, as we can readily recognise one instrument from another. But what is it about the sound that we recognise as different? Is it possible to measure it?

According to the ANSI standard of Acoustical Terminology [82], timbre is defined as:

> That attribute of auditory sensation which enables a listener to judge that two nonidentical sounds, similarly presented and having the same loudness and pitch, are dissimilar...

If a person is asked to compare the sounds taken from the steady state of a given note played by two different instruments (e.g. a trumpet and a flute)

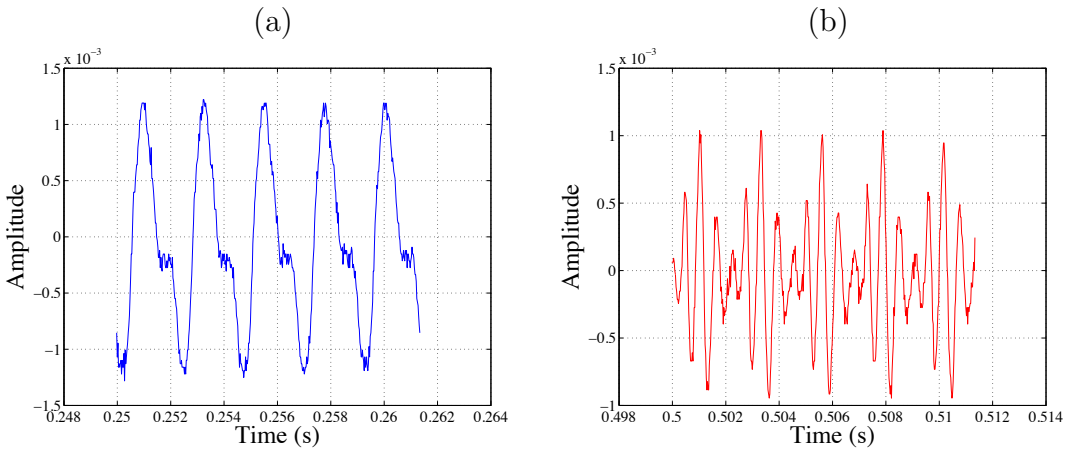

Figure 3.9: Steady state waveform for note A_4 played with (a) voice and (b) oboe

recorded under similar conditions and having the same loudness and pitch, he or she will probably recognise that the sounds are different, but will not necessarily be able to identify what instrument is playing. This is because the transient at the start of the standing wave generation (often called the attack of the note) has been found to be crucial in recognising the timbre of an instrument. Very often when the transients are removed, the instrument as such is no longer recognisable [43]. Also, the timbre of a particular instrument will change along its playing range. For most wind instruments, the timbre also depends on the loudness: the louder it gets, the richer in harmonics the spectrum will be.

If we measure the sound of two musical instruments, and plot their respective steady state waveforms, we will find that they differ significantly in their shape. Figure 3.9 shows the time waveforms of the note A_4 played with voice (vowel /a/) and with an oboe. It is clear that the waveforms for voice and oboe are different, and indeed different musical instruments in general will produce different waveforms. But the same musical instrument can also generate different waveforms, and still be recognised as being that particular instrument. The specific waveform of a particular musical instrument will depend on the relative amplitudes and phases of the harmonics that compose it.

3.4.1 Harmonic spectrum

The harmonic spectrum of a sound gives us information about the relative amplitudes and phases of the harmonics that form it. For a given amplitude spectrum,

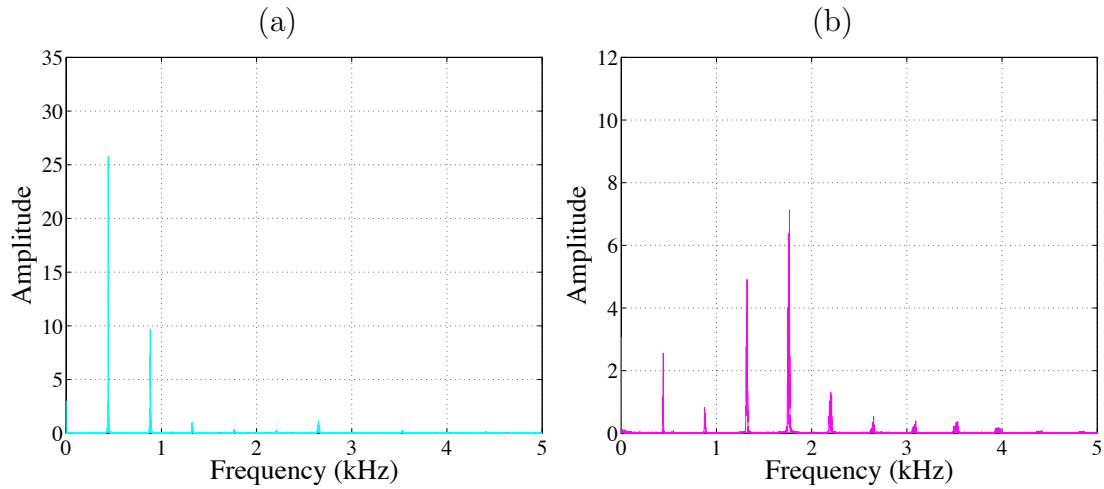

Figure 3.10: Amplitude spectrum for note A_4 played with (a) voice (vowel /a/) and (b) oboe

the particular shape of a waveform will depend upon the phase spectrum. If we were to replicate the waveforms shown in Figure 3.9, we would have to add each of the harmonic components with its own amplitude and phase, but to replicate the timbre we could ignore the phase information of the spectrum, as the ear is mostly insensitive to phase changes [20], [70]. This makes the amplitude spectrum of a sound a better representation of what we actually hear. Figure 3.10 shows the amplitude spectrum of the signals presented in Figure 3.9. Figure 3.10 (a) shows a prominent first harmonic, a second harmonic about half the amplitude of the first, and not much after that. Figure 3.10 (b), in contrast, shows that the most prominent harmonic is the 4^{th}.

If we make repeated measurements of these sounds, and plot their respective spectra, we will find that the general shape of the spectrum will remain, but the amplitudes of the harmonics will vary, without being regarded as having different timbre. These variations will depend on the relative position of the microphone with respect to the source, the characteristics of the room in question (as this will change the way the sound is reflected), the small variations that the musician adds to the note, and the particular radiation pattern of the instrument. For this reason, a better representation of the timbre of a sound is its average spectrum.

Experiments have been performed to assess the dependence of spectral shape or profile in the detection of timbre [28], [41]. They have concluded that humans recognise that a sound comes from certain source depending on its spectral profile.

fine	coarse
reserved	obtrusive
dark	bright
dull	sharp
soft	hard
smooth	rough
broad	narrow
wide	tight
clean	dirty
solid	hollow
compact	scattered
open	closed

Table 3.2: Some verbal scales used to describe the timbre of a particular sound (taken from [20])

3.4.2 Multidimensional representation of timbre

Both pitch and loudness are said to be one-dimensional, as both can be completely described in one scale: The loudness of a sound is said to vary from soft to loud, whereas the pitch varies from low to high. Humans have assigned a number of subjective descriptions or verbal scales in order to describe the timbre of different sounds. Some of them are listed in Table 3.2 [20].

von Bismarck [87] found that the dull–sharp scale is particularly important, as experiments showed consistent results amongst listeners. He also found that sharpness is an attribute that can be distinguished even if sounds differ in pitch and loudness.

In principle, timbre could be represented in an N-dimensional space, N being the number of harmonics of the sound. Experiments performed by Grey and Gordon [42] using Mutidimensional Scaling techniques have shown that three dimensions are sufficient to describe timbre. One of the dimensions that he found is correlated to the spectral energy distribution. On the low end of this dimension lie the sounds with narrow spectral bandwidth and a concentration of low frequency energy. On the high end of this dimension lie the sounds with wide spectral bandwidth and less concentration of low frequency energy.

3.4.3 The tristimulus diagram

An important attempt to correlate timbre into three measurable dimensions was made by Pollard [71]. He used as coordinates the loudness of the fundamental, the loudness of the mid-range harmonics (harmonics 2, 3 and 4), and the loudness of the higher harmonics of the sound (harmonics 5 and onwards), all loudnesses given as proportions of the total loudness measured in sones [20]. The three coordinates x, y and z are calculated as follows:

$$N = N_1 + N_2^4 + N_5^n \tag{3.17}$$

$$x = \frac{N_5^n}{N} \tag{3.18}$$

$$y = \frac{N_2^4}{N} \tag{3.19}$$

$$z = \frac{N_1}{N} \tag{3.20}$$

where N is the total loudness of the sound in sones, N_1 is the loudness of the fundamental, N_2^4 is the equivalent loudness of partials 2 to 4, and N_5^n is the equivalent loudness of partials 5 to n. As $x + y + z = 1$, it is sufficient to plot only two of these, as the third one can be inferred by subtracting the sum of the other two minus one.

A tristimulus diagram plots the loudness of the high-range harmonics vs the mid-range harmonics. A pure tone will only have a fundamental component, so it would lie on the origin, a sound with strong mid-frequency partials will lie near the (0,1) point, and a sound with strong high frequency partials will lie near the (1,0) point. An advantage of this representation is that transients of the sound can also be represented as curves in the tristimulus diagram.

3.4.4 Spectral centroid

The sharpness scale proposed by von Bismarck [87] has been related to the centroid of the loudness spectrum of the sound [71] and to the spectral energy distribution of the sound [42]. The spectral centroid has been found to be correlated to the perception of brightness of the sound.

The normalised spectral centroid of a sound is defined as [12] [53]:

$$NSC = \frac{\sum_{k=1}^{n} k \cdot A_k}{\sum_{k=1}^{n} A_k} \tag{3.21}$$

where n is the total number of harmonics of the sound, k is the harmonic number, and A_k is the amplitude of the kth harmonic.

A more recent study by Schubert et al. [76] showed that the perceived brightness of the sound is better correlated to the spectral centroid, rather than to the normalised version. They defined spectral centroid as:

$$SC = \frac{\sum_{k=1}^{n} F_k \cdot A_k}{\sum_{k=1}^{n} A_k} = F_1 \cdot NSC \tag{3.22}$$

where F_k is the frequency of the kth harmonic. The units of spectral centroid are Hz.

3.4.5 Just noticeable difference

Kendall and Carterette [53] found that synthesised sounds with 5 harmonics whose normalised spectral centroids differ by as little as 0.2 (unitless measure) are distinguishable. However, further experiments showed that signals with different spectral profile but identical normalised spectral centroids were also distinguishable, which indicates that the normalised spectral centroid does not describe timbre completely. Despite this, and because of the correlation between perceived brightness and spectral centroid (Hz), this was chosen as a representation of timbre of the sound for the remainder of this work.

3.4.6 Measuring spectral centroid

The spectral centroid was measured with the program SNDAN [12] (see Section 3.2.7). The spectral centroid variation over time (in Hz) is defined as:

$$SC(t) = f_a \cdot \frac{\sum_{k=1}^{n} k \cdot A_k(t)}{\sum_{k=1}^{n} A_k(t)} \tag{3.23}$$

where

$$n = \frac{f_s}{2 \cdot f_a} - 1 \tag{3.24}$$

is the maximum possible number of harmonics of a sampled signal with sampling frequency f_s. This is given by the Nyquist limit, where the maximum frequency of a sampled signal is $\frac{f_s}{2}$. It is worth noting that in order to take into account n harmonics the noise level in the higher harmonics must be low, otherwise the program will give an overestimate of the spectral centroid, taking the noise energy that lies in the place of the harmonics as being a true harmonic.

Chapter 4

Influence of the mouthpiece on the timbre of the trombone

4.1 Introduction

Manufacturers of mouthpieces have developed many designs of mouthpieces with slight differences claiming that these help to produce a better sound and control. Table 4.1 shows data extracted from the Denis Wick catalogue of trombone mouthpieces. It shows a wide range of mouthpieces with slight differences in their parameters, such as the cup diameter and the throat diameter (called "bore" in the catalogue). Each of these has a brief description of the timbre attributed to the instrument while being played with the stated mouthpiece. For example, the description given to the trombone mouthpiece 5BS is: "Gives medium bore trombone the qualities of large bore".

Previous work has been done on how small differences in a physical parameter of a musical instrument result in perceptible changes in timbre. Benade [17] investigated the influence of the mouthpiece on the impedance peaks of brass instruments, stating that the two most important parameters of mouthpieces that help the musician to set up a successful regime of oscillation are the mouthpiece cup volume and the throat diameter, both of which directly influence the "popping" frequency of the mouthpiece. This is the note obtained when the rim of the mouthpiece is slapped against the palm of the hand, causing the mouthpiece to sound a note at its Helmholtz resonance frequency [62].

Model	**Cup Diam.** (mm)	**Overall Diam.** (mm)	**Rim Width** (mm)	**Bore** (mm)	**Back Bore**	**Description**
4BS	25.90	39.44	6.77	7.13	Medium	For well developed embouchures that need a large cup on small bore trombones
5BS	25.73	39.00	6.64	6.87	Medium	Gives medium bore trombone the qualities of large bore
6BS	25.40	37.92	6.26	6.66	V-type	All-round best seller. Good in all registers
7CS	25.40	37.92	6.26	6.24	Medium	Super efficient. Fantastic high range
9BS	25.00	37.92	6.46	6.66	V-type	Perfect mouthpiece for beginners
12CS	24.5	37.92	6.71	6.10	V-type	Excellent jazz model, rounded rim contour

Table 4.1: Dimensions of various parameters of medium bore trombone mouthpieces taken from the Denis Wick catalogue

Coltman [25] noted how changes in the spectral parameters of a sound affect the timbre, and investigated how this correlation takes place. He resynthesised sounds from different notes of a flute, changed the amplitude of one harmonic at a time, and with these signals he made psychoacoustic tests to find the just noticeable difference (JND). He found that the changes had to be between 0.7 and 3 dB depending on which harmonic was changed, its amplitude relative to neighbouring harmonics, and whether the amplitude was increased or decreased. Finally, he analysed the differences in harmonic content of a flute played with two different headjoints, and with the results he had obtained concluded that the differences should be perceptible.

Wright and Campbell [90] studied the differences in the sound of trumpets and cornettos when played with different mouthpieces, and did psychoacoustic tests to confirm that these were perceptible. They found that even when the differences in the spectra of the sounds were very small, the listeners could still distinguish between different mouthpieces. Then with the aid of synthesised sounds, they tried to find which were the features of the sound to which the

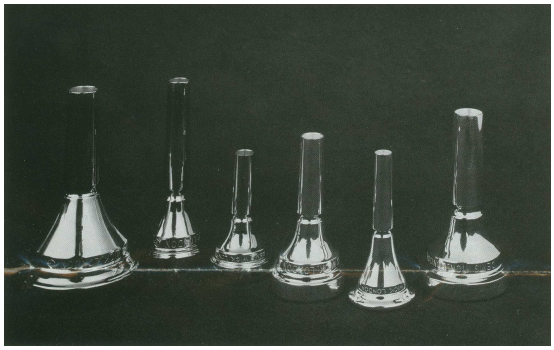

Figure 4.1: Picture of several brass mouthpieces taken from the Denis Wick catalogue

listeners were sensitive. They concluded that the amplitudes of partials relative to the noise floor are more important than the absolute amplitudes. Similarly, the high frequency components are used as a "reference level" by which to measure changes at lower frequencies.

Plitnik and Lawson [68] made an experiment with french horn mouthpieces, in which they aimed to correlate the psychoacoustic parameters "playability" and "tonal responsiveness" to the acoustical parameters impedance peak amplitude, Q_n and spectral envelope. They described "playability" as the combination of:

- the range from the softest to the loudest tones possible
- the smoothness and consistency sensed by the player
- the ease with which the performer can slip from resonance peak to resonance peak

and "tonal responsiveness" as the combination of:

- the quality of the tone produced
- the smoothness and rapidity of the initial attack
- how well the pitch "locks in"

They gave a professional french horn player a number of mouthpieces on a blind test. He was asked to rate them on a like–dislike scale according to those psychoacoustic parameters. They analysed the results from the blind test to correlate

these to the acoustical variables mentioned. They concluded that these psychoacoustic parameters are well correlated to the mean of the magnitude of the impedance peaks (Z_{max}) and its standard deviation.

This Chapter focuses on the determination of the threshold of perception of similar musical sounds: specifically, sounds of a trombone played with different mouthpieces. The small differences in the parameters of, in this case, the mouthpiece, will in turn produce different spectra. Thus, the perceptual effect of small changes in the harmonic content of a signal is evaluated, by studying the spectral differences of the sounds of a trombone played with two different mouthpieces.

Preliminary results of a psychoacoustic test in which listeners compared real and synthesised sounds from a trombone using two different mouthpieces show that both the harmonic content and the high frequency aperiodic components of the signal are crucial for distinguishing two sounds as different. The analysis and synthesis of the sounds are done in a way which allows each of these attributes to be modified separately. Finally, tests are carried out on sounds recorded using two mouthpieces differing only in throat diameter, to evaluate the perceptual significance of this parameter.

Section 4.2 describes in detail how the signals from the trombone sounds were produced and recorded. Section 4.3 describes in detail the differences found in the spectra of the sounds from the trombone playing the two mouthpieces. Section 4.4 examines three methods of synthesis that were attempted, including the results of the psychoacoustic tests made to find out whether the synthesised sound was indistinguishable from the original. It also highlights the different attributes of the sound that appear to give the listener important cues to distinguish between similar sounds. Section 4.5 describes a psychoacoustic test that presents to the listener these synthesised sounds with small changes in the partial amplitudes in order to find out a threshold of distinguishability between similar trombone sounds. Section 4.6 presents a psychoacoustic test, where the pairs of sounds described in Section 4.5 were presented to the subject in randomised order, so as to be able to determine the just noticeable difference. Section 4.7 presents an experiment in which two identical mouthpieces were taken, one of which had its throat diameter increased by 4%. The signals were analysed and using the results from Section 4.5 and 4.6 we were able to predict whether the listener would be able to distinguish between these sounds or not. A psychoacoustic test was also

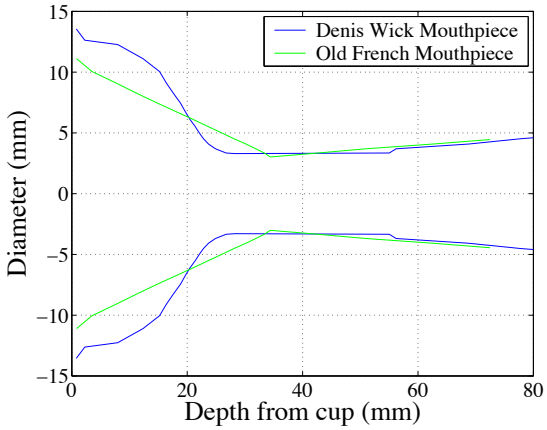

Figure 4.2: Bore profile of the mouthpieces used for the experiments

performed, proving the prediction previously made.

4.2 Recordings of trombone sounds using two different mouthpieces

A semi-professional trombone player was asked to play a tenor trombone model King 2B with two different mouthpieces: a standard Denis Wick model 6BS and a nineteenth century French mouthpiece from the Edinburgh University Collection of Historic Musical Instruments, catalogue number 3726. The bore profile of both mouthpieces is shown in Figure 4.2. A preliminary psychoacoustic test showed that the sounds produced by this trombone using the two mouthpieces were easily distinguishable.

A DAWE sound level meter model D-1422 was placed about one metre away from the bell of the instrument, where the player could clearly see the value measured. It measured around 80 dB SPL when the player was playing at what he considered a piano dynamic level. Hence, he was asked to play in such a way that the sound level meter would measure 80 dB SPL, and to play the notes steadily and without vibrato.

To minimise reflections that could change the shape of the spectrum, the recordings were made in an anechoic chamber, using an Audio-Technica omni-directional condenser microphone model ATM10a placed at a distance of 1 bell

	Denis Wick	**Old French**
$B_2^\flat$	82.18	83.14
$B_3^\flat$	81.69	82.04

Table 4.2: Calculated loudness levels in phons of signals with equal RMS values

diameter as described in [20] and [17], as this would produce a spectrum like that of having averaged several spectra taken at different places in a reverberant room.

The microphone was connected to a TASCAM mixer model M–08 and the level of the signals was adjusted to be as high as possible without saturating. This adjustment was done once at the beginning of the measurements. The output of the mixer was then connected to a TASCAM DAT recorder model DA-20mkII, which recorded at a sampling frequency of $f_s = 44.1$ kHz.

The player played a few arpeggios and some steady notes. From these recordings, two notes from each of the mouthpieces were selected: $B_2^\flat$ and $B_3^\flat$ (concert pitch). These notes had been played steadily for about 4 seconds. This allowed a few windows to be taken from each signal, to get an average of the spectra of the two notes.

4.3 Analysis of recorded signals, and comparison of spectra of signals from the two mouthpieces

A window of duration of 0.5 s which was stable in pitch and amplitude was taken from each mouthpiece and the selected notes. The RMS value of these signals was equalised. The loudness of these signals was calculated using a MATLAB program written by Marek Dziubinski from the Technical University of Gdansk, Poland, based on a method developed by Glasberg and Moore [38] (see section 3.3.7). Table 4.2 shows the maximum value of the short-term loudness of the signals. The difference in loudness between the signals of the two mouthpieces was less than 1 phon.

The signals were windowed (Hanning) and zero-padded so as to have 44100 samples. Fast Fourier Transforms (FFT) were taken from these, hence the frequency resolution was 1 Hz. Figures 4.3 and 4.4 show the spectra of these signals.

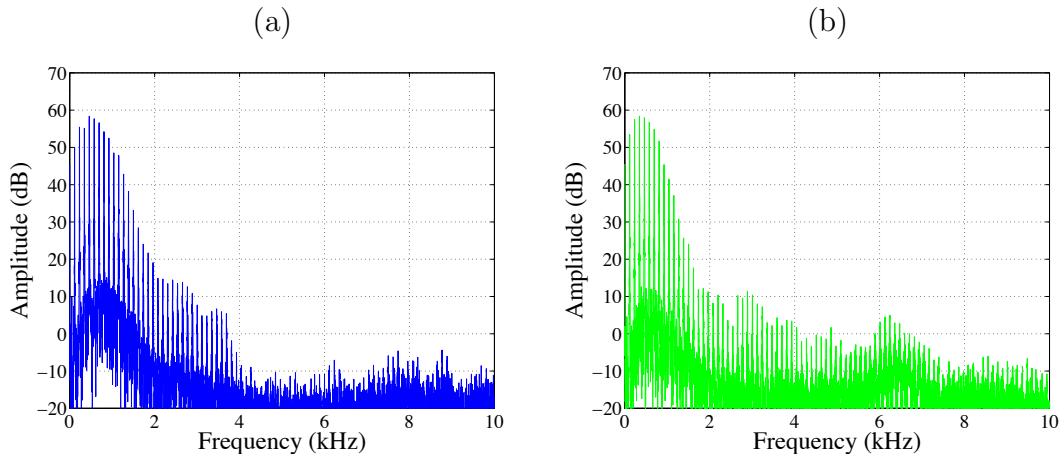

Figure 4.3: Spectra of signals from (a) Denis Wick and (b) Old French mouthpieces for $B_2^\flat$

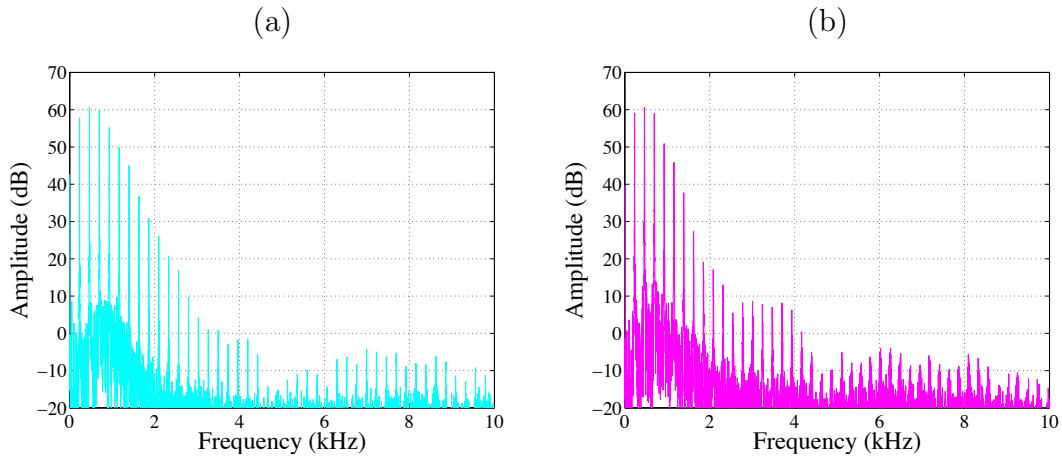

Figure 4.4: Spectra of signals from (a) Denis Wick and (b) Old French mouthpieces for $B_3^\flat$

Figure 4.5 shows a comparison of the spectral envelopes. Figure 4.6 shows the difference in amplitude (dB) of each harmonic between Denis Wick and Old French mouthpieces. In this figure, the height of the bars represents the extent to which the Denis Wick mouthpiece harmonic amplitude in dB exceeded that of the Old French mouthpiece. Negative values imply that the Old French mouthpiece harmonic was higher than that of the Denis Wick mouthpiece.

The main differences found in the signals of these two mouthpieces are:

1. Amplitudes of partials differ, as shown in Figure 4.5. As can be seen in Figure 4.6 these differences vary from 0 to 13 dB.

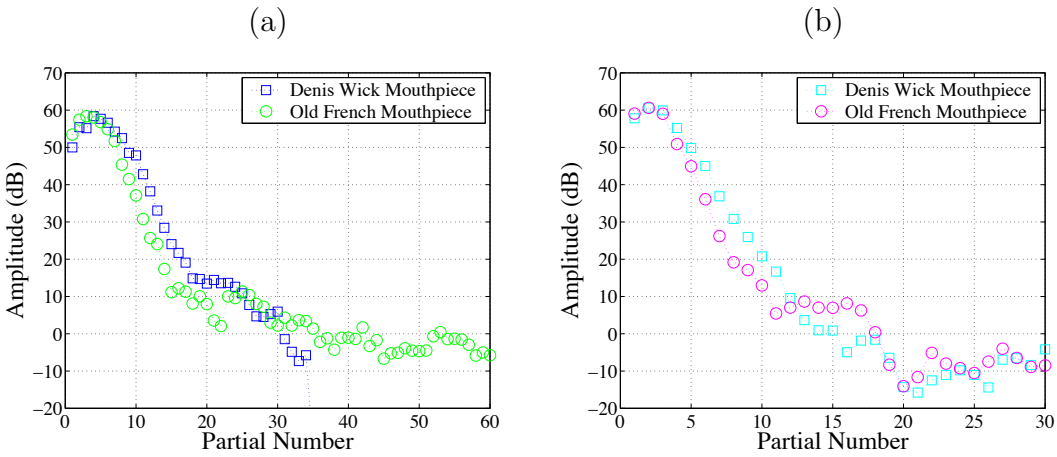

Figure 4.5: Spectral envelopes of signals from Denis Wick and Old French mouthpieces for (a) $B_2^\flat$ and (b) $B_3^\flat$

2. When playing the note $B_2^\flat$ with the Denis Wick mouthpiece, partials above 4 kHz (partial number 34) are covered by noise, whereas in the Old French mouthpiece components are still higher than the noise floor up to 10 kHz (partial number 60).

3. Slow temporal variations differ, such as the vibrato effects and the amplitude envelopes of individual partials. Figure 4.7 shows the normalised composite weighted-average frequency over time (see Section 3.2.7)

   Figures 4.8 and 4.9 show the amplitude variation over time of each harmonic for both mouthpieces. The data for Figures 4.7, 4.8 and 4.9 were calculated using the program SNDAN [12]. Even when a musically trained subject is asked to play steadily and without vibrato, this is not an easy task, mainly because musicians have been trained to produce beautiful sounds that have at least certain degree of vibrato.

4. Frequencies of partials differ slightly. Figure 4.7 shows that the note $B_2^\flat$ in the two mouthpieces as well as note $B_3^\flat$ in the Old French mouthpiece were played 10 to 15 cents flat, whereas the note $B_3^\flat$ on the Denis Wick mouthpiece was played well in tune, according to the frequencies that correspond to an equally tempered scale.

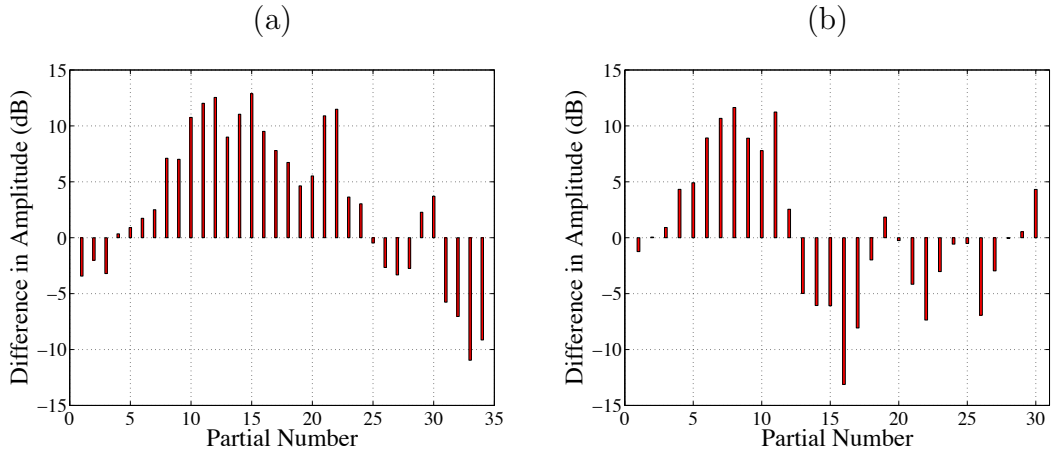

Figure 4.6: Spectral differences in harmonic content between Denis Wick and Old French mouthpieces for (a) $B_2^\flat$ and (b) $B_3^\flat$

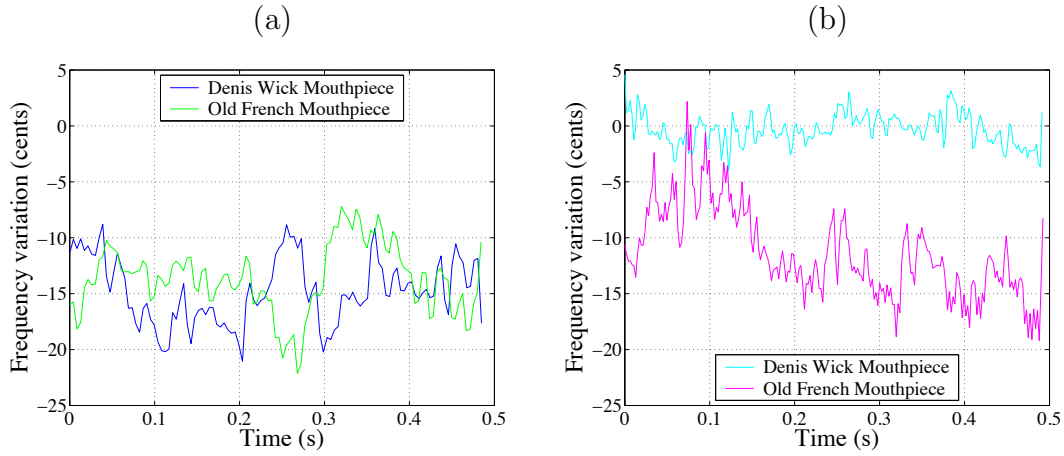

Figure 4.7: Frequency variations of Denis Wick and Old French mouthpieces for note (a) $B_2^\flat$ and (b) $B_3^\flat$. 0 cents represents the frequency of these notes on an equally tempered scale

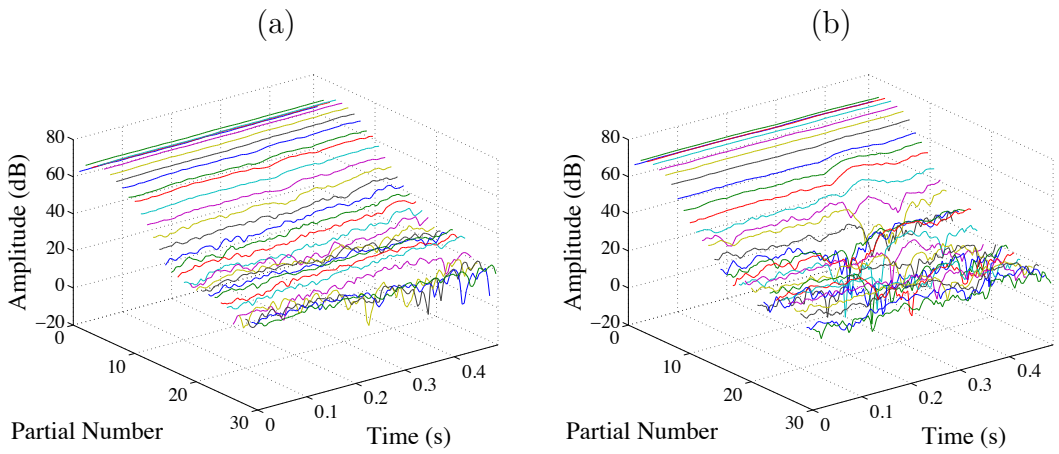

Figure 4.8: Amplitude envelopes of (a) Denis Wick and (b) Old French mouthpieces for note $B_2^\flat$

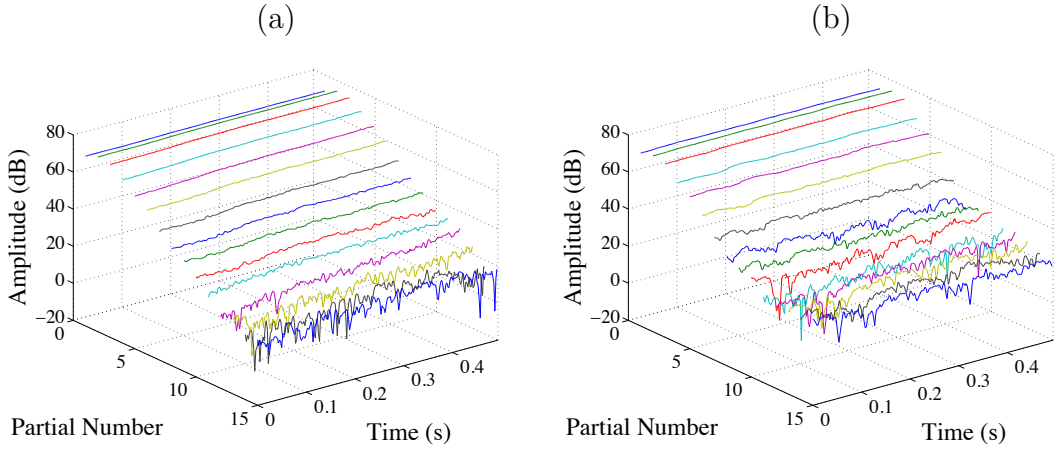

Figure 4.9: Amplitude envelopes of (a) Denis Wick and (b) Old French mouthpieces for note $B_3^\flat$

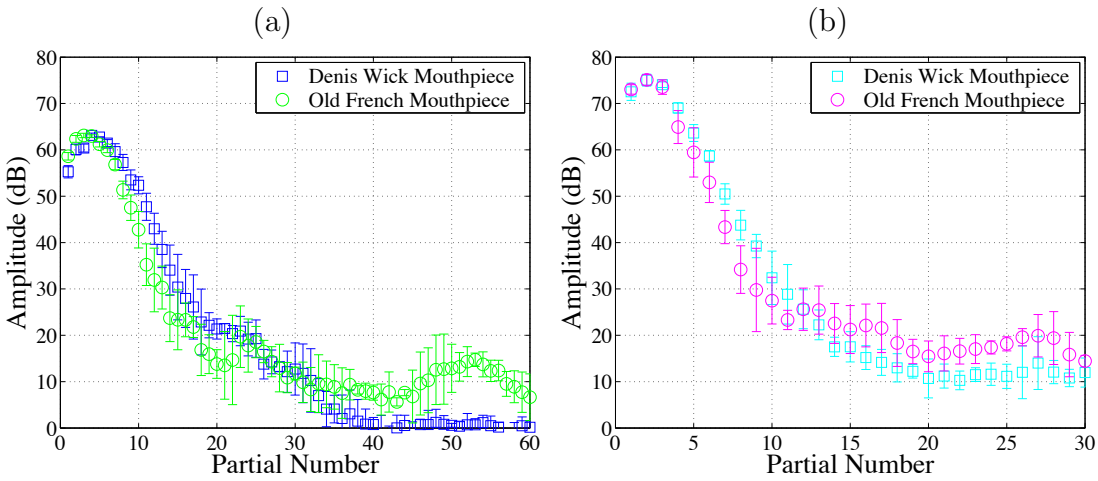

Figure 4.10: Mean and standard deviation of harmonic components for three windows taken from notes (a) $B_2^\flat$ and (b) $B_3^\flat$

To make sure that the window selected for each mouthpiece was typical for that mouthpiece, and that the differences shown so far between these signals were not due to slight variations in the way the instrument was played, two more windows for each note were taken. The mean and standard deviation of the amplitude of each harmonic component for the three windows of each mouthpiece are shown in Figure 4.10. This figure shows that the variations due to normal playing are smaller than those introduced by the different mouthpieces.

4.4 Description of analysis/synthesis methods and of psychoacoustic tests

As the perceptual effect of small differences in the harmonic content of a signal was to be evaluated, it was necessary to have a set of signals that were as close as possible in timbre to the recorded trombone signals, and to be able to modify all the perceptually important parameters of the spectrum independently in a controlled way.

When synthesising the recorded signals, the initial objective was to obtain signals that were indistinguishable from the original trombone sounds. Once this was achieved, the components of the synthesised signals were changed in a controlled way. Sounds from these signals were then presented to subjects in psychoacoustic tests to find what was the amount of change that was necessary

in a signal for the listeners to hear a difference.

Three methods of synthesis were developed, each of which is described in this Section. There were 14 subjects in total who volunteered to do at least one of the following psychoacoustic tests. All of them but two play or have played at least one instrument and are considered to be musically experienced. One of the subjects has a music degree, and another one conducts an orchestra of semiprofessional players. All the sounds of the following tests were played through a pair of Sennheiser headphones model HD455 preset at a comfortable volume level.

The subjects were presented with pairs of sounds which were:

- Original – Original
- Original – Synthesised
- Synthesised – Original
- Synthesised – Synthesised

There was one separate test for each note. In each test, 20 pairs of sounds were presented to the subjects in randomised order. The instructions given to the subjects were:

> In this test, you will be presented with 20 pairs of sounds produced by both real recordings and resynthesised versions of trombone sounds. For each pair, please indicate whether the sounds on each pair are THE SAME or DIFFERENT.

Each answer was recorded as 1 if it was correct, and as 0 if it was incorrect. Distinguishability was defined as the average of the recorded results, giving the fraction of correct answers that each subject had.

If the pairs Original – Synthesised and Synthesised – Original were very different, then the upper bound of 1 would be easily reached, as it would be very easy for people to state when the two sounds were the same and when different. In this case, all the answers to all the pairs would be correct.

It is important to note that the lower bound of distinguishability would be 0.5, and not 0. The lower bound would be reached whenever the Original – Synthesised and Synthesised – Original pairs were so similar that listeners could

	Distinguishability	**StdDev**
$B_2^\flat$	0.96	0.07
$B_3^\flat$	0.87	0.14

Table 4.3: Distinguishability of first synthesis method: The distinguishability is well above the 0.5 limit, meaning that the resynthesised sounds were easily distinguishable from the originals

no longer recognise them as being different. In this case, the listener would answer "THE SAME" in all four pairs. As all tests had nine or ten "THE SAME" pairs and ten or eleven "DIFFERENT", then the lowest bound for distinguishability would be between 0.50 and 0.55. In the following tests, the aim was to get as close as possible to this lower bound, as the resynthesised versions of the sounds were meant to be indistinguishable from the originals.

4.4.1 First synthesis method and results of psychoacoustic test

From the FFT of the signal described in Section 4.3, each partial was isolated, and for each of those the values of frequency, amplitude, and phase were taken. The synthesised signal was generated by adding pure sine waves with the values taken. The bandwidth for the synthesised version of the note $B_2^\flat$ was 1.7 kHz (first 15 partials were taken), whereas for the note $B_3^\flat$ it was 2.3 kHz (first 10 partials were taken).

This test was done with 5 subjects. Table 4.3 shows the results of this test: the distinguishability was well above 0.5, meaning that subjects could easily identify the sounds that were the same and the sounds that were different.

It is worth noting that the note $B_3^\flat$ had a slightly lower distinguishability. As the bandwidth of the synthesised $B_3^\flat$ was higher than that of the note $B_2^\flat$, it was thought possible that the increased bandwidth was the reason why it was more difficult to identify the original signal from the synthesised: the higher the bandwidth the lower the distinguishability. This would follow from the fact that if the synthesised signal had a higher bandwidth, it would also have more information about the original signal, hence making it more difficult to distinguish.

	Distinguishability	**StdDev**
$B_2^\flat$	0.93	0.09
$B_3^\flat$	0.90	0.17

Table 4.4: Distinguishability of second synthesis method: The distinguishability is still well above the 0.5 limit

4.4.2 Second synthesis method and results of psychoacoustic test

To eliminate a possible bias due to the difference in bandwidth of the synthesised signals, this method included components up to 4 kHz in both notes, which correspond to taking the first 34/17 partials of the note $B_2^\flat$/$B_3^\flat$ respectively.

This test was done with 4 subjects. As can be seen in Table 4.4 the distinguishability was still well above 0.5. Even though the bandwidth of the two notes was higher than in the previous test, the distinguishability did not drop significantly towards the 0.5 limit.

As these two signals are still easily distinguishable from the originals, there must still be significant components in the original signals that are missing in the synthesised version. Two possible reasons for this are considered.

1. The synthesised signals do not include any information above 4 kHz. Even in the Denis Wick $B_2^\flat$ case, where the partials of this signal are too small to be isolated, there are noise components that might aid the recognition process

2. The synthesised signals are generated with pure sine waves, which means that all the amplitudes and frequencies of all the partials remain constant for the duration of the sound. However, as was previously shown, these parameters are not constant in the original signals (see Figures 4.7, 4.8 and 4.9). This might also provide cues to the listener

At this point, it has been noted that the two attributes of the signal that are still missing from the synthesised sounds are the high frequency components such as noise, and the slow temporal variations of both frequency and amplitude that the original signals had. This might be the reason why the two synthesis methods described previously had distinguishabilities well above the 0.5 limit.

4.4.3 Third synthesis method and results of psychoacoustic test

The synthesised signals must have all the attributes that allow people to discriminate between one signal and the other. The following procedure allowed the synthesised signals to include high frequency components such as noise, and the slow temporal variations of both frequency and amplitude that the original signals had. The procedure to do this was:

1. The partials of the original signals were located
2. Each of these partials was filtered using a MATLAB band-pass FIR 4000^{th}-order filter (window method), with a bandwidth of 2 Hz. This bandwidth would allow a variation of ± 15 cents in the $B_2^\flat$ note and of ± 7 cents in the $B_3^\flat$ note
3. All the information above the highest partial was filtered using a MATLAB high-pass FIR 4000^{th}-order filter (window method)
4. The synthesised signal was generated by adding the output of filters (2) and (3)

A schematic of this synthesis method is shown in Figure 4.11. The frequency response of one of the band-pass filters and the high-pass filter used in the signal recorded from the Denis Wick mouthpiece playing the note $B_2^\flat$ are shown in Figure 4.12.

The filters used had a transient of around 90 ms, corresponding to 4000 samples approximately. The selected windows from the original signals were extended to 26050 samples, so that the first 4000 samples of the filter transient were discarded. The samples that were kept (4001 to 26050) corresponded to the steady state of the filter. The 0.5 s duration of the sounds was maintained.

As was mentioned in the previous Section, the two parameters that were still missing in the synthesised signal were the high frequency aperiodic components and the slow temporal variations of the original signal. For this test, they were added to investigate its significance:

- The high frequency aperiodic components were included as the output signal of the high-pass filter

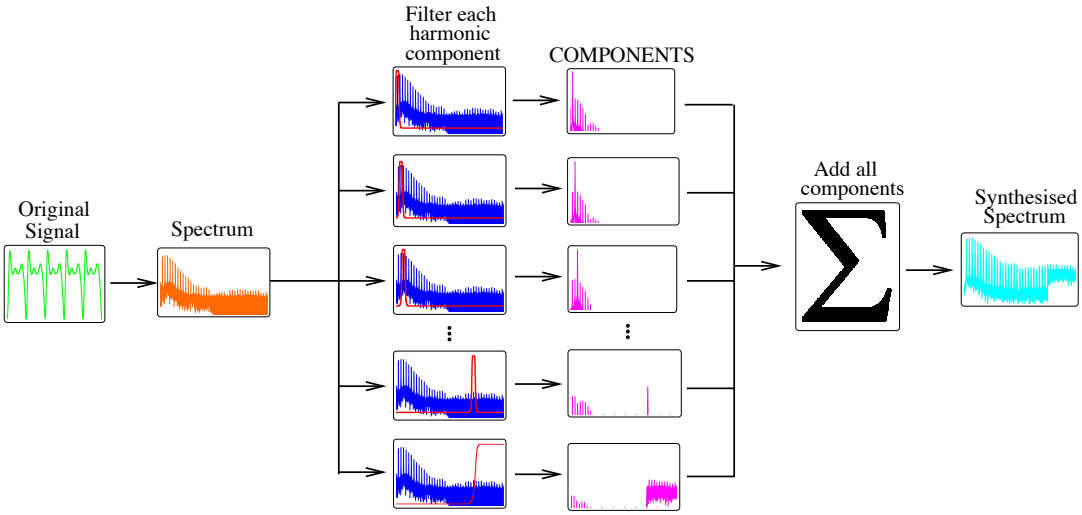

Figure 4.11: Schematic showing the Third synthesis method

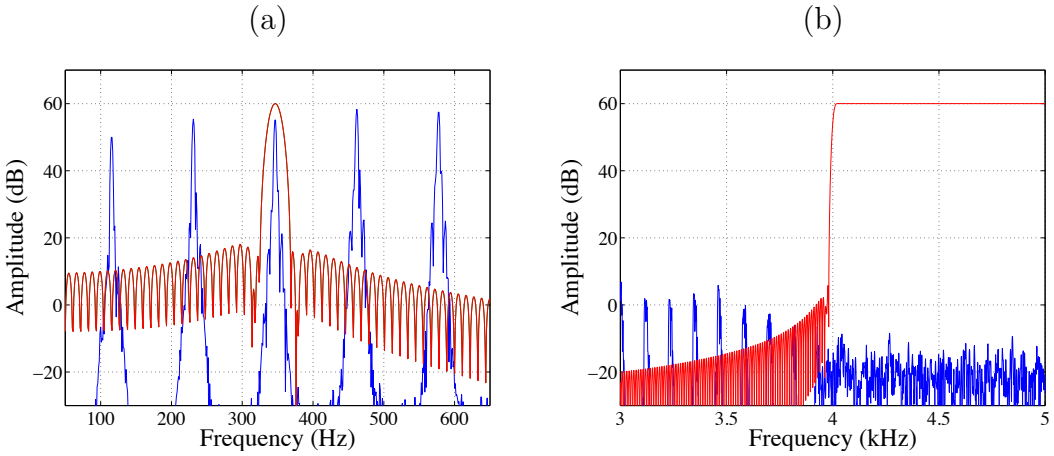

Figure 4.12: Frequency response of (a) third band-pass and (b) high-pass filter used in the analysis of the signal from the Denis Wick mouthpiece playing the note $B_2^\flat$. The blue plot shows the spectrum of the signal, and the red plot shows the corresponding filter

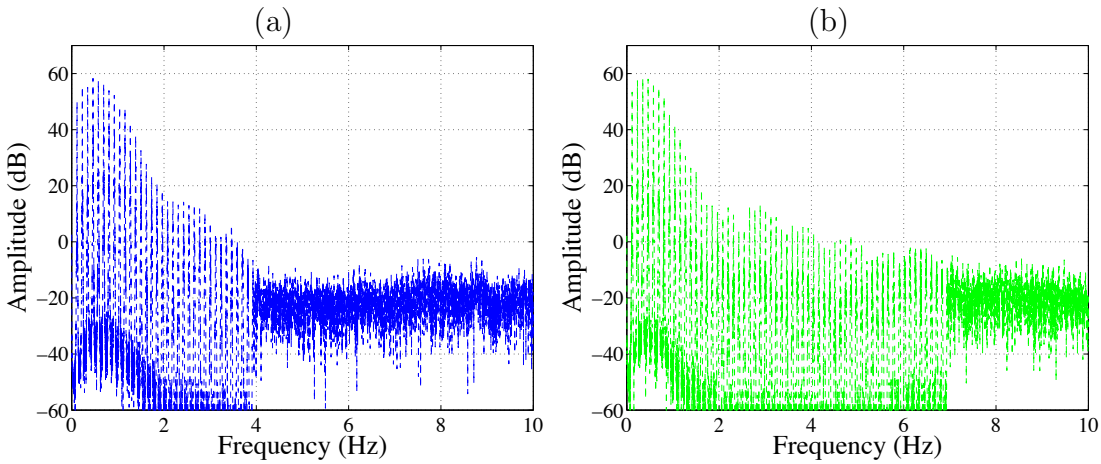

Figure 4.13: Spectra of synthesised signals from (a) Denis Wick mouthpiece and (b) Old French mouthpiece for $B_2^\flat$. Notice that the noise level in between partials is lower than that of the original signals

- The slow temporal variations of the original signals were copied to the synthesised signals, because the partials of the original signals were filtered and then added unaltered to the synthesised signal

The spectra of the synthesised signals are shown in Figures 4.13 and 4.14. These figures show that the main difference between original and synthesised signals was that the spectra of the synthesised signals had a lower noise level in between partials. The band-pass filters used to filter out the partials were such that the noise level in between partials was reduced by around 40 dB.

It is worth noting that the synthesised signal generated from the note $B_2^\flat$ of the Denis Wick mouthpiece had partials only up to 4 kHz, because of the characteristics of the original signal noted in the last section, whereas the other signals (Denis Wick $B_3^\flat$, Old French $B_2^\flat$ and Old French $B_3^\flat$) were synthesised with partials up to 7 kHz (60 partials for $B_2^\flat$ and 30 for $B_3^\flat$). The components higher than this were included by adding the output of the high-pass filter.

The frequency variations of the synthesised signals are shown in Figure 4.15, and the amplitude envelopes are shown in Figures 4.16 and 4.17. Comparison of these figures with Figures 4.7, 4.8 and 4.9 show that at least some of the slow temporal variations were kept in the synthesised version.

The calculated loudness of the synthesised signals is shown in Table 4.5. All four synthesised signals had a loudness comparable to those of the original signals,

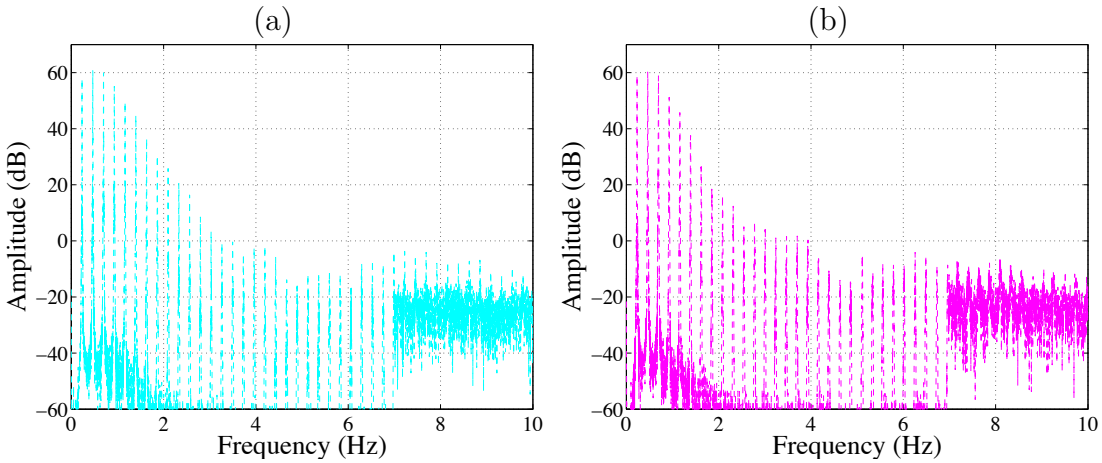

Figure 4.14: Spectra of synthesised signals from (a) Denis Wick mouthpiece and (b) Old French mouthpiece for $B_3^\flat$. Notice that the noise level in between partials is lower than that of the original signals

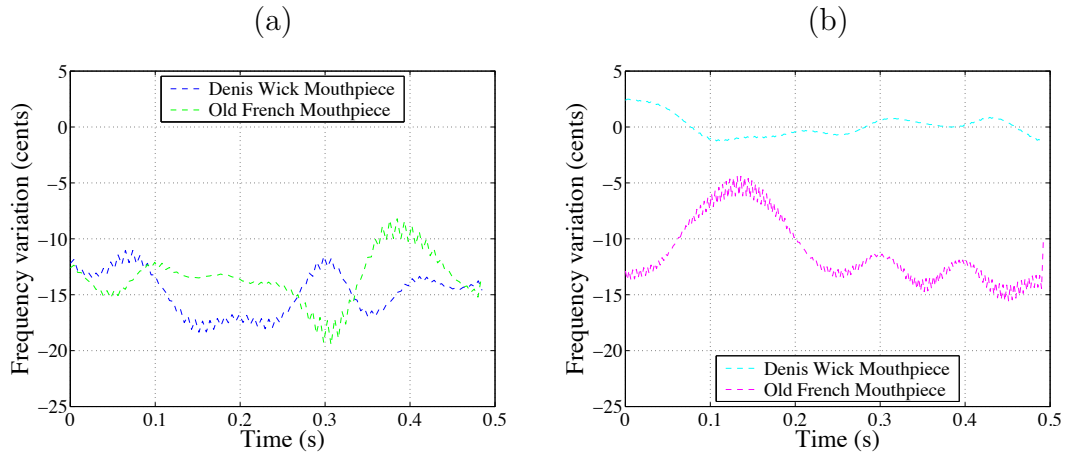

Figure 4.15: Frequency variations of synthesised versions from Denis Wick and Old French mouthpieces for note (a) $B_2^\flat$ and (b) $B_3^\flat$. 0 cents represents the frequency of these notes on an equally tempered scale

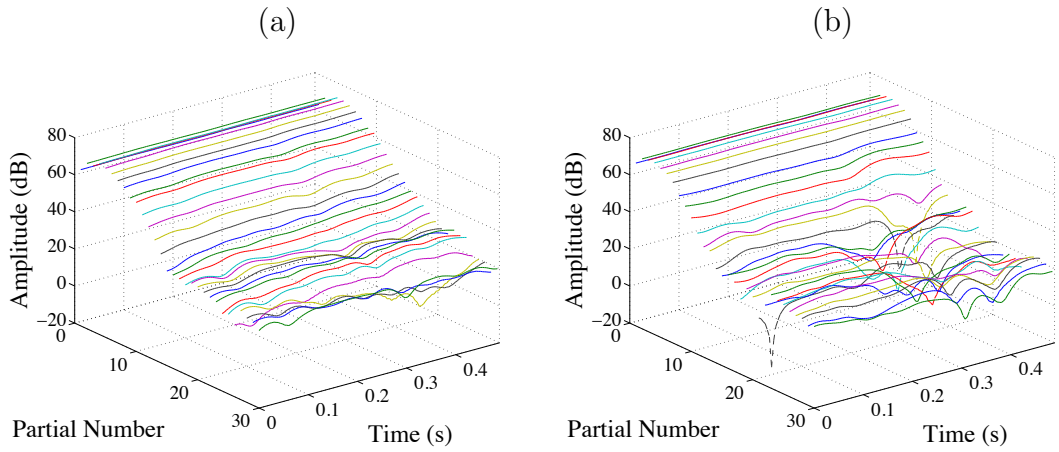

Figure 4.16: Amplitude envelopes of synthesised versions of (a) Denis Wick and (b) Old French mouthpieces for note $B_2^\flat$

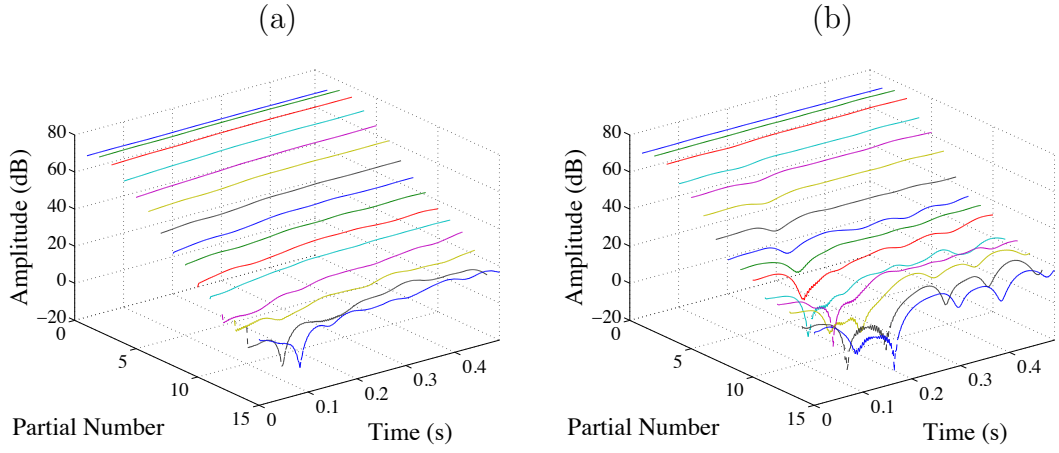

Figure 4.17: Amplitude envelopes of synthesised versions of (a) Denis Wick and (b) Old French mouthpieces for note $B_3^\flat$

	Denis Wick	**Old French**
$B_2^\flat$	82.07	83.00
$B_3^\flat$	81.75	81.85

Table 4.5: Calculated loudness levels in phons of synthesised signals

	Distinguishability	**StdDev**
$B_2^\flat$	0.57	0.14
$B_3^\flat$	0.59	0.04

Table 4.6: Distinguishability of third synthesis method. With this synthesis method, the distinguishability dropped significantly to be very close to the 0.5 limit

differing at the most by 0.2 phons.

This test was done with 5 subjects. As can be seen in Table 4.6, the distinguishability between the original and the synthesised signals using this method dropped significantly compared with the other two methods, being quite close to the 0.5 limit. This is why this method was used for the remainder of this Chapter.

The fact that the distinguishability was at this point very close to the 0.5 limit is a strong indication that the synthesised signals had most of the psychoacoustic attributes of the original signal that allow a subject to discriminate between the two signals. These attributes are:

- The amplitudes and frequencies of the harmonics
- Most of the slow temporal variations in amplitude and frequency of each harmonic
- The high frequency aperiodic components

All of these together were necessary to make the synthesised signal indistinguishable from the original. It is worth noting at this point that even though the slow temporal variations of the synthesised signals were not identical to those of the original signals, the information that was kept in the synthesised signals was enough to make them almost indistinguishable from the originals.

4.5 Psychoacoustic test to determine the threshold of distinguishability between similar trombone sounds

At this point, the differences in spectra between the two mouthpieces were known, and the analysis described in Section 4.3 separated each of the components of the signals. The amplitudes of the partials of one mouthpiece can be gradually changed so as to have the same amplitudes as those of the other mouthpiece.

The idea of modifying the partials of one mouthpiece until they have the same amplitudes as the other mouthpiece allows us to keep the high frequency components and slow temporal variations unaltered. In this way, it is possible to study the perceptual significance of the amplitudes of partials.

4.5.1 Description of psychoacoustic tests

The psychoacoustic tests performed in this Section consisted of presenting subjects with pairs of sounds, the first of which was always kept unaltered, and will be referred to as the "reference sound". The second sound was gradually modified in some way, and will be referred to as the "test sound". Every pair presented played the reference sound first, and then the test sound. Whenever a new pair was played, the test sound would be changed slightly more than before. This was done repeatedly until the end of each test.

Figure 4.6 shows the difference in partial amplitudes between the Denis Wick and the Old French mouthpieces playing the notes $B_2^\flat$ and $B_3^\flat$. Each partial difference was divided into 30 equal steps, each of which was $\frac{1}{30}$ of the total difference shown in that Figure. The test sound had all its partials modified by one step at a time. The subject was presented then with at the most 30 pairs of sounds, consisting of the reference sound and 30 different test sounds, corresponding to different degrees of similarity or difference between the two mouthpiece spectra. The subject was allowed to hear any pair as many times as desired before answering.

There are two tests that were done:

1. Starting with two equal sounds, the reference sound was changed gradually until they were perceived different. The instructions to the subjects were:

> In this test you'll hear pairs of sounds, and you'll be asked to state whether they are THE SAME or DIFFERENT. The first pair that you'll hear will be the "REFERENCE" pair, and ONLY this pair WILL BE THE SAME. Then the second sound will be gradually changed until your answer is DIFFERENT. If you hear a click, or can't make up your mind, you can always hear the previous pair as many times as you like before answering.

If the subject answered THE SAME, then the next pair was presented. If the subject answered DIFFERENT, the test stopped and the degree of change made to the test sound up to that point was recorded.

2. Starting with two different sounds, the reference sound was changed gradually until they were perceived the same. The instructions to the subject were:

> In this test you'll hear pairs of sounds, and you'll be asked to state whether they are THE SAME or DIFFERENT. All the pairs you'll hear in this test will be different, including the first one, but the second sound of each pair will be gradually changed so as to be more similar to the first sound, until your answer is THE SAME. The first pair that you'll hear will be the "REFERENCE" pair. If you hear a click, or can't make up your mind, you can always hear the previous pair as many times as you like before answering.

If the subject answered DIFFERENT, then the next pair was presented. If the subject answered THE SAME, the test stopped and the degree of change made to the test sound up to that point was recorded.

As there are two mouthpieces, there are two possibilities for each test. Tables 4.7 and 4.8 show these two possibilities for both Test 1 and Test 2. The "Start" column shows what the reference and the test sounds were in the first pair, and the "End" column shows what the test sound would be in the last pair, if the test were allowed to continue until all 30 pairs were presented. For example, Table 4.7 α shows that the reference sound and the test sound started at Denis Wick, and the test sound finished at Old French. This means that the test sound was gradually changed from its initial spectrum corresponding to the Denis Wick mouthpiece towards the spectrum of the Old French mouthpiece (from equal to different). Correspondingly, in Table 4.8 γ the reference sound started at Denis Wick, whereas the test sound started as Old French. This means that the test

	Start		**End**
	Reference sound	*Test sound*	*Test sound*
α	Denis Wick	Denis Wick	Old French
β	Old French	Old French	Denis Wick

Table 4.7: Two cases for Test 1. The "Start" column indicates the state at which the reference sound and the test sound started, and the "End" column indicates what the test sound would be at the end of the test, if continued to play all 30 pairs. Notice that both sounds start the same, and the test sound gradually becomes more different than the reference sound. This test stops when the subject answers "DIFFERENT"

	Start		**End**
	Reference sound	*Test sound*	*Test sound*
γ	Denis Wick	Old French	Denis Wick
δ	Old French	Denis Wick	Old French

Table 4.8: Two cases for Test 2. The "Start" column indicates the state at which the reference sound and the test sound started, and the "End" column indicates what the test sound would be at the end of the test, if continued to play all 30 pairs. Notice that the test sound starts being different from the reference sound, and the former is then gradually changed to become more and more similar to the latter. This test stops when the subject answers "THE SAME"

sound was gradually changed from its initial spectrum corresponding to the Old French mouthpiece spectrum towards the spectrum of the Denis Wick mouthpiece (from different to equal).

Each of these tests was done separately with the notes $B_2^\flat$ and $B_3^\flat$.

4.5.2 Results of Tests 1 and 2 with their two cases

Tables 4.9 and 4.10 show the results of Tests 1 and 2 with their respective two cases for both notes $B_2^\flat$ and $B_3^\flat$. These results represent the degree of difference that the test signal had with respect to the reference signal at the time when the subjects stopped the test. 0 would mean that the two signals were the same (the amplitudes of the partials of the test sound matched those of the reference sound), and 1 would mean that that the signals had the biggest difference (the partials of the test sound had the amplitudes of the other mouthpiece).

Figures 4.18 and 4.19 show graphically the results presented in Table 4.9. The red bars represent, for the purpose of reference, the difference in spectra

(a)

	Difference	**StdDev**
α	0.30	0.12
β	0.32	0.23

(b)

	Difference	**StdDev**
α	0.26	0.09
β	0.35	0.21

Table 4.9: Results of Test 1 for notes (a) $B_2^\flat$ and (b) $B_3^\flat$. These results represent the degree of difference that the test signal had with respect to the reference signal at the time when the subjects stopped the test. 1 corresponds to the biggest difference

(a)

	Difference	**StdDev**
γ	0.64	0.23
δ	0.57	0.25

(b)

	Difference	**StdDev**
γ	0.70	0.23
δ	0.59	0.25

Table 4.10: Results of Test 2 for notes (a) $B_2^\flat$ and (b) $B_3^\flat$ These results represent the degree of difference that the test signal had with respect to the reference signal at the time when the subjects stopped the test. 1 corresponds to the biggest difference

between the two mouthpieces, which would correspond to the biggest difference. The yellow bars show the differences in spectra between the signals in the pair in which subjects stated they perceived a difference. In this yellow plot all partials had a difference below 4 dB. Because in the starting pair the reference and the test sounds were the same, this result means that the difference in partials between the two sounds had to be increased to at least 4 dB for subjects to perceive them different.

Figures 4.20 and 4.21 show graphically the results presented in Table 4.10. The red bars represent the difference in spectra of the starting pair, which has the biggest difference. The white bars show the differences in spectra between the signals in the pair in which subjects stated that the signals were the same. In this white plot all the partials have a difference of below 8 dB. Because the starting pair was the pair with the highest difference, this result means that this difference had to be reduced to less than 8 dB for subjects to perceive them the same.

The results presented previously suggest that the threshold of hearing two sounds as being the same or different is between 4 and 8 dB of difference in partials. That is, two sounds can still be judged as being the same as long as the difference in partials does not exceed 4 dB, and two sounds will be perceived as different until the difference in partials is less than 8 dB.

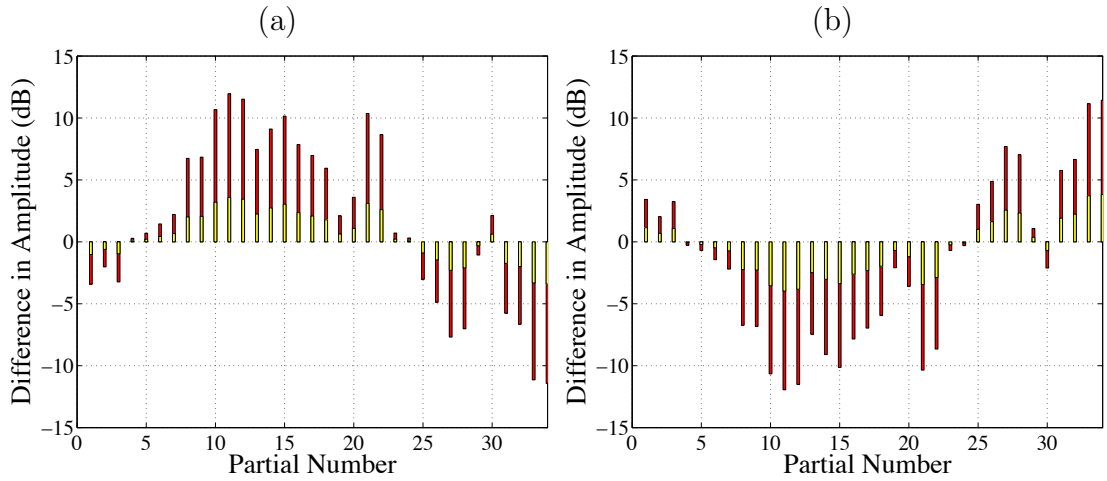

Figure 4.18: Spectral differences in harmonic content of signals described in Test 1, note $B_2^\flat$, (a) α (b) β. The red bars show the biggest difference possible. The yellow bars show the spectral differences between the test and reference signal at the time when the test was stopped

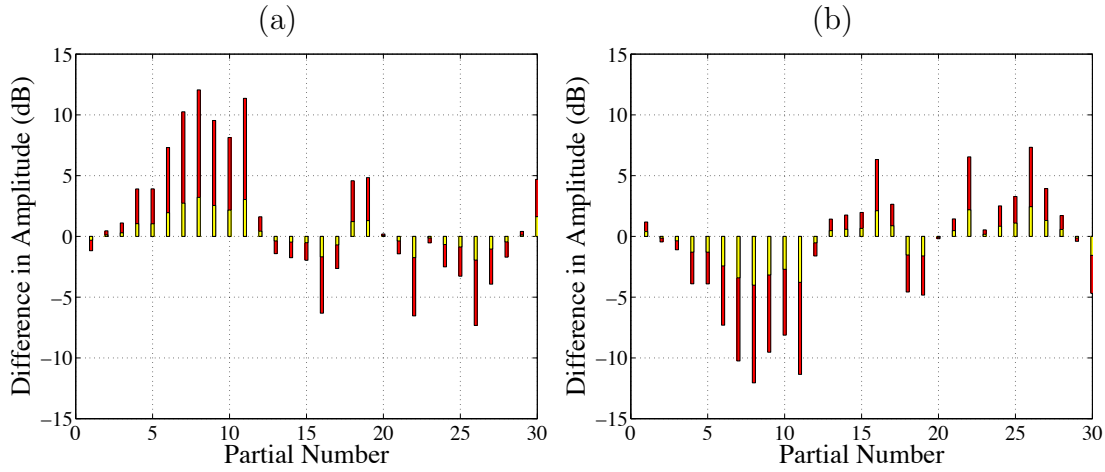

Figure 4.19: Spectral differences in harmonic content of signals described in Test 1, note $B_3^\flat$ (a) α (b) β. The red bars show the biggest difference possible. The yellow bars show the spectral differences between the test and reference signal at the time when the test was stopped

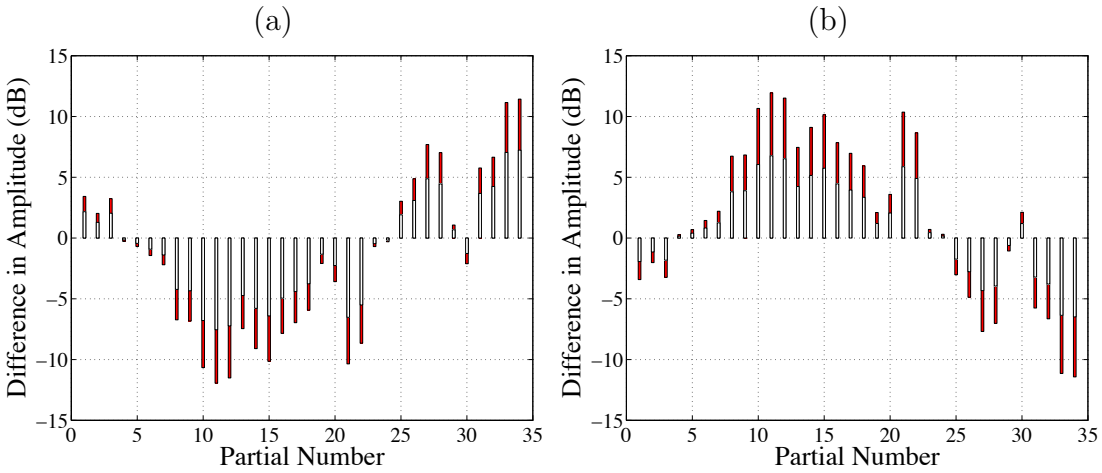

Figure 4.20: Spectral differences in harmonic content of signals described in Test 2, note $B_2^\flat$, (a) γ (b) δ. The red bars show the difference in spectra of the starting pair (biggest difference). The white bars show the spectral difference between the test and reference signals at the time when the test was stopped

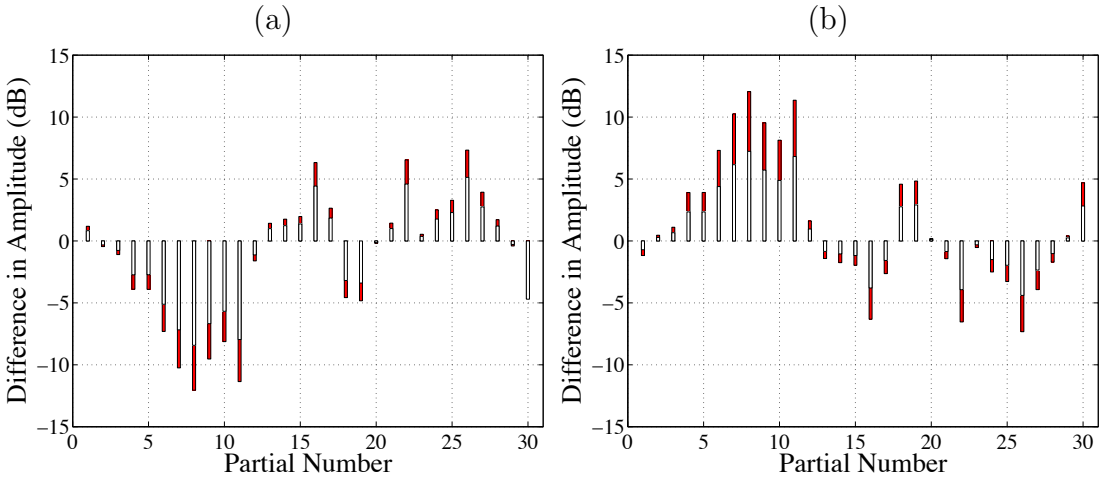

Figure 4.21: Spectral differences in harmonic content of signals described in Test 2, note $B_3^\flat$ (a) γ (b) δ. The red bars show the difference in spectra of the starting pair (biggest difference). The white bars show the spectral difference between the test and reference signals at the time when the test was stopped

This apparent "hysteresis" effect could be due to the fact that the subjects were predisposed to hearing the following pair either the same (in the case of Test 1) or different (in the case of Test 2). In order to avoid this bias in the subject's response, it is necessary to present pairs with different degrees of difference in randomised order. The following Section presents an experiment done to find the just noticeable difference in timbre between the sounds of one of the notes presented in this Section.

4.6 Just noticeable difference in timbre of trombone sounds

As mentioned in Section 3.1, the just noticeable difference between two sounds is the smallest change in a stimulus that is perceivable by a human being [59]. It is a statistical quantity, therefore it is necessary to conduct many trials in order to determine the threshold. It usually indicates the difference that a person notices on 50% of the trials.

In Section 4.5 pairs were presented sequentially with gradual bigger or smaller differences. Also, each pair was presented only once, and the test was stopped at the point when the subject noted a difference. Under these conditions, it was found that for note $B_3^\flat$ the threshold of perception lay between 0.32 and 0.57, where the biggest difference is represented by 1.

In order to find the just noticeable difference, each pair has to be presented many times, and in random order. This Section describes such a test done for the note $B_3^\flat$, aiming to find the just noticeable difference in timbre.

4.6.1 Description of psychoacoustic test

The subjects used for this experiment were Physics students in the University of Edinburgh, who were asked to volunteer in a psychoacoustic test "that has to do with how humans perceive sound". There were 24 subjects in total, out of which 13 were considered musically experienced, and 11 non musically experienced. This was determined after a short interview held at the end of the test.

The sounds chosen were the first 15 steps out of 30 described in Section 4.5. The difference between the first sound and the 15^{th} sound would correspond to

0.5. It was determined by a short listening test that this pair contained two sounds that were easily distinguishable. Each pair consisted of the "reference sound", which was the original sound, and another sound which had a degree of difference from the "reference sound" between 0 (the "reference sound" was played twice) and 0.5. Every sound had a duration of 0.5 s.

The test was made using a computer program, that presented the subjects the pairs in randomised order. Each pair was presented 20 times, giving a total of 320 presentations. Out of these 320 pairs, only 20 of them consisted of the "reference sound" played twice. The subjects were unaware of this. The sounds were presented through a pair of Sennheiser headphones model HD433. The volume was preset at a comfortable level at the start of each test. The test was performed in a sound proof laboratory. Every pair presented played one sound, followed by a 0.5 pause, followed by the second sound. The subjects were allowed to listen to every pair as many times as desired before answering. There was a training session prior to the test, in which all the 16 pairs were presented in randomised order, to allow the subject to familiarise him/herself with the procedure.

The instructions to the subjects were:

> In this test you'll hear pairs of sounds, and you'll be asked to state whether they're
>
> THE SAME
>
> or
>
> DIFFERENT
>
> You'll be able to hear each pair as many times as you like before answering. You'll state your answers by pressing the buttons labelled THE SAME or DIFFERENT, and you'll be able to hear the pair again by pressing the button labelled PLAY AGAIN.
>
> It will start with a short training session, so that you familiarise yourself with the procedure. During the training session your answers will not be recorded. To start the training session press START SESSION

These instructions remained on screen during the training session. After the training session the instructions presented on the screen were:

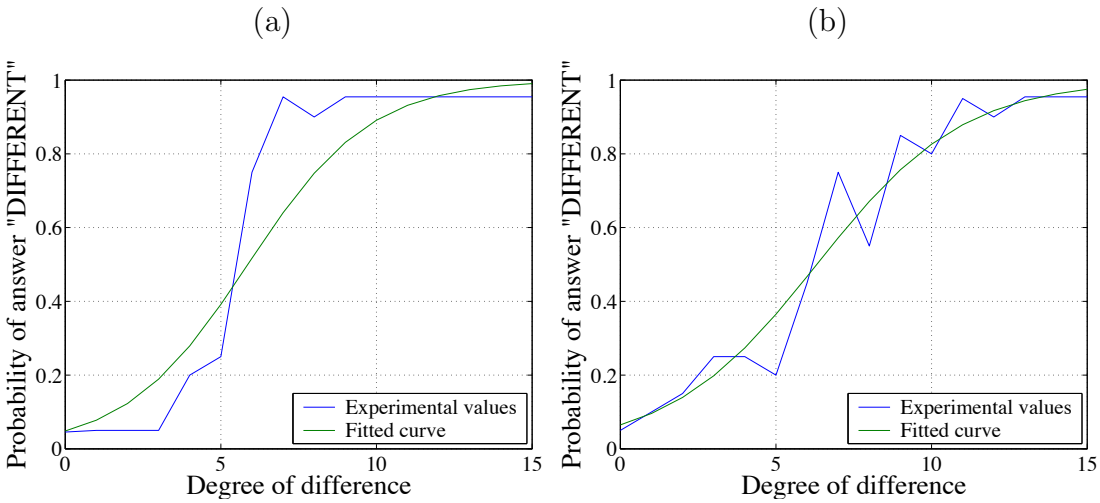

Figure 4.22: Plots of q_i vs x_i for two subjects: (a) musically experienced ($R^2 = 0.82$, $JND = 0.1955$) and (b) non musically experienced ($R^2 = 0.94$, $JND = 0.2104$)

TRAINING SESSION FINISHED

Now you can start the Main Test by pressing the button labelled START SESSION again.

After this, the screen included a progress bar, an example of which is shown below:

MAIN TEST STARTED

Progress 30%

****

Subjects were allowed to take a short pause in the middle of the test, if so they wished.

4.6.2 Results of the psychoacoustic test

The JND for each subject was calculated using the method described in [18]: The probability that the subject answered DIFFERENT (q_i) was computed for each of the 16 pairs (x_i). The logistic transformation was calculated for each pair:

$$l_i = ln\left(\frac{1-q_i}{q_i}\right) \tag{4.1}$$

For the plot l_i vs x_i, a linear regression was performed. The 50% point corresponding to the JND is calculated as follows:

$$JND = \frac{b}{m} \tag{4.2}$$

where m is the slope and b is the y-intercept. This gives a number between 0 and 15, which corresponds to the difference between the pair at which the subject answered 50% the same and 50% different. This JND was divided by 30 in order to be comparable with the results obtained in Section 4.5. The correlation coefficient R^2 was also calculated, a value between 0 and 1 which is a measure of how well the predicted line fits the measured data. Results that gave an $R^2 < 0.8$ were discarded. The data sets that remained corresponded to 12 of the musically experienced subjects, and 5 of the non musically experienced subjects. Figure 4.22 shows two examples, where $R^2 = 0.82$ and $R^2 = 0.94$.

The JND's for the musically and non musically experienced subjects are shown in Table 4.11. The JND found with this test is much smaller than the results obtained in Section 4.5. In Section 4.5, the subject would stop the test once he/she was sure that the sounds were either different (for Test 1) or the same (for Test 2). The JND obtained in this Section corresponds to the point where the subject does not know if the sounds heard are the same or different, hence when presented with the same pair many times, he/she would give each answer 50% of the time. The 75% JND would correspond to an approximate value of 0.3, or 4 dB of difference in partials, which conforms with the results presented in Table 4.9 and Figure 4.19. The test presented in this Section lasted approximately one hour in average, whereas that of Section 4.5 lasted ten minutes. The latter gives a good approximation to the JND in a simpler and more convenient test.

The JND between musically and non musically experienced subjects is not statistically different. However, it appears to be that musically experienced subjects tend to get better results in terms of R^2 than non musically experienced subjects, as the results of half of the latter had to be discarded.

Figure 4.23 shows the differences in spectra between the "reference signal" and the signal corresponding to the 50% JND. These differences are below 2.5

	Mean JND	**StdDev**
Musically experienced	0.1855	0.0752
Non musically experienced	0.2062	0.0514

Table 4.11: Just noticeable difference in timbre between trombone sounds. 1 corresponds to the biggest difference, as defined in Section 4.5

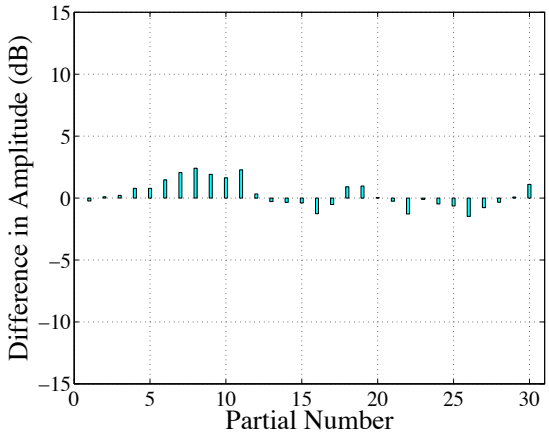

Figure 4.23: Spectral differences in harmonic content between the "reference signal" and the signal that corresponds to the JND obtained in this experiment

dB. This means that if two signals have spectral differences of 2.5 dB, subjects will be able to tell the difference between one another 50% of the time.

4.7 Change in throat diameter

According to the Denis Wick catalogue of trombone mouthpieces, the throat diameter of mouthpiece 6BS is 6.66 mm, and that of mouthpiece 5BS is 6.87 mm (see Table 4.1). For this experiment, two 6BS mouthpieces were taken, and the throat diameter of one of them was drilled out to 6.90 mm. The sounds of the trombone playing these two mouthpieces were recorded as described in Section 4.2 and 4.3, and psychoacoustic tests performed as described in Section 4.4 to find out if the subjects were able to tell the difference.

The spectral envelopes and differences in spectra of one window are shown in Figures 4.24 and 4.25, respectively. In the previous Section it was found that the JND between similar trombone sounds is 2.5 dB in the harmonic with the highest

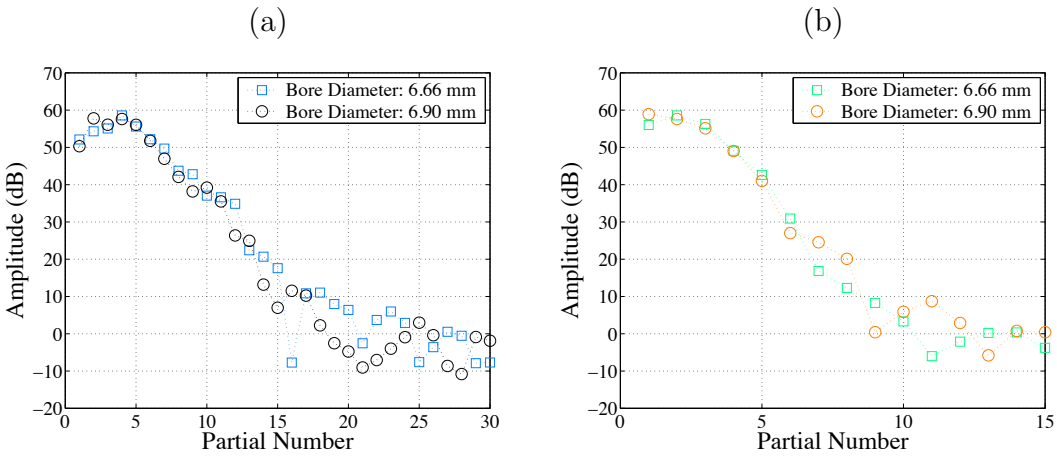

Figure 4.24: Spectral envelopes of signals from mouthpieces with throat diameter of 6.66 mm and 6.90 mm for (a) $B_2^\flat$ and (b) $B_3^\flat$

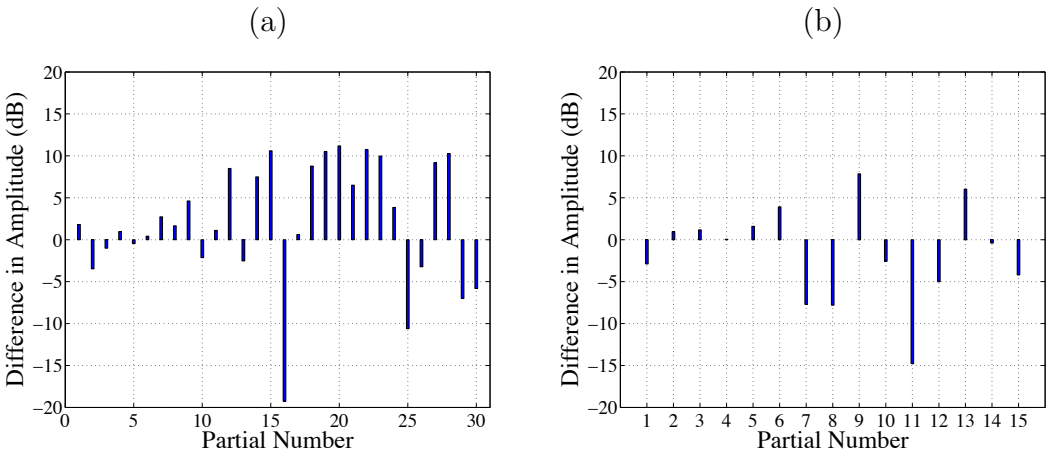

Figure 4.25: Spectral differences in harmonic content between mouthpieces with throat diameter of 6.66 mm and 6.90 mm for (a) $B_2^\flat$ and (b) $B_3^\flat$

difference. Figure 4.25 shows that half of the harmonics of the two mouthpieces differ by more than 5 dB. Hence, it is predicted that these two sounds will be distinguished easily from one another.

This test was done with 5 subjects. Table 4.12 shows that it is possible to distinguish these two sounds. However, it is important to determine if the differences between these two signals are only due to the change in throat diameter or to slight variations in the way the notes were played. Figure 4.26 shows the mean and standard deviation of the amplitude of each harmonic component for four windows taken for each mouthpiece. This Figure shows that the variations in playing are greater that those introduced by the change in throat diameter

	Distiniguishability	StdDev
$B_2^\flat$	0.82	0.10
$B_3^\flat$	0.82	0.14

Table 4.12: Distinguishability between mouthpiece 6BS and mouthpiece 6BS with its throat diameter increased to 6.90 mm

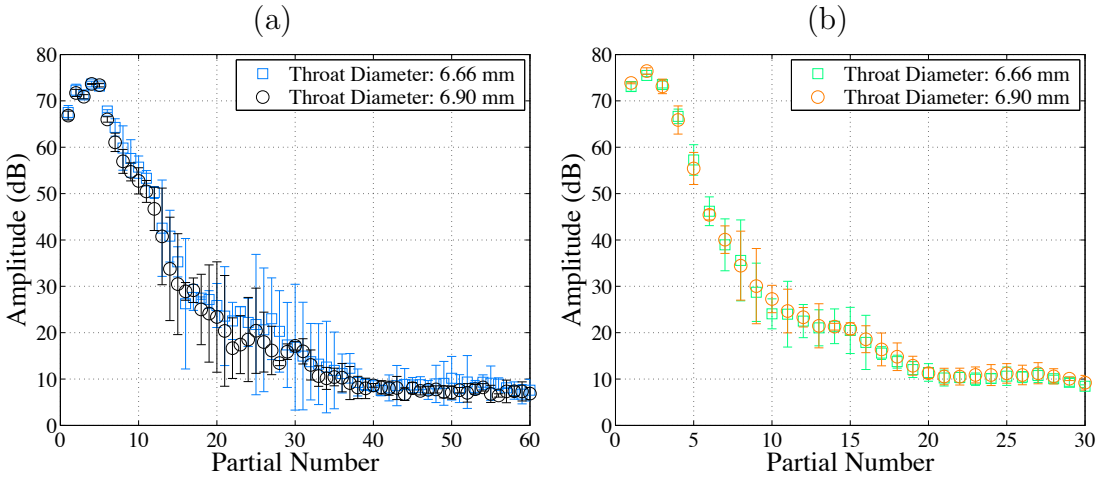

Figure 4.26: Mean and standard deviation of harmonic components for four windows taken from notes (a) $B_2^\flat$ and (b) $B_3^\flat$

in one of the mouthpieces. However, the fact that the two signals tested in the psychoacoustic test are still distinguishable, means that people are able to perceive the change in timbre introduced by the musician due to slight variations in the way he plays.

4.8 Conclusions

It has been shown that the main attributes that allow subjects to distinguish between the original and synthesised versions of signals from a trombone played with two different mouthpieces are:

- the relative amplitudes of the partials of the signal
- the high frequency aperiodic components
- the slow temporal variations induced by effects like vibrato.

This was determined by means of analysis and resynthesis of the original signals, and by psychoacoustic tests in which the subjects compared the original and synthesised signals. The synthesis method used included all these attributes, allowing to change only the amplitudes of the partials of the studied signals, and to keep the other attributes unaltered.

By gradual manipulation of signals of trombone sounds, it has been shown that the threshold of distinguishability is between 4 and 8 dB in difference in amplitude of the partials of the compared signals. A further test where the pairs were presented in randomised order, allowed to find the 50% JND, which was found to correspond to a difference in amplitude of the partials of 2.5 dB.

A small change of about 4% in the throat diameter was made to a mouthpiece. Psychoacoustic tests showed that the signals taken from the two mouthpieces are easily distinguishable. However, further analysis of these signals show that the differences were due to slight variations in the way of playing, and not to the change in throat diameter. The importance of this result lies on the fact that people are able to perceive the changes in timbre that the player introduces in the sound while he/she plays.

Chapter 5

Relationship between pressure, pitch and timbre on bagpipe sounds

5.1 Introduction

Bagpipe traditional folk music has flourished in most European countries: Scotland, Ireland, England, France, Belgium, Spain, Portugal, Italy, Poland, Czech Republic, Slovakia, Hungary, Rumania, Yugoslavia, Bulgaria and India, although many of these have become obsolete. Until now, the Scottish Great Highland Bagpipe is by far the most popular, although some other bagpipes are still played, notably in Great Britain, Ireland, Spain and Bulgaria [24].

A bagpipe is a wind instrument which consists of a chanter and one or more drones, all supplied with air from a bag, which is compressed under the player's arm to provide a constant pressure. The chanter is usually fitted with a double reed, and the drones with a single reed [24].

Scotland has three predominant types of bagpipes [24]:

1. *Great Highland Bagpipe* (Figure 5.1). It consists of three cylindrical drones, two tenor and one bass, a conical chanter, and is mouth-blown. The scale of the chanter consists of the notes G_4, A_4, B_4, $C_5^\sharp$, D_5, E_5, $F_5^\sharp$, G_5 and A_5. The two tenor drones play the note A_3, and the bass one octave below the tenors

Figure 5.1: Scottish Great Highland Bagpipe. It consists of three cylindrical drones (two tenor and one base), and a conical chanter (taken from [24])

2. *Lowland or Border Bagpipe* (Figure 5.2). It consists of three cylindrical drones (two tenor and one bass), a conical chanter, and is usually bellows blown, although it can also be found mouth-blown. The scale of the chanter is the same as that of the Great Highland Bagpipe. The three drones are placed in one stock, the tenors are tuned in A_4, and the bass one octave below. The chanter and drone are slightly smaller than those of the Great Highland Bagpipe

3. *Small-pipe* (Figure 5.3). It consists of three cylindrical drones placed in one stock, and a cylindrical chanter. The smallest drone is tuned in unison with the second deepest note of the chanter, the biggest one an octave below, and the middle one a 5^{th} in between. It can be both mouth and bellows blown. It usually comes in the scale of A (an octave below that of the Great Highland Bagpipe) or D (a 4th higher), but it can also be found in the scales of $C^{\sharp}$ and $B^{\flat}$

Bellows blown bagpipes have a long tradition in many European countries (Scotland, Italy, Poland and Serbia) and interest in these instruments has grown in recent years [24]. However, little has been studied about how small changes in the playing parameters affect the way this instrument sounds. It is generally considered that there is a feedback loop in the way wind instruments are played, in which parameters such as blowing pressure and embouchure are changed to adjust

Figure 5.2: Lowland or Border Bagpipe. It consists of three cylindrical drones placed inside a common stock (two tenors and one bass), and a conical chanter. The drones and chanter are smaller than those of the Great Highland Bagpipe (taken from [24])

the pitch and timbre dynamically. In the case of the bellows blown bagpipes, the only parameter that appears to be controlled by the player for a given fingering is the pressure exerted on the bag of the instrument.

There has been relatively little work done about the production of sound in bagpipes. Allan [1] measured the frequencies of the nine notes of eight different Highland bagpipe chanters. He found that there was significant irregularity between the eight chanter tunings, and that there did not seem to be a standard scale associated with them. He also measured the frequency of the tone when the reed is blown on its own. Three reeds gave frequencies of 1250, 1400 and 1540 Hz. He also measured the resonance of the air column for all the notes of the chanter by blowing in the same manner pan-pipes are blown. These resonances lay between 580 and 2260 Hz. He noted that the pitch at which the chanter sounds is the result of the coupling between the reed and chanter system (which he referred to as "coupling tone"), being flatter in pitch than the resonance of the pipe. He postulated that variations in the playing frequency of the chanter are in part due to changes in moisture from the breath of the player (increased humidity would tend to reduce the pitch), and from changes in the pressure applied to the bag, which could cause a shift in pitch of up to a semitone.

Lenihan and McNeill [55] also measured the frequencies of the notes of the

Figure 5.3: Small-pipe. It consists of a cylindrical chanter, and three drones placed inside a common stock. The drones are tuned as follows: The smallest one is tuned in unison with the second deepest note of the chanter, the biggest one an octave below, and the middle one a 5^{th} in between (taken from [24])

Highland bagpipe chanter, following Allan's work [1]. They found discrepancies in what Allan had measured, although they coincided in that the scale they found does not correspond to either just intonation or equal temperament. They suggested the adoption of a standard pitch for Highland bagpipes, setting A to 459 Hz.

Harris et al. [44] measured the spectra produced by the drones and chanter in normal playing conditions from a Highland Bagpipe. They found that the drone spectrum changes significantly when the length is reduced or increased. They measured the playing frequency of each note in four different chanters, finding good agreement with the measurements done by Lenihan and McNeill [55]. They also measured a particular chanter-reed-piper combination in two occasions, the second one three months after the first, in an attempt to find the effect of aging of the reed in the sound of the chanter. The reed was given a considerable use during these three months. They found a particular high frequency formant in the spectrum of the chanter. When the reed was new, this formant was very evident, three months later it was suppressed, changing both the quality of the tone and the SPL of the chanter. This latter sound was described as "mellower". They made a further experiment in which they measured the pressure exerted on the bag, and measured the sound of the chanter at a distance of 1 m. They compared

the spectra of the chanter sounding the note A vs pressure. Their results show an increase of amplitude in the fourth harmonic as pressure increases from 5.5 kPa (below this pressure the reed fails to vibrate) to 9 kPa (the maximum pressure that a player could provide, being limited by the lung capacity of the player). They found that a difference in SPL between the lowest pressure and the highest pressure was about 4 dB. They measured the pressure at which the bag is pressed under typical blowing conditions, being approximately 7.35 kPa.

Carruthers [22] measured the sound radiation of three representative notes of the Highland Bagpipe (low G, low A and E). He found that the sound is radiated in a nearly omnidirectional fashion. He also measured the relative SPL of each of its notes. He found that the two most intense notes are low G and low A, and the least intense note is high A. He found that the absolute SPL of individual notes depends mainly on the condition of the reeds, their tuning positions and the pressure change of the air in the bag.

Carruthers [23] measured how the temperature of the air in the bag affects the pitch of the notes low A and D played in the chanter of a Highland Bagpipe, throughout 50 minutes of playing, keeping the pressure as steady as possible. He fitted both temperature and pitch curves with a polynomial regression. He concluded that the bag would take a finite time to reach thermal equilibrium, which depends mainly on the atmospheric temperature, and that the pitch shift in the bagpipe is dependent on how the temperature changes inside the bag. He considered it plausible that the maximum temperature inside the bag should be in the centre of the bag, thus making the top end of the chanter warmer than the rest, which could account for the fact that the maximum pitch shift for note D (37 cents), was higher than that found in low A (24 cents). He also acknowledged that the moisture coming from the player's breath will probably reduce the resonance frequency of the reed, as predicted by [1].

Firth and Sillitto [31] measured the input impedance of each note of the Highland bagpipe chanter, using an iophone and measuring with a microphone the reflected waveform. The first impedance peaks were between 399 Hz (for low G) and 908 Hz (for high A), contrasting with what Allan [1] found. They measured the spectra of the reed blown on its own, finding coincidences between the spectral peaks of the reed spectrum with the spectra of the played notes.

Allan [1] and Carruthers [23] hinted at the role of humidity in the physical

properties of the reed (increased humidity would tend to reduce the resonance frequency of the reed), and on the sound of the chanter and reed system (increased humidity would reduce the pitch). There is no work known by the author that has attempted to investigate this effect experimentally. Thus it is important to consider if and how changes in the environment affect the pitch and timbre of the bagpipe.

This Chapter describes studies carried out on a Scottish bellows blown Border bagpipe chanter and reed, and it is organised as follows: Section 5.2 presents evidence of significant fluctuations in pitch and timbre of a bagpipe chanter played by an expert player both mouth-blown and with bellows, suggesting that there are other parameters apart from the changes in relative humidity inside the bag that affect both the pitch and timbre of the bagpipe. In order to remove the variations in pitch and timbre that result from the way the musician plays the bagpipe, an artificial blowing machine was built. Section 5.3 describes in detail the equipment used for the experiment with the artificial blowing machine. It also describes how the measurements were taken, and the calculations that were performed in order to get the results presented. Section 5.4 presents a detailed analysis on the effect of variations in relative humidity in two of the notes studied. Finally, Section 5.5 presents the results obtained from performing the same measurements on a plastic reed. The comparison between the results from the cane reed and from the plastic reed suggests that relative humidity affects the behaviour on cane reeds, which in turn affects the pitch and timbre in some ways.

5.2 Effect of relative humidity on the pitch and timbre of a Scottish border bagpipe chanter and reed

A preliminary study was made that aimed at finding out how the relative humidity introduced by the player's breath in a mouth-blown Border bagpipe affected the pitch and timbre of the chanter and reed.

When the same bagpipe is played with bellows, these take air from the atmosphere to fill the bag, which is pressed to create a flow of air through the reed making it vibrate. The relative humidity in general varies during the day, nev-

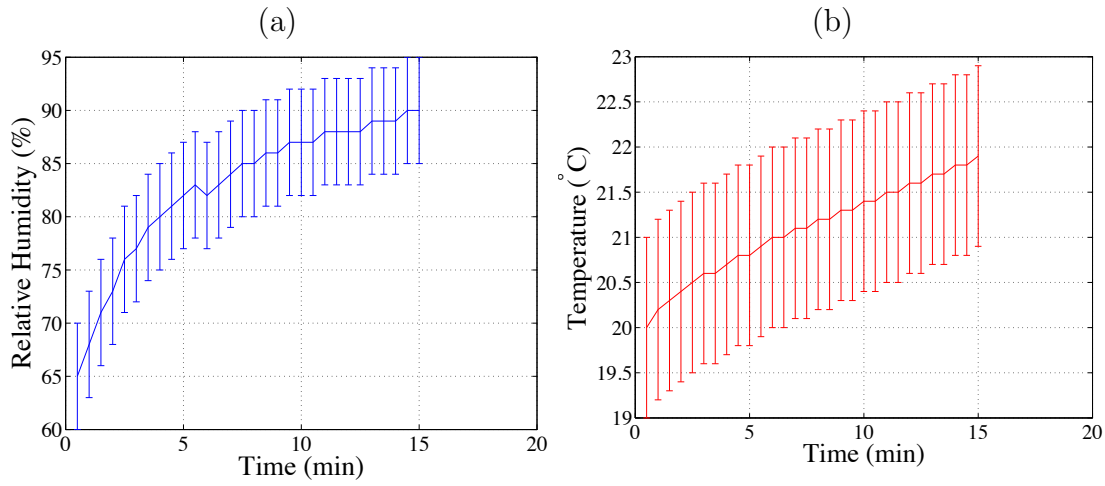

Figure 5.4: (a) Relative humidity and (b) temperature variations inside the bag of a mouth-blown bagpipe during the first 15 minutes of playing

ertheless a player will play the bagpipe for a period of about one hour. It is in this time that the relative humidity of the environment was considered to remain constant.

Figure 5.4 shows how the relative humidity and temperature inside the bag increase over time when the bagpipe chanter is mouth-blown during the first 15 minutes of playing. This measurement was done by inserting the probe of a Dostmann electronic model P320 humidity and temperature sensor inside one of the holes of the stocks where the drones are normally inserted. The bagpipe was played without the drones.

Recordings of an expert piper were made under two conditions: bellows blown, and mouth blown. The results obtained from this study revealed that the pitch and timbre of the bellows blown chanter vary considerably over time, even when the relative humidity does not change. Figure 5.5 shows these variations over the first five minutes of playing.

This implies that there are other significant parameters that affect the pitch and timbre of a given note, apart from changes in relative humidity. For a given fingering, the only parameter that appears to be changed by the player while playing the bagpipe is the pressure exerted on the bag of the instrument. The following Section describes experiments done with an artificial blowing machine, aimed at finding how the pitch and timbre of the chanter and reed system change with varying pressure.

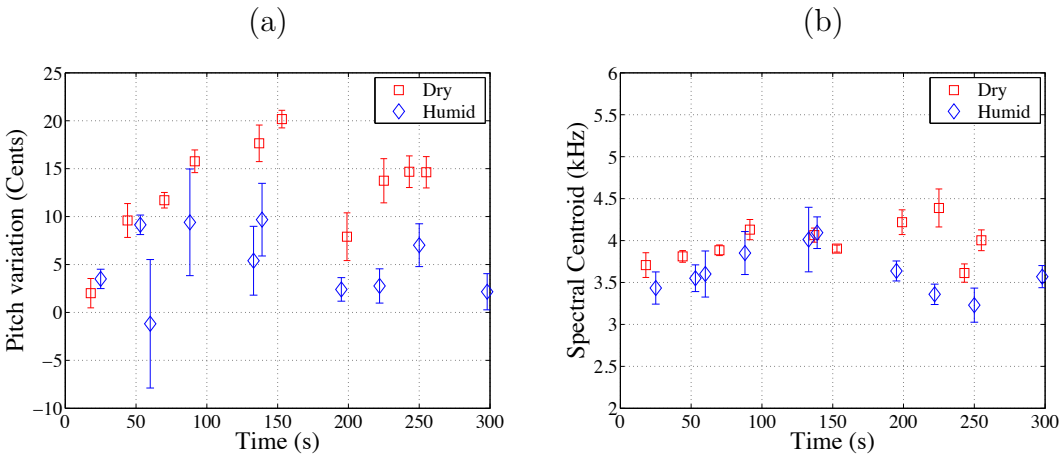

Figure 5.5: Variations in (a) pitch and (b) spectral centroid over time of note E_4 played with bellows (dry) and mouth-blown (humid)

5.3 Experiments using an artificial blowing machine

The experiment described in the previous Section reveals the fluctuations of pitch and timbre that occur during normal playing. These could be due to the way the musician plays the instrument. To minimise the small variations that a human player would introduce while playing the bagpipe, it was decided to build an artificial blowing machine.

Previous studies using an artificial blowers have described the use of artificial means of playing a musical instrument, mainly for the following reasons:

- to eliminate the variations in playing that a human player introduces
- to be able to measure things such as the vibrations of the reed or the pressure inside a cavity that serves as a substitute for the player's mouth, that would not be possible otherwise
- to be able to control the playing parameters such as blowing pressure and lip pressure independently
- to be able to test the quality of a musical instrument

Backus [5] designed an artificial blowing machine to study the vibrations of a clarinet reed. He had a cavity where the air from a vacuum cleaner was connected to provide the air pressure, and an artificial lip/teeth arrangement made

from neoprene and a brass wedge respectively. He measured the motion of the reed by illuminating it with a stroboscope. He found that there are no transverse oscillations in the reed while the instrument is being played under normal conditions. On a different setup, be shone light through the mouthpiece, and a photomultiplier received the light, the latter being connected to an oscilloscope. In this setup, the oscilloscope readings gave the reed displacement as a function of time. He found that the reed closes completely for nearly half of the cycle during loud playing. He compared these latter results for cane reed and plastic reed, showing that the plastic reed motion had a bigger amplitude, and hypothesised that this could be due to the reduced stiffness and increased mass compared to those of the cane reed. He concluded that the reed is mainly stiffness controlled, and that the size and shape of the oral cavity do not have an influence in the tone produced by the clarinet.

Backus [6] developed a theory to explain the fact that the clarinet player has control over the playing frequency by adjustment of the embouchure, and the existence of a threshold pressure needed to start the vibrations of the instrument. He tested his theory by means of measuring the response of a clarinet artificially blown.

Bak and Dømler [9] developed an artificial blowing machine to investigate the relationship between blowing pressure and playing frequency in the clarinet. The idea was to find if clarinetists are right when they say that the playing frequency falls as the pressure is increased. With the use of an artificial blowing machine, they were able to control the blowing pressure independently, which would not be possible with a human player. They placed the clarinet inside a box, inside which a vacuum cleaner was connected via a hose. They fitted the reed with an artificial embouchure made from a water-filled balloon to mimic a human lip. They measured the sound of the clarinet just inside the mouthpiece. They measured the frequency of the played sound by amplifying the signal from the microphone until it clipped, and then connected it to one of the inputs of a phase-locked loop (PLL) device. The other input of the PLL had a reference tone with a frequency of the note of the equally tempered scale that corresponded to the note of the clarinet being tested. The PLL gives a DC signal that measures the deviation of the clarinet playing frequency from the reference tone. They always found a positive correlation between blowing pressure and playing frequency,

contrary to the clarinetists opinion. They noted that the playing frequency does not depend only on the blowing pressure, but also on the lip pressure.

Idogawa et al. [48] used an artificially blown clarinet to investigate the different vibratory states that can be excited in this instrument. They built a transparent acrylic cavity to which air at a constant pressure was provided. The clarinet mouthpiece was placed between two rubber lips inside the cavity, along with a pressure meter. They shone a parallel beam through the mouthpiece, and measured it with a photodiode that was placed just outside the cavity. This photodiode measured the position of the reed. With the artificial setup they were able to control the lip position and pressure on the reed, and the pressure inside the cavity. They studied in detail the different vibratory states that resulted from several configurations. They found that they could excite, apart from periodic vibrations and high pitched "squeals", aperiodic vibrations that were highly complicated. The vibratory state that was excited at one particular time depended on the previous vibratory state, as well as on the change of pressure.

Petiot et al. [67] developed an artificial blowing machine with the aim of testing the quality of brass instruments, and thus aid the instrument maker in the design and testing process of these instruments. This artificial machine consisted of a cavity to which "artificial lips" (rubber lips filled with water) were fitted. The mouthpiece of the instrument is then pressed against these lips. The following parameters could be adjusted: the water pressure inside the lips, the mechanical pressure on the jaw, the tension of the lips, and the blowing pressure. The lips were made with Polyurethane tubes. They carried out several tests with this blowing machine on two different trumpets of different makers. They found different behaviour between these two instruments, regarding the threshold pressure, which could be correlated to the ease of play, and playing frequency, which could be correlated to good tuning.

Richards [74] developed an artificial mouth for playing brass instruments, to study the nature of the lip reed. It consisted of an airtight box fed by an air pump, corresponding to the mouth of the player. The lips were mimicked with latex tubes filled with water. The mouthpiece was pressed against the lips, and when the pressure inside the cavity was increased, a note was produced. He constructed a transparent trombone mouthpiece in order to be able to view the motion of the lips. He filmed the motion of the lips with a high speed camera,

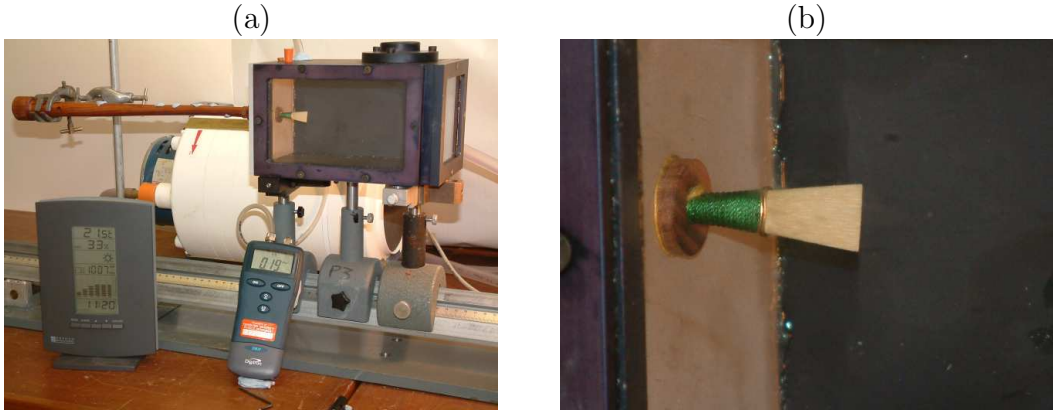

Figure 5.6: (a) Artificial blowing machine, and (b) close up image of the reed inside the cavity of the apparatus

and he found the motion to be two-dimensional, i.e. the motion was not only up-down, but also front-back. He could also place a loudspeaker instead of the air pump, and excite the lips with a sinusoidal waveform. Under these conditions, he measured the phase of the lip movement with respect to the driving force at resonance. He found that this phase could correspond to both an inward striking reed or an outward striking reed, depending on the embouchure. This explains why a brass player can play both above and below the impedance peak of the instrument.

5.3.1 Experiments with an artificially blown chanter

The artificial blowing machine (Figure 5.6) that was used for the experiments described in this Chapter is an adapted version of that used by Richards [74]. It is capable of providing a steady pressure through an ACI air pump model 8MS11 to a cavity in which the top of the chanter with the reed is introduced. A Digitron manometer model 2001P was also connected inside the cavity to measure the pressure given by the pump. This pressure can be varied from 0 to 8 kPa by adjusting a valve. The main difference to that used by Richards is the front plate, which allowed the introduction of the chanter top inside the cavity.

In the experiment, starting with 0 Pa the pressure was gradually increased until the reed started vibrating. When the manometer gave a steady measurement, the sound that the chanter produced was recorded via an Audio-Technica condenser microphone model ATM 31a into a TASCAM DAT recorder model

DA-20mkII with a sampling frequency $f_s = 44.1$ kHz. The microphone was placed approximately 1.5 m away from the chanter, off axis. The pressure was then increased in steps of 200 Pa, and the sound recorded at each of these points where the manometer gave a steady measurement. When the maximum pressure that the pump can provide was reached (8 kPa) the pressure was then reduced in steps of 200 Pa until the manometer could no longer give a steady measurement (i.e. the pressure kept falling even when the valve was kept untouched), at which point the reed eventually stopped vibrating.

5.3.2 Analysis of recorded signals

The two parameters that were monitored were the variation of pitch and of spectral centroid as the pressure changed. Studies by Kendall and Carterette [53] and Schubert et al. [76] found that the spectral centroid is correlated to the perceived degree of brightness of a sound.

The program SNDAN [12] provided by James Beauchamp from the University of Illinois at Urbana-Champaign was used to calculate the pitch variation over time (Section 3.2.7), and the spectral centroid variation over time (Section 3.4.6). The analysis frequency f_a was selected initially to be the frequency at which each fingering was supposed to sound, taking into account the intonation of a bagpipe chanter. Table 5.1 shows the frequencies that correspond to each of the notes of the chanter. This information was provided by Nigel Richards from Garvie Bagpipes [73], who designed this particular chanter. Once the analysis was done with this initial value of f_a, a new f_a value was taken from SNDAN, which suggests a frequency that lines the harmonics up with the analysis bins as well as possible (as SNDAN performs a pitch-synchronous analysis, the analysis performance is best when the analysis frequency is set as close as possible to the fundamental. See Section 3.2.7 for more details). The analysis was then repeated with this new f_a. This last analysis file is the one from which all the results presented in this Section were calculated. A typical measurement of pitch and spectral centroid variation over time of a note from the bagpipe chanter taken under the conditions described in this experiment is shown in Figure 5.7.

The mean and standard deviation of these results were taken and plotted in graphs of pitch and spectral centroid vs blowing pressure. In all such curves, 0 cents represents the frequency of the note that is shown in Table 5.1, unless

Note	Frequency (Hz)
G_4	385
A_4	440
B_4	495
$C_5^\sharp$	550
D_5	586.67
E_5	660
$F_5^\sharp$	733.33
G_5	770
A_5	880

Table 5.1: Intonation table for the bellows blown bagpipe chanter used in this experiment. Note that it corresponds to an A major scale tuned in just intonation with a flattened 7^{th} (taken from [73])

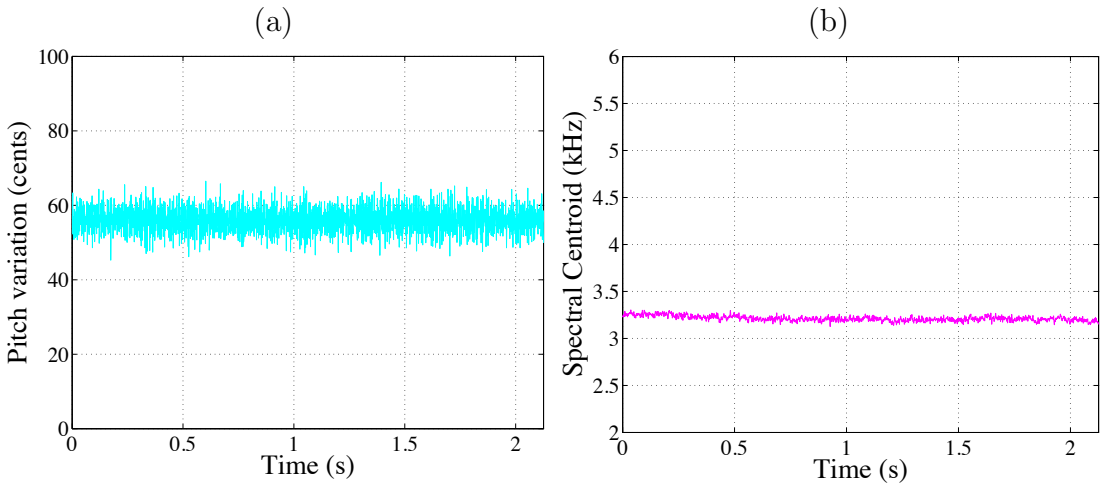

Figure 5.7: Typical measured values of (a) pitch and (b) spectral centroid variation over time of a bagpipe chanter note, while being artificially blown

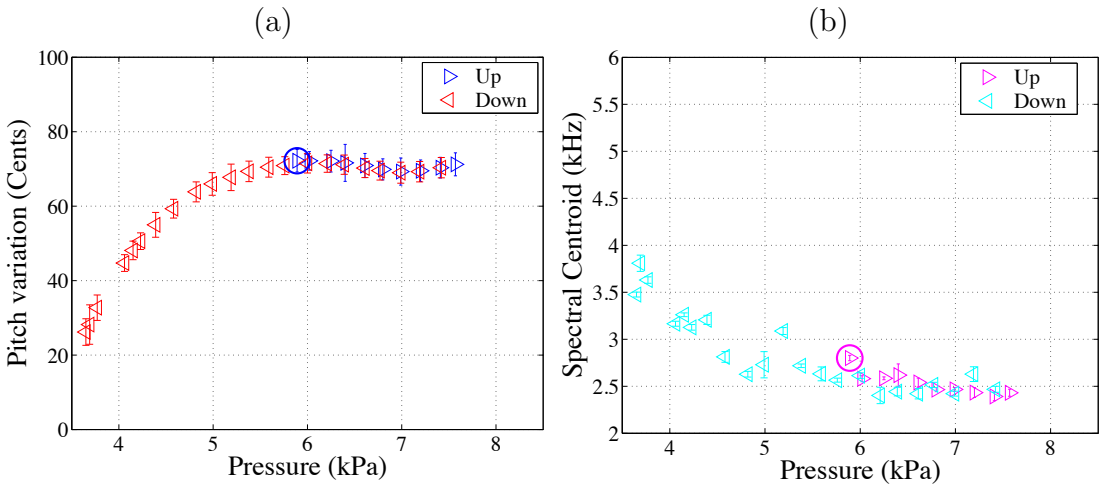

Figure 5.8: Variation of (a) pitch and (b) spectral centroid vs pressure for note G_4

otherwise stated.

5.3.3 Preliminary measurements and results

In a preliminary study, all nine notes of the bagpipe were recorded and analysed as described in Sections 5.3.1 and 5.3.2. Figures 5.8 to 5.16 show the results obtained for each note. The threshold pressure at which the reed started vibrating is indicated in these figures by a circle. As can be seen in these figures, all nine notes played sharp at all the pressures measured, except for note A_5. Nigel Richards, who built this particular chanter, also noted that the reed used in this experiment played significantly less loud than an optimum reed would play. It is his opinion that the reason for these is the fact that this particular reed was "soft", and the opening between the blades was slightly narrower than that of an optimum reed.

These figures also reveal that each note has a particular profile of pitch and spectral centroid variation with pressure. That is, the shape of the curves pitch vs pressure and spectral centroid vs pressure are different for each of the notes presented here. Furthermore, all notes had hysteresis, in the sense that the pressure at which the reed had to be subjected before starting to vibrate (around 6 kPa) was higher than the lowest steady pressure at which it could play while already vibrating (around 4 kPa).

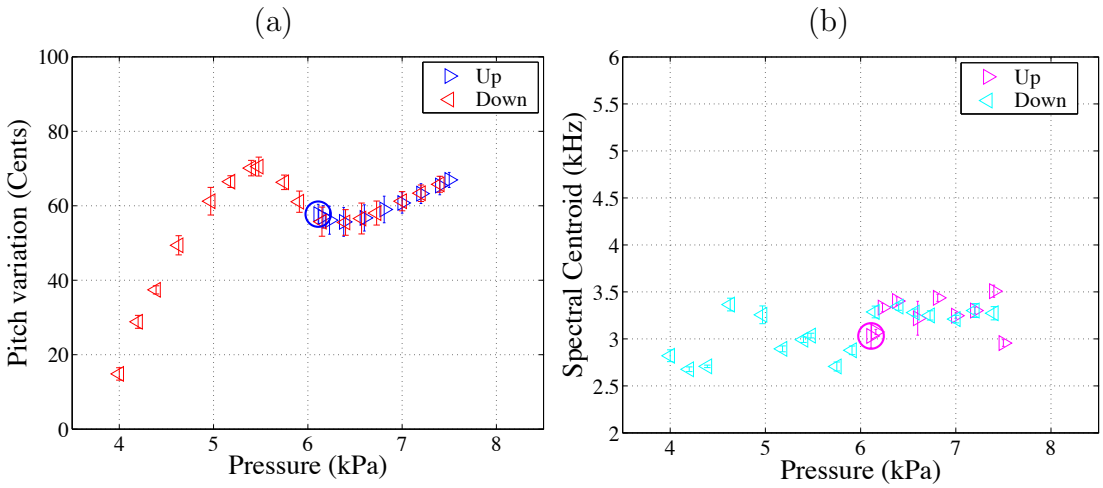

Figure 5.9: Variation of (a) pitch and (b) spectral centroid vs pressure for note A_4

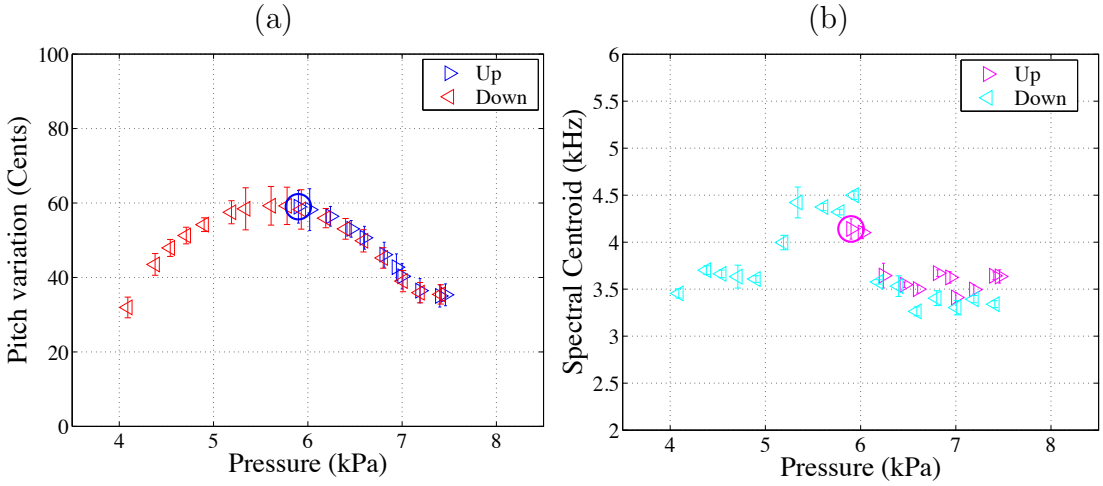

Figure 5.10: Variation of (a) pitch and (b) spectral centroid vs pressure for note B_4

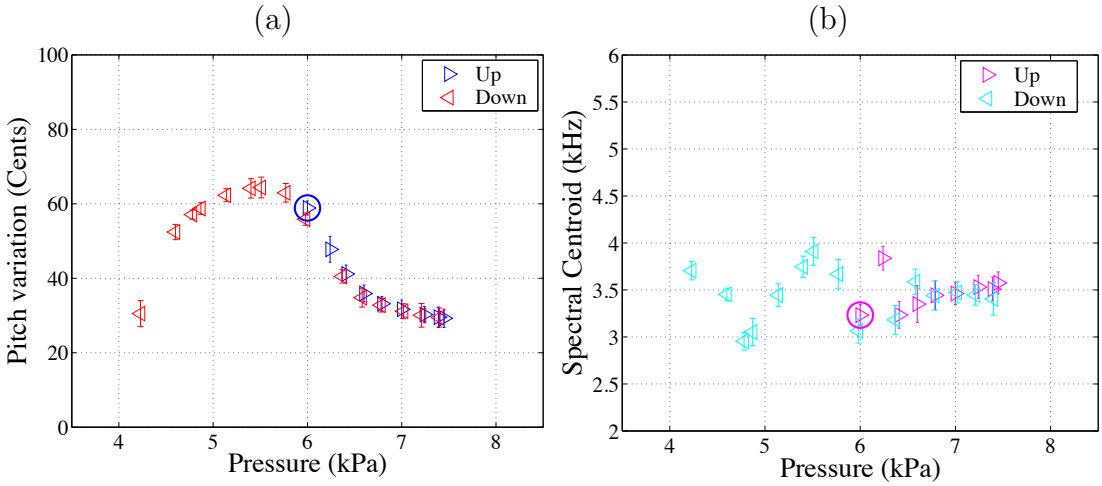

Figure 5.11: Variation of (a) pitch and (b) spectral centroid vs pressure for note $C_5^\sharp$

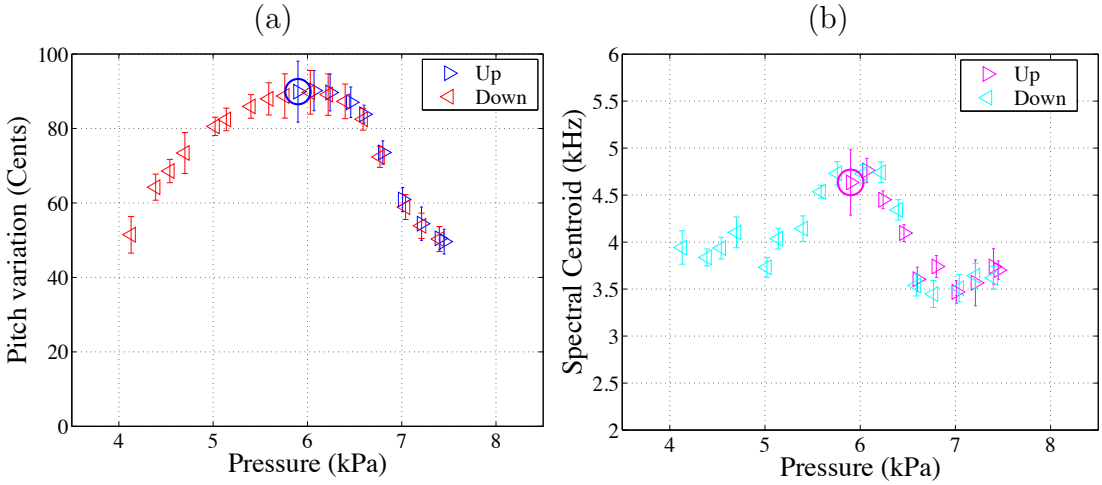

Figure 5.12: Variation of (a) pitch and (b) spectral centroid vs pressure for note D_5

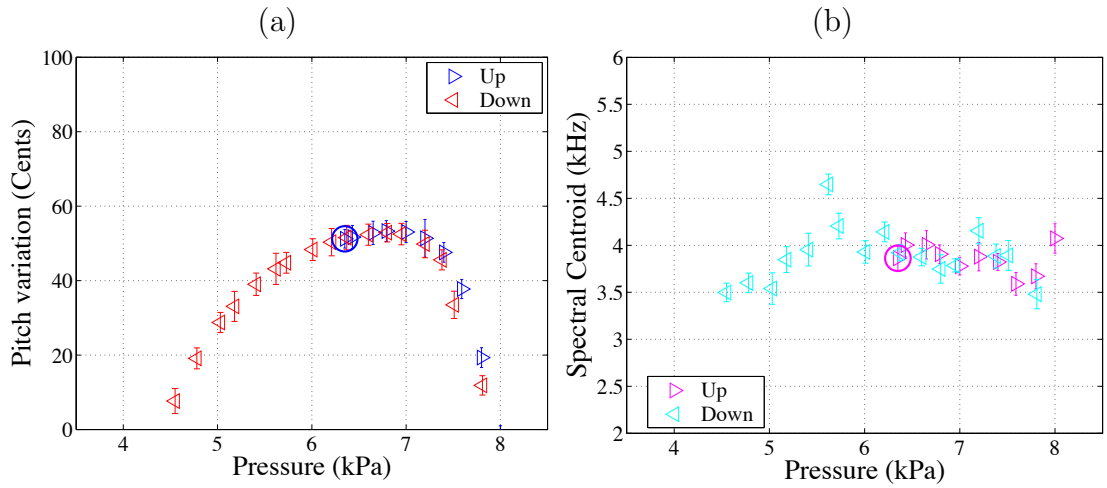

Figure 5.13: Variation of (a) pitch and (b) spectral centroid vs pressure for note E_5

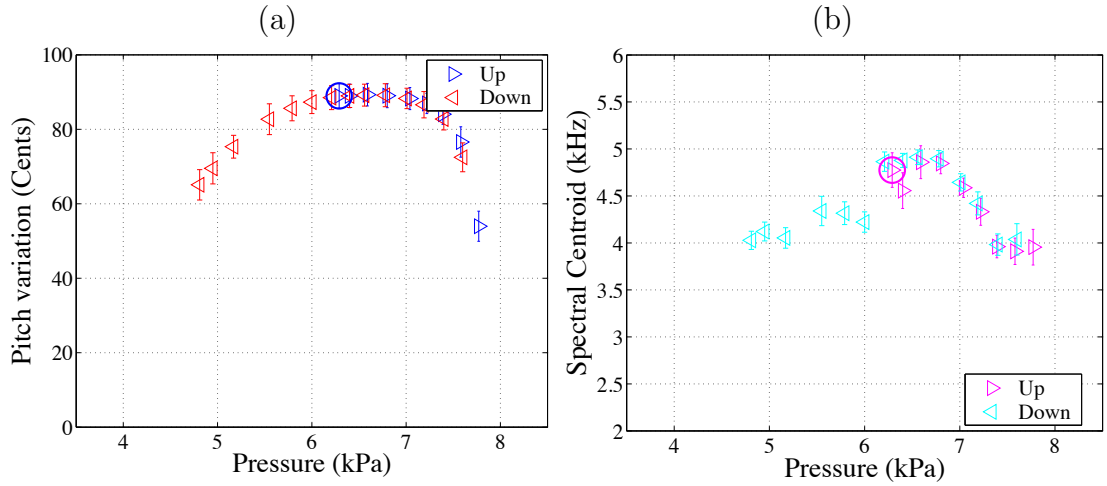

Figure 5.14: Variation of (a) pitch and (b) spectral centroid vs pressure for note $F\sharp_5$

A further measurement was done with the reed inside the cavity without the chanter. The results of this experiment are shown in Figure 5.17, where 0 cents corresponds to 695 Hz. This figure shows two different pitches, one being about one octave below the other. The high pitch occurred at a high pressure, and at a very low pressure. The low pitch occurred in between the high and low pressure regimes. These measurements are more or less in agreement with what Firth and Sillitto [31] found:

> Blowing hard, a smooth, high-pitched tone is heard; blowing at a reduced pressure, a good reed will emit a rather harsh, high-pitched croak. Between the croak and the smooth tone there is another unstable oscillation which occurs at a lower pitch. This unstable sound is referred to here as the

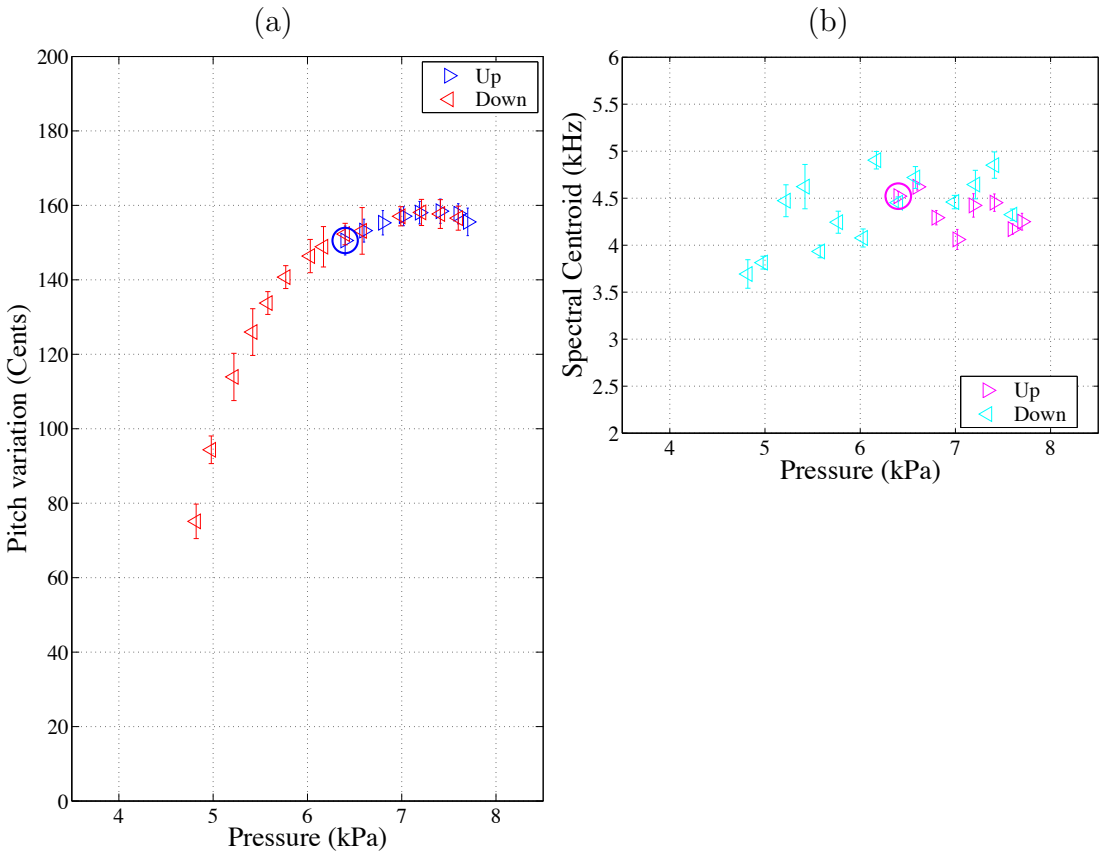

Figure 5.15: Variation of (a) pitch and (b) spectral centroid vs pressure for note G_5

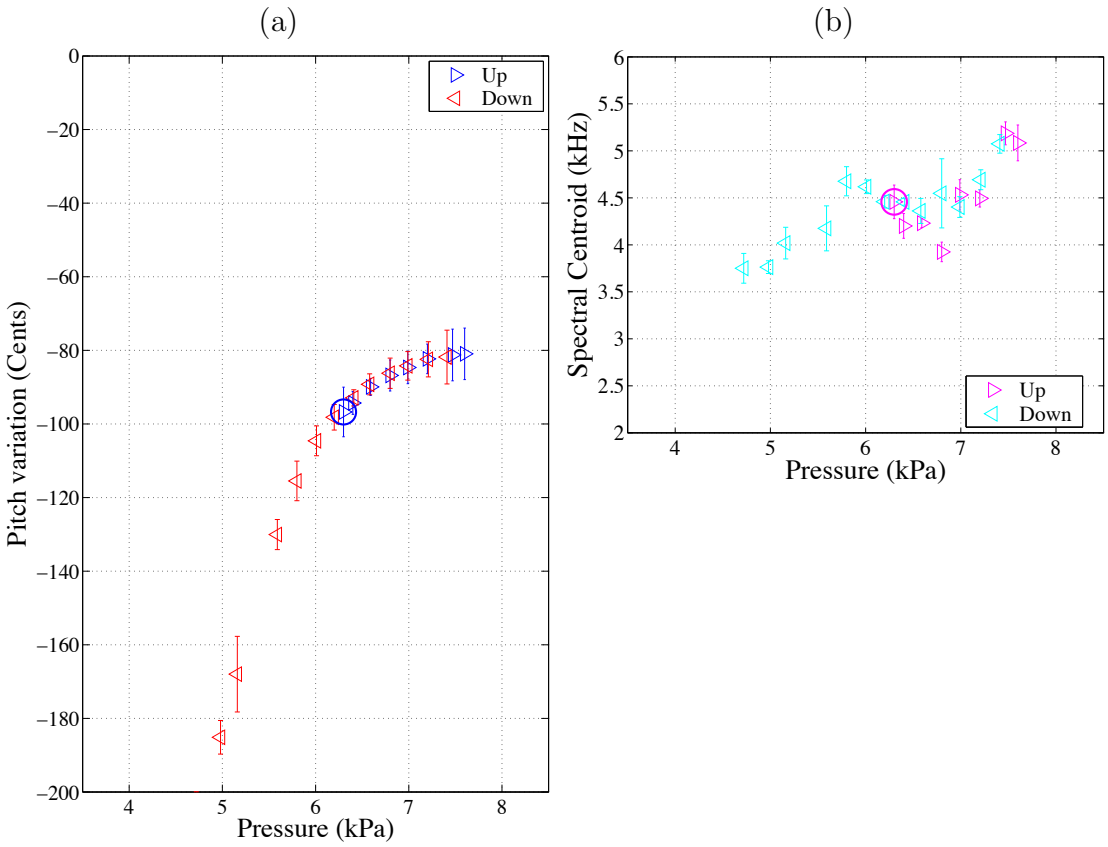

Figure 5.16: Variation of (a) pitch and (b) spectral centroid vs pressure for note A_5

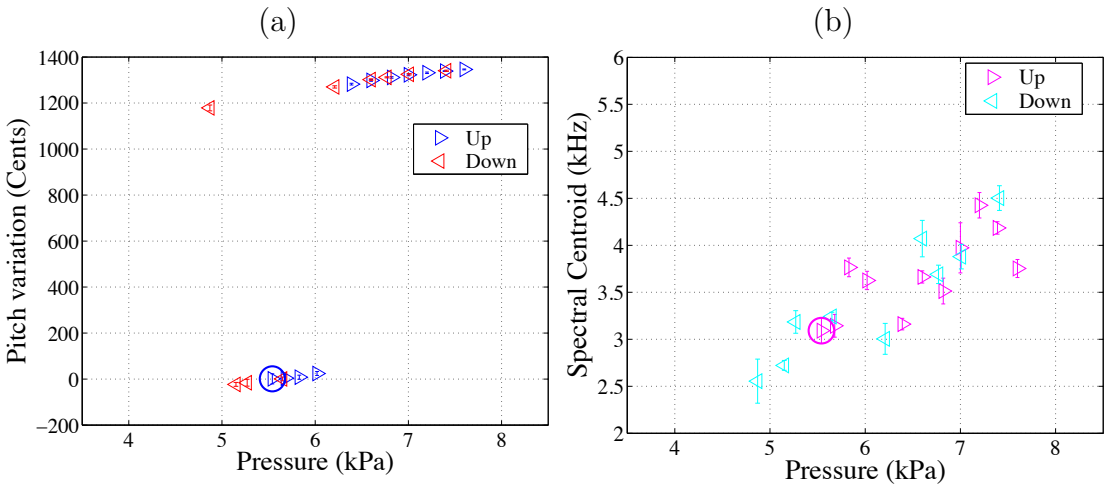

Figure 5.17: Variation of (a) pitch and (b) spectral centroid of reed without the chanter. 0 cents corresponds to 695 Hz

sub-harmonic mode because measurements of its spectra show that its fundamental oscillation is at about a half of the fundamental frequency of the smooth tone.

The spectral centroid values in this case are much lower than those of the notes recorded with the chanter. This measurement also presented the hysteresis effect described before.

This particular chanter and reed were also played in its bag by an expert player, and measurements of the pressure inside the bag were recorded with the same manometer. The mean of these measurements was 3.74 kPa, and the standard deviation 130 Pa. However, the pressure at which the vibrations started in the experiments described so far, was above 6 kPa, or very close to 6 kPa (this threshold pressure is shown in Figures 5.8 to 5.16 by a circle). This implies that to start playing, the player has to initially press the bag with a pressure significantly higher to that of normal playing just to start the vibrations of the reed. Also, the player chooses to play in the bottom end of the hysteresis found in the figures presented, where the pitch curve shows the highest slope. This might be to allow pitch and timbre modulations that make musical instruments interesting to the human ear. As an illustration of this, a closer look at Figure 5.13 reveals that in order to have the 20 cent variation in pitch shown in Figure 5.5, the player only needed to change the pressure by about 10%.

It is worth noting that the pressure at which this bagpipe is played (around 4

kPa) is much lower than the findings of Harris et al. [44], who measured a typical pressure of around 7 kPa. This is because Harris et al. measured the pressure when playing a Highland bagpipe, whereas this particular Scottish Border bagpipe is designed to be played at a lower pressure, making it suitable to play indoors.

The notes G_4 and D_5 were selected for further study on the grounds of having the widest variation in spectral centroid at the pressures measured.

5.4 Effect of relative humidity on the curves of pitch and spectral centroid vs pressure for notes G_4 and D_5

The previous Section presented a preliminary study where the pitch and spectral centroid variations vs pressure were measured for all the notes of the chanter being studied. In this Section, these measurements were repeated for the notes G_4 and D_5, as these were the notes that showed the widest variation in pitch and spectral centroid with varying pressure. The measurements were done at different relative humidity conditions, with the aim of finding out whether the environmental conditions affect the way this instrument sounds.

The temperature and relative humidity in the laboratory were recorded using an Oregon Scientific Deluxe 7 Line Weather Forecaster in four different days. For each day, the measurements of pitch and spectral centroid curves were done twice to find out whether the results obtained were reproducible. The results presented in this Section show the two measurements done in a given day on the same graph, one on top of the other, differentiated by colour. It will be shown that the results taken on the same day were essentially the same, although results from different days varied in many ways, even when the temperature and relative humidity conditions varied not more than 1°C and 4% respectively.

5.4.1 Results for note D_5

Figure 5.18 shows the measurements done at a temperature of 18.5°C and a relative humidity of 45% and 44%. Figure 5.19 shows the measurements done at a temperature of 20.5°C and 19.5°C respectively, and a relative humidity of 33% and 36%. These figures show two measurements in each plot (corresponding

to the two measurements that were done on the same day), each of which is of a different colour. As can be seen in these plots, the measurements that were done on the same day were reproducible, as the difference between them is well inside their standard deviations. However, a comparison between measurements that were done in different days shows that both the pitch and spectral centroid changed in several ways, even in the cases where the relative humidity was within the tolerance of the instrument.

Although the shape of the pitch curve remained the same in all the measurements, the following variations were noted:

- In Figure 5.18, the pitch curve in the top panel is flatter than the bottom panel for about 20 cents. The same is the case in Figure 5.19, the pitch in the bottom panel is around 20 cents flat compared to the top panel
- The pressure at which the pitch had its maximum value varied between 5 and 5.5 kPa

There does not appear to be a direct correlation between the changes in relative humidity and the changes in pitch noted in these measurements.

The shape of the spectral centroid curve also varied in several ways.

- In Figure 5.18 there is an increased spectral centroid between 5 to 6 kPa, and in the rest of the pressure range it remains lower, although the bottom measurement appears to have an overall higher spectral centroid
- In Figure 5.19 the increased spectral centroid region is wider: between 4.5 and 6 kPa, again the bottom measurement being somewhat higher

The relative humidity appears to have an effect on the overall shape of the spectral centroid curve, nevertheless the overall height does not seem to be directly related to relative humidity variations.

To make sure that these changes were not due to the relative positioning of the reed in the chanter, the note D_5 was recorded several times at a pressure of 6 kPa, repositioning the reed in between measurements. The variations in pitch and spectral centroid are shown in Figure 5.20. The scale in this figure was intentionally left as it was in previous measurements, for the sake of comparison. The variation in pitch is much smaller than the 20 cents shown in the previous

figures. Although the variation in spectral centroid is of the same magnitude as the changes seen in the measurements, the only measurement that would be affected by a repositioning of the reed would be the one shown at the top of Figure 5.18, as in the other measurements the reed was kept in place.

5.4.2 Results for note G_4

Figure 5.21 shows measurements done at a temperature of 20.5°C and 19.5°C and a relative humidity of 33% and 36%. Figure 5.22 shows a measurement done at a temperature of 18.5°C and a relative humidity of 44%. Again, these figures show two measurements in each plot (corresponding to the two measurements that were done on the same day), each of which is of a different colour. As can be seen in these plots, the measurements that were done on the same day were reproducible, as the difference between them is well inside their standard deviations. However, a comparison between measurements that were done in different days shows that both the pitch and spectral centroid changed in several ways, even in the cases where the relative humidity was within the tolerance of the instrument.

These results differ from the previous measurement shown in Figure 5.8 as there is a jump of about an octave in pitch between 5 and 7 kPa, as the chanter was overblown at these pressures. This is surprising as these types of bagpipes are not usually overblown. The shape of the spectral centroid curve is also very different. In the former measurement, the spectral centroid decreases as pressure increases, whereas in the latter measurements its shape is more like a letter "W", with the central peak at around 5.5 kPa.

Figure 5.21 shows two measurements done at similar relative humidity conditions. It was expected to have similar results when the relative humidity conditions were similar (33% for the top and 36% for the bottom). However, the bottom measurement seems to be more similar to that of Figure 5.22, even though the relative humidity in the latter Figure was higher (45%). For example, the pitch jump in Figure 5.22 happened at 5.5 kPa and at 7.5 kPa. The bottom measurement of Figure 5.21 shows that behaviour as well, but the pitch jump in the top measurement happened at 5 kPa and at 6.5 kPa. These changes do not seem to be correlated directly to variations in relative humidity.

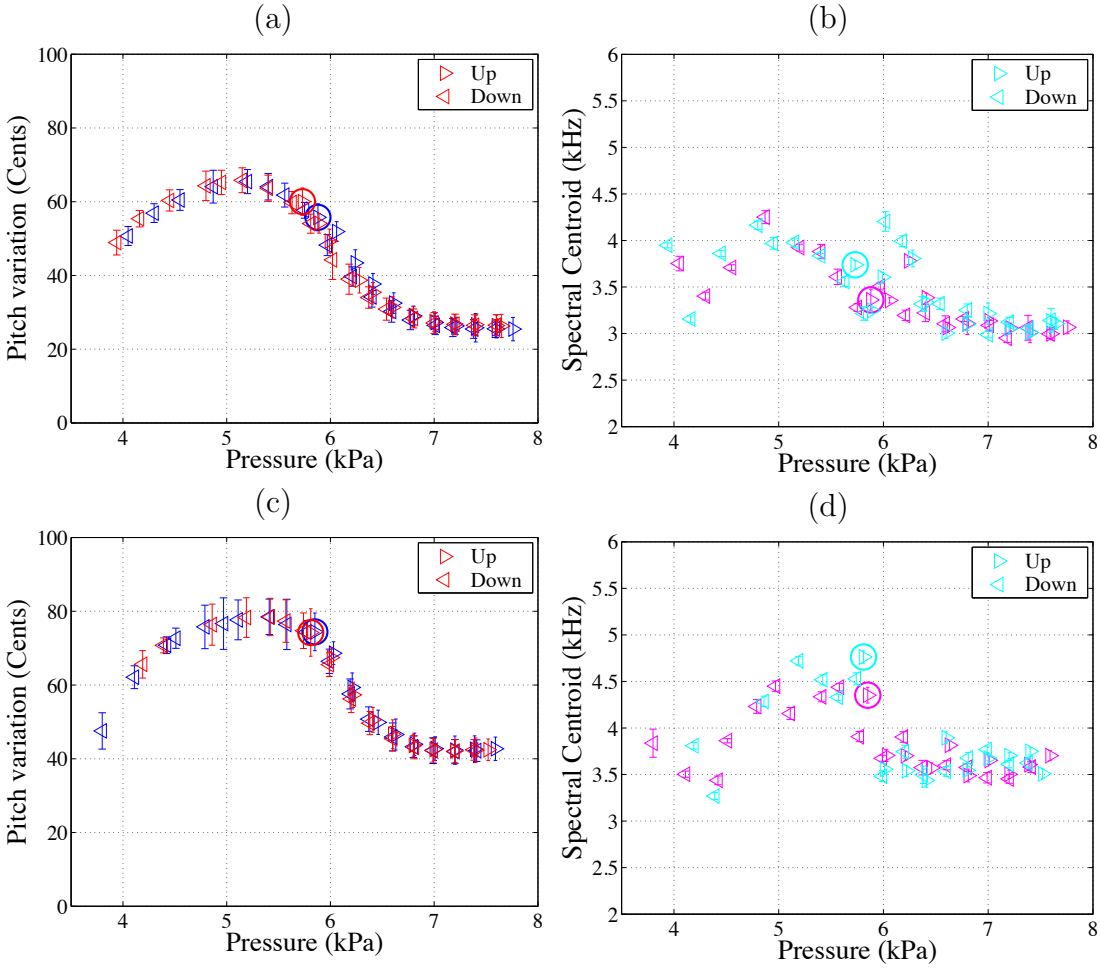

Figure 5.18: Variation of (left) pitch and (right) spectral centroid vs pressure for note D_5.
(top) Temperature = 18°C, relative humidity = 45%
(bottom) Temperature = 18.5°C, relative humidity = 44%.
Each colour represents one measurement

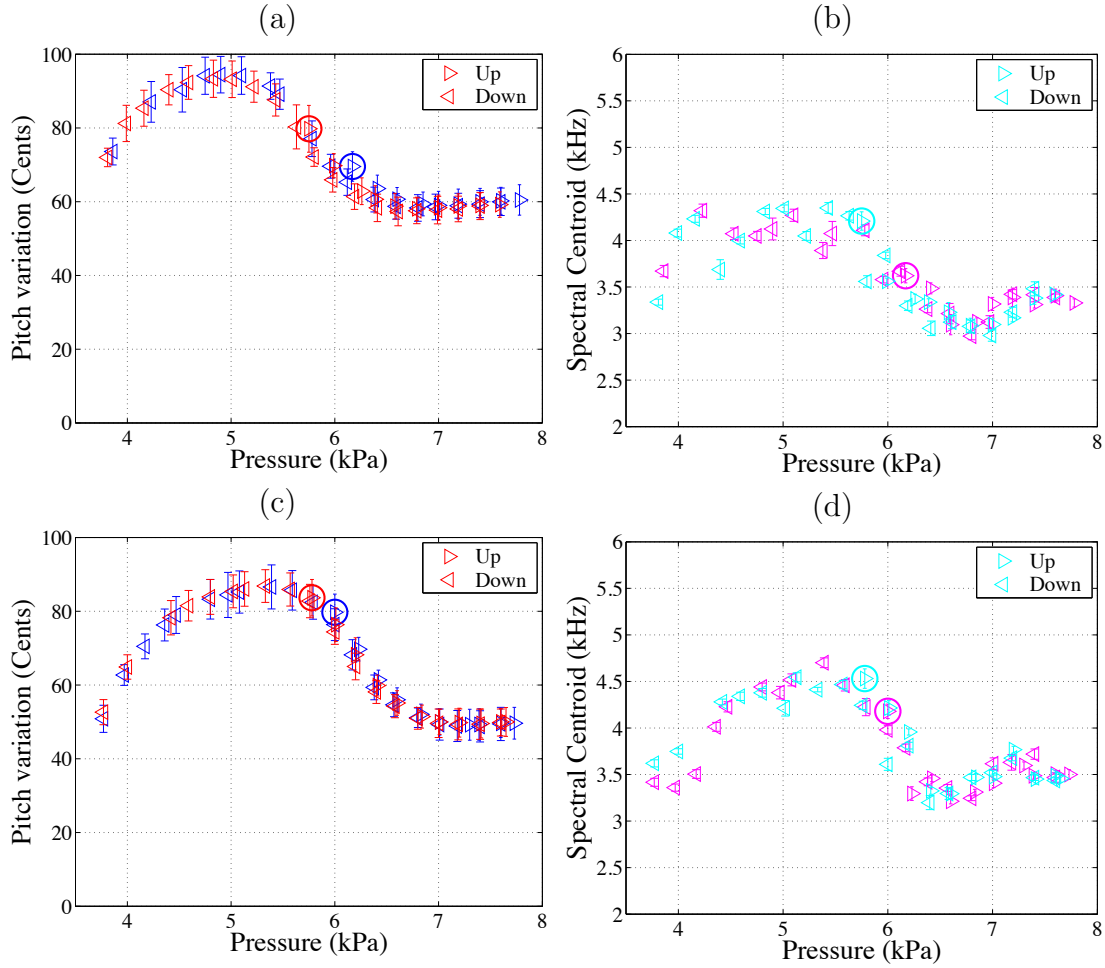

Figure 5.19: Variation of (left) pitch and (right) spectral centroid vs pressure for note D_5.
(top) Temperature = 20.5°C, relative humidity = 33%
(bottom) Temperature = 19.5°C, relative humidity = 36%.
Each colour represents one measurement

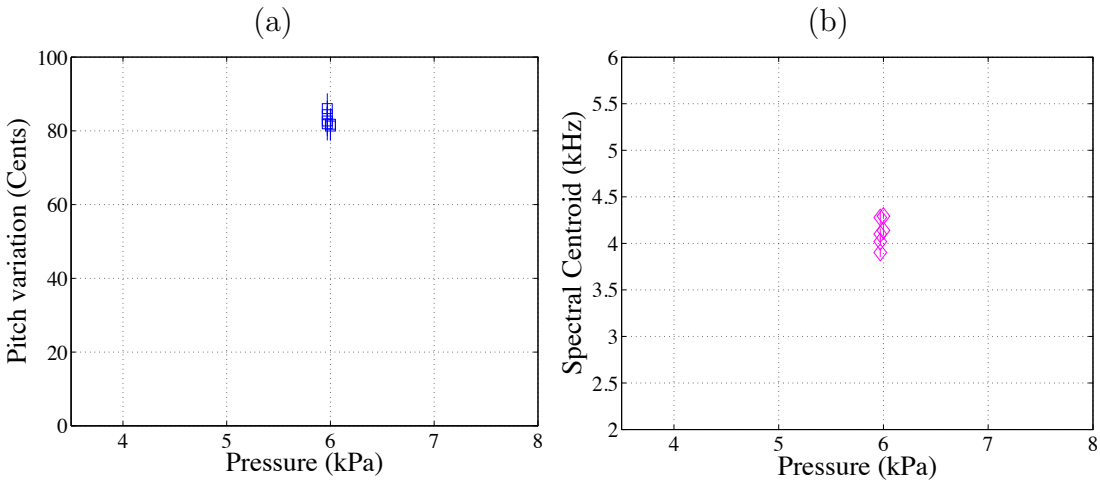

Figure 5.20: Variation of (a) pitch and (b) spectral centroid for note D_5 at a constant pressure of 6 kPa

It is worth noting that some of the notes recorded during this experiment had a strong beating, which is an acoustical phenomenon resulting from the interference of two sound waves of slightly different frequencies, where the number of beats per second equals the difference in frequency between the two notes [40]. In the two figures (5.21 and 5.22), there is a gap just above and below 5 kPa. All the notes in this region were those coming down, as the starting pressure was above 5.5 kPa in these measurements. In the spectral centroid curves two or three values are above most of all the others, and are just above 5 kPa. This is best seen in the bottom panel of Figure 5.21 and in Figure 5.22. These were some of the notes that had strong beating. This effect happened after the pitch had been high, then the notes started beating, and then the pitch finally stabilised in the low register. An example of one of these notes is shown in Figure 5.23. In this note, the beating frequency was around 30 Hz. Figure 5.24 shows the spectrum of this signal, and a zoom into the higher harmonics. The latter shows the presence of subharmonics at a frequency interval or around 30 Hz, showing a strong nonlinearity in the chanter and reed system.

Although some of the changes noted in the experiments performed with notes D_5 and G_4 could be attributed to variations in relative humidity, there are other factors that might be affecting the way the reed behaves. Some of them could be due to:

- Changes in geometry of the reed

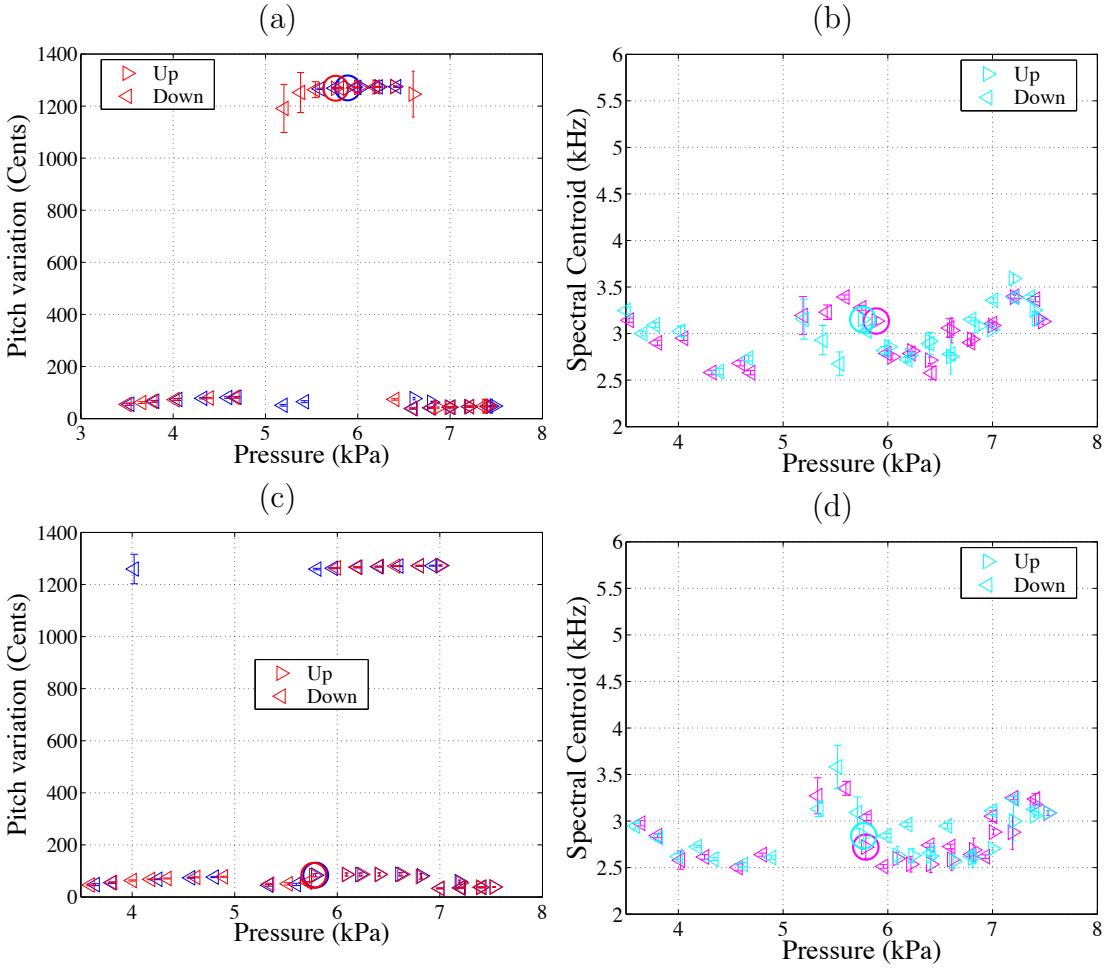

Figure 5.21: Variation of (left) pitch and (right) spectral centroid vs pressure for note G_4.
(top) Temperature = 20.5°C, relative humidity = 33%
(bottom) Temperature = 19.5°C, relative humidity = 36%.
Each colour represents one measurement

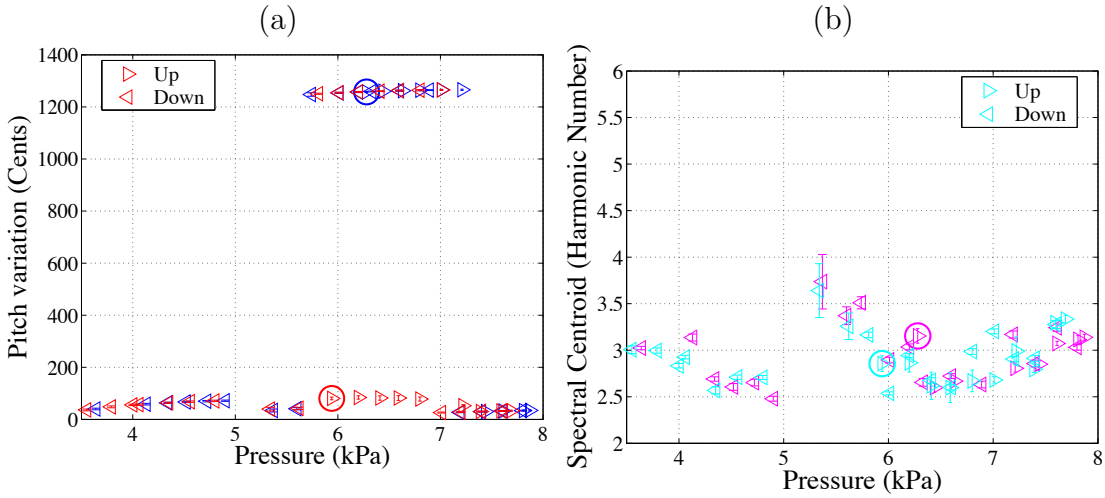

Figure 5.22: Variation of (a) pitch and (b) spectral centroid vs pressure for note G_4. Temperature = 18.5°C, relative humidity = 44%. Each colour represents one measurement

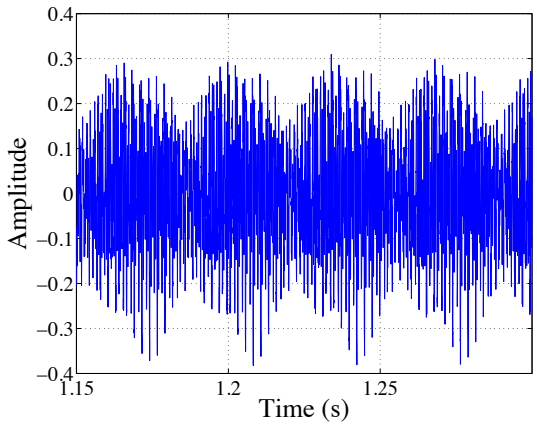

Figure 5.23: Time waveform of beating note. The beating frequency is around 30 Hz

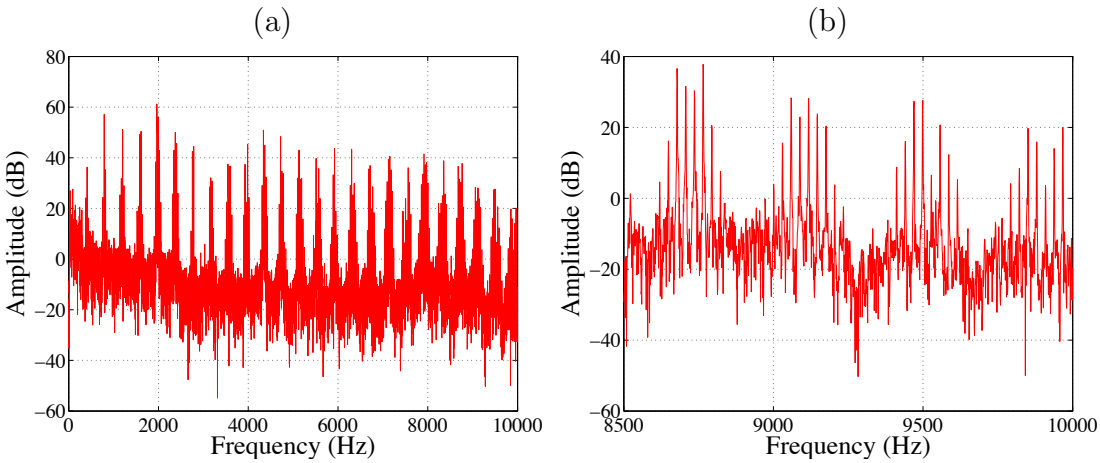

Figure 5.24: Spectrum of the beating note (b) Zoom of higher harmonics. Note the presence of subharmonics. The separation between subharmonics is around 30 Hz

- Ageing of the reed

- Moisture content of the reed. It is worth noting that this parameter is related to the relative humidity of the air that surrounds the reed, but because the cane will take certain time to absorb or release the moisture in order to reach an equilibrium state, the "instantaneous" relative humidity measurement (such as the one presented so far) would not necessarily reflect the moisture content that the reed actually had at the time of the measurement

None of these parameters were recorded in these measurements.

At this point it was hypothesised that the moisture content of the reed could be the source for the differences found so far. The moisture content of the reed depends on the relative humidity of the air around it. So it is possible that the relative humidity indeed affects the sound of this instrument, but in an indirect way. The first approach to proving this hypothesis was to measure a plastic reed, as it would not absorb/release moisture from/to the air around it, hence its moisture content would remain constant, and so would its own physical properties. Further on, Chapter 6 presents further evidence to support this hypothesis.

5.5 Measurement of pitch and spectral centroid curve vs pressure on a plastic reed at different relative humidity conditions

To make sure that the changes reported so far were due to variations in the moisture content of the reed, some more measurements were done with a plastic reed, as it would not absorb/release moisture from/to the air surrounding it, hence its physical parameters would remain constant with changing relative humidity.

The experimental setup was modified in several ways from that described in Section 5.3.1 when these measurements were taken. These measurements were done using a Brüel & Kjær PULSE data acquisition front-end hardware, which consists of a 4/2 channel input/output module type 3109 and la LAN interface module type 7533. A computer with the PULSE Labshop version 6.1 software for Windows 2000 was connected via the LAN interface.

There was a cardboard tube surrounding the chanter, with a hole through which a Brüel & Kjær microphone model 4938 was inserted. This accounts for the fact that the spectral centroid curves were different from those shown so far. The microphone was connected to the input module, and the data acquired by this card was transfered to the computer via the LAN connection. The sounds that were recorded were sampled at $f_s = 44.1$ kHz.

Figure 5.25 shows the results obtained from measuring a plastic reed on three different days with the following temperature and relative humidity conditions: 19.5°C and 37%, 18.3°C and 45%, 19°C and 31%. These figures show each measurement in a different colour, allowing direct comparison between measurements. Although the relative humidity conditions varied in these measurements as much as those made in Section 5.4, the curves of pitch and spectral centroid did not change significantly. Even though the experimental conditions were different, if there had been any effect of relative humidity on the behaviour of the plastic reed, it would have been reflected in these latter results.

This provides evidence that the amount of moisture that the cane reed has absorbed/released might be responsible for the variations in the pitch and spectral centroid curves shown in Section 5.4. As mentioned before, the moisture content of the reed is related to the relative humidity of the air that surrounds it, but by knowing the "instantaneous" relative humidity only, the moisture content of the

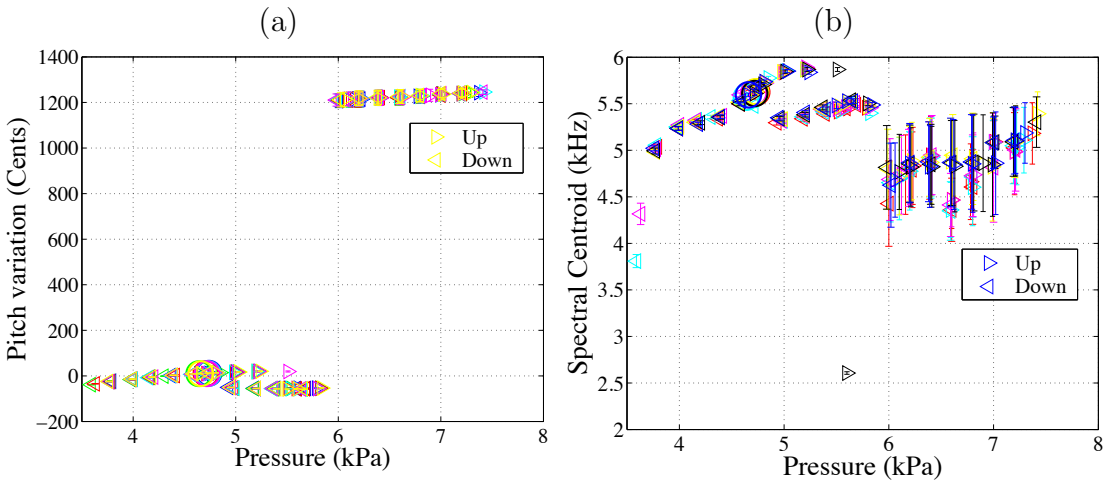

Figure 5.25: Variation of (a) pitch and (b) spectral centroid vs pressure for note D_5 played with a plastic reed at three different relative humidity conditions: 37%, 45% and 31%

reed cannot be predicted.

There was also a pitch jump in these measurements that did not happen in all the other measurements with the cane reed playing the note D_5. A reason for this could be that plastic reeds have different physical properties compared to cane reeds as hypothesised by Backus [5], hence its physical behaviour and the way the reed couples to the air column could account for the difference in the sound of the instrument.

5.6 Conclusions

A preliminary study carried out to find how the relative humidity from the player's breath affected the sound of the chanter while playing the bagpipe led to results that suggested that there are other parameters that affect the way this instrument sounds. A study of how the sound changes with blowing pressure was made. It was found that there is a complex relationship between pitch, spectral centroid, and blowing pressure, that involves hysteresis. Evidence of nonlinear behaviour was also found, as there were some cases where subharmonics were present, notes were beating, and jumps in pitch were observed. The measurements recorded on a given day were reproducible, but those made in different days differed significantly, when the reed used was the standard cane reed. This is possibly due to changes in moisture content, geometry, and ageing of the reed.

The fact that the results were independent of relative humidity conditions when the plastic reed was measured supports the hypothesis that the relative humidity affects the way the chanter and reed produce sound, even if this effect is indirect, i.e. by changing the moisture content of the reed.

The results also revealed that this instrument is played in the range in which significant variations in pitch take place when the pressure is changed only by a small percentage, which in turn allows for wide modulations in pitch and timbre.

In order to understand how the chanter and reed produce sound, it is important to know how the reed parameters such as stiffness and resonance frequency vary. SThis would also help to develop more realistic physical models. It has been shown how the relative humidity might have an indirect effect on the sound of the chanter and reed. The main hypothesis drawn is that the relative humidity would affect the moisture content of the reed, this being the reason for the changes in the sound shown so far. Chapter 6 presents how the reed parameters, both physical (stiffness, damping factor and resonance frequency) and psychoacoustic (pitch and timbre) change reproducibly with variations in moisture content.

Chapter 6

Effect of the reed moisture content on the physical behaviour of the reed, and on the psychoacoustics of the chanter sound

6.1 Introduction

Bagpipe chanter reeds, as well as oboe, bassoon and clarinet reeds, are traditionally made from the stem of the cane *Arundo donax*. This material has been used for this purpose since at least 3000 B.C. [10]. It is a common view among bagpipe players that humidity variations in the reed are responsible for its rapid degradation. Commercial products are available which claim to protect the bagpipe reed from mildew (too humid environment) and from splitting (too dry environment), by maintaining optimum moisture conditions [8].

Apart from the fact that humidity might reduce the lifetime of a reed, there are other questions that are worth investigating: Does relative humidity affect the produced sound of the chanter? Are those changes perceptible?

In Chapter 5 it was found that the pitch and timbre of a Scottish Border bagpipe chanter played by an artificial blowing machine varied significantly over

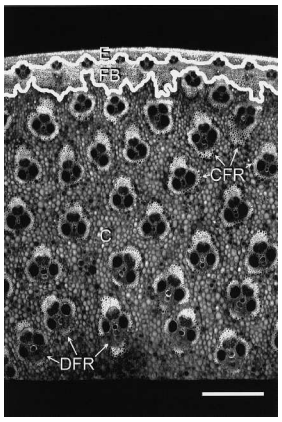

Figure 6.1: Confocal image of cross section through heel of clarinet reed manufactured from *Arundo donax*. E, epidermis and outer cortical cells; FB, fibre band; C, inner cortex; CFR, vascular bundles with continuous fibre rings; DFR, vascular bundles with discontinuous fibre rings. Bar=500 μm (taken from [54])

different days. It was hypothesised that this could be due to variations in relative humidity of the air around the reed, as this would affect its moisture content, thus its physical parameters, and in turn the sound produced by the instrument as a whole.

Work has been done on finding the properties of cane that make good reeds, including how relative humidity affects them. Kolesik et al. [54] gave 75 reeds to two clarinet players, who assessed the reeds as good, fair or poor. The reeds that received the same score by the two clarinet players were selected. The selected reeds were analysed by means of confocal laser scanning microscopy. The cane has three concentric rings of epidermis and outer cortical cells, fibre band, and an inner cortex (see Figure 6.1). They found that good reeds had vascular bundles with more fibre and less proportion of xylem (tissue that carries water up the root and stem) and phloem (tissue that carries organic nutrients, particularly sucrose to all parts of the plant where needed) compared to bad reeds (see Figure 6.2).

Glave et al. [39] analysed the cane of oboe reeds that were rated as good and bad by professional oboists. Preliminary observations using light microscopy and scanning electron microscopy showed that the cane of inferior reeds had more occluded vessels than that of superior reeds. They hypothesised that this could be due to disease or injury of the cane. They also scanned the cane using particle induced X-Ray emission, looking for concentration of specific chemicals in the

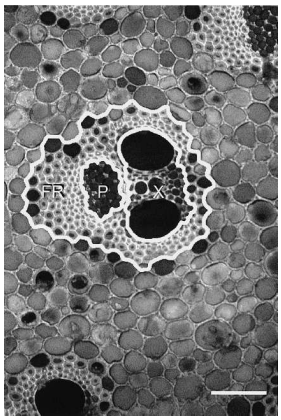

Figure 6.2: Confocal image of vascular bundle in inner cortex of clarinet reed manufactured from *Arundo donax*. FR, fibre ring; P, phloem; X, xylem. Bar=100 μm (taken from [54])

cane. They compared elemental maps (concentration of Si, P, S, Cl, K and Ca) of good and bad reeds. Their statistical tests revealed that there are no significant differences in chemical elements between good and bad reeds.

Obataya and Norimoto [65] studied the effect of natural extractives (glucose, fructose and sucrose) on the acoustic properties (stiffness and internal friction) and quality of the reed at different relative humidity conditions. The acoustic properties were measured under the following conditions: They removed the extractives of the reeds by soaking them in water for 4 days, and then dried them and steamed them. Then they impregnated the reed with glucose (the most abundant extractive found in cane). They measured the stiffness and the internal friction of the reeds at each stage of the process (untreated, water-extracted and glucose-impregnated). They found that the extractives enhanced the stiffness of the reed and increased the internal friction at high frequencies. The quality of the reeds was assessed as follows: They made a sensory test with 32 professional clarinet players. Each player was given 10 reeds and asked to assess their quality. After this evaluation, 4 of those reeds were water extracted, two of which were also impregnated with glucose. The quality of these 4 reeds was evaluated again. The results from these tests suggested that the extractives improved the tone quality, but that the quality of the extracted reeds could be recovered by glucose-impregnation.

It is well known amongst woodwind players that reeds change constantly. A

good reed today might be a bad reed tomorrow. Kolesik et al. [54] and Glave et al. [39] were looking in the anatomy of the reed for quality indicators. It is hard to see how the anatomy of a reed would change so dramatically from one day to the next, making what used to be a very good reed convert to a very bad reed in a matter of days, or even hours. The method they used for testing the reeds involved destroying them (making a cross section cut through the heel of the reed [54] or cutting 2 mm thick sections [39]). Is it possible then, to design a method for testing the quality of a reed, that does not involve destroying it? If this is the case, the source for these sudden quality changes must be identified first.

This Chapter presents how storing the reed under different humidity conditions affects both the physical parameters of the reed and the sound the chanter produces. The reed was stored inside test tubes where the relative humidity was being controlled, for 6 to 8 days. After this period, the reed was subjected to the following measurements:

1. Physical attributes of the reed
    - Stiffness
    - Resonance frequency and damping factor
2. Psychoacoustic attributes of the chanter sound
    - Pitch and timbre variation vs blowing pressure

At the end of the measurements, the reed was stored in another test tube, and the procedure repeated again.

Section 6.2 presents the method by which the relative humidity was controlled in the test tubes, as well as the relationship between the moisture content of the reed and the relative humidity. Section 6.3 describes the experimental setup and the results obtained in the measurements of the physical attributes of the reed. Section 6.4 presents how the pitch and timbre of the chanter sound vs pressure change with varying relative humidity.

6.2 Relationship between relative humidity and moisture content of the reed

The moisture content of wood depends on the relative humidity and temperature of the air that surrounds it. If wood remains long enough in air where the relative humidity and temperature remain constant, the moisture content will reach a constant value referred to as Equilibrium Moisture Content (EMC) [79].

It is standard practice in the timber industry to express the moisture content of wood as a percentage of the mass of the oven-dry wood [86]:

$$MC(\%) = \frac{W_f - W_d}{W_d} \times 100 \tag{6.1}$$

where W_f is the fresh weight of wood and W_d is the weight of oven-dry wood. It is possible to measure the moisture content of a bagpipe chanter reed by weighing it. As its dried weight will always be constant, relative changes in the moisture content can be observed by monitoring variations on the weight of the reed.

The method described in [35] was used to control the relative humidity of the air contained inside small test tubes. A small amount of a given salt solution (see table 6.1) was placed in the test tube. The reed was introduced inside the test tube, above the solution. The relative humidity inside the test tube was monitored using a Rotronic hygrometer model HygroPalm 2, with a 5 mm probe HygroClip SC05, which was also introduced in the test tube. The test tube was closed air tight (see Figure 6.4). The hygrometer was connected to a PC via an RS-232 cable, through which the hygrometer sent to the computer the measured values of temperature and relative humidity every minute. These values were saved in a file. Typical curves of relative humidity inside the tube vs time are shown in Figure 6.3. As the reed is introduced in a new relative humidity environment, it starts absorbing/releasing moisture from/to the air around it, until the reed and the environment reach an equilibrium state. From the plots shown in Figure 6.3, especially those corresponding to salts NaCl and K_2SO_4, it was decided that a period of at least 4 days (100 hours) was required to reach an equilibrium state. Under these grounds, it was decided to leave the reed inside the container for a period of 6 to 8 days.

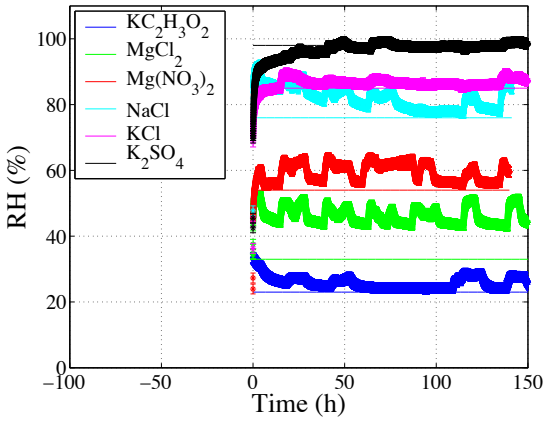

Figure 6.3: Typical curves of relative humidity vs time inside the containers for different salts. Straight lines correspond to values of humidity as in Table 6.1

After a period of 6 to 8 days, the reed was taken out of the test tube, and weighed. The measured values of relative humidity that had been saved in a file were averaged, giving a mean relative humidity at which the reed was stored during this period. Figure 6.5 shows the weight of the reed after this period vs the mean relative humidity.

When the reed was stored in the test tube containing K_2SO_4, the hygrometer measured 100% in several occasions, and the probe had condensation on it, thus the relative humidity was above the saturation point. This explains why the weight of the reed falls into a wide range, although it is always higher than in the case of any other salt. Figure 6.5 (b) shows a the mean and standard deviation of the measurements shown in Figure 6.5 (a) for the first five salts (excluding salt K_2SO_4). In all cases, the mean relative humidity observed was higher than that shown in Table 6.1 (see for example Figure 6.3), which was taken from [35]. These discrepancies could be due to variations in the amount of water with which each salt was prepared. As both the mean relative humidity and the weight of the reed were reproducible when the reed was stored in the same container, these discrepancies were considered irrelevant to this study.

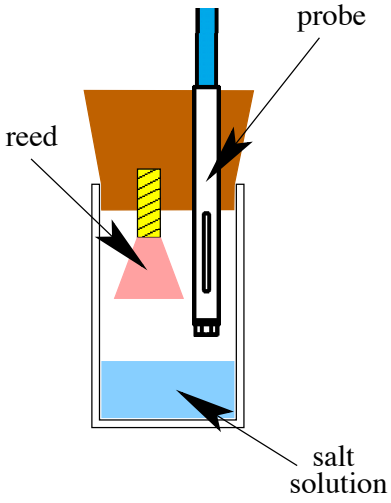

Figure 6.4: Test tube with an aqueous salt solution used for storing the reed in a controlled relative humidity environment

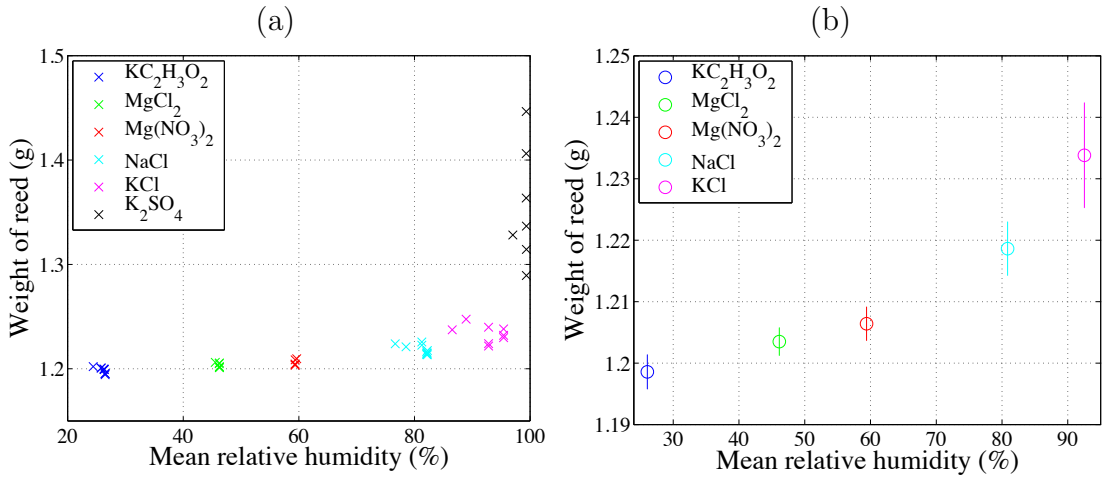

Figure 6.5: Weight of the reed vs mean relative humidity. (a) Shows independent measurements made in different occasions, and (b) shows the mean and standard deviation of these measurements for the first five salts

Salt	**Relative humidity (%)**
$KC_2H_3O_2$	23.1
$MgCl_2$	33.1
$Mg(NO_3)_2$	54.4
NaCl	75.5
KCl	85.1
K_2SO_4	97.6

Table 6.1: Salts that were used to control the relative humidity of the air enclosed in small test tubes, and the relative humidities associated with each of them, according to [35]

6.3 Measurements of the physical attributes of the reed

Almeida et al. [2] have provided evidence that the two blades of a double reed have symmetric displacement. This means that the motion of only one blade needs to be modelled as a simple damped harmonic oscillator, as described in Section 2.3:

$$\frac{\mathrm{d}^2 y}{\mathrm{d}t^2} + g_r \frac{\mathrm{d}y}{\mathrm{d}t} + \omega_r^2 y = -\frac{1}{\mu_r} \Delta P \tag{6.2}$$

where y is the displacement of the reed, g_r its damping factor, ω_r its resonance frequency, μ_r its mass per unit area, $\Delta P = p_m - p$, p_m is the pressure inside the mouth or wind cap and p is the pressure inside the reed. The stiffness k of the reed is

$$k = \mu_r \omega_r^2 \tag{6.3}$$

In order to be able to model the behaviour of the reed, it is necessary to know its physical parameters. Physical modelling provides a way of predicting how the instrument will behave. The following Sections describe the experiments done to measure the stiffness, resonance frequency, and damping factor of the reed.

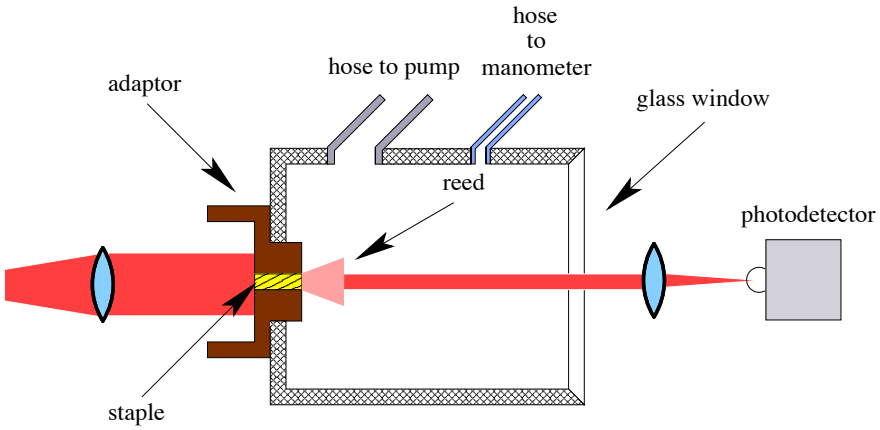

Figure 6.6: Experimental setup used for measuring the stiffness of the reed

6.3.1 Quasi-static regime: Stiffness measurement

The experimental setup for measuring the stiffness of the reed was based on experiments performed by Almeida et al. [3] on oboe reeds. The reed entrance was covered by a transparent plastic film. The reed was placed in an adaptor (see Figure 6.6), which was then inserted into the cavity of the artificial blowing machine (described in Section 5.3), where a pressure difference can be applied to the reed: The pressure inside the cavity acts on the blades of the reed, and as there is no flow through the reed, the pressure at the staple end is atmospheric.

The height of the reed opening was measured as follows: A HeNe HUGHES laser model 3225H-C with an Ealing spatial filter attached to it was placed on an optical rail. The laser beam was expanded into a collimated beam by means of a converging lens. Crossed polarisers were placed after the converging lens, in order to control the intensity of the beam. The artificial blowing machine was also placed on the optical rail, in such a way that the light from the collimated beam went through the reed slit opening. Another converging lens focused the light into a photodetector model IPL10530DAL, which gives a voltage proportional to the amount of light. Calibration tubes were built to investigate the relationship between the reed height opening and the voltage given by the photodetector. The dimensions of the calibration tubes were as follows: their inside and outside diameters were as those of the staple, the length was the total length of the reed plus staple. They were open on one end, and partially closed on the other end, except for a small rectangular slit. The width of this slit was as that of the staple

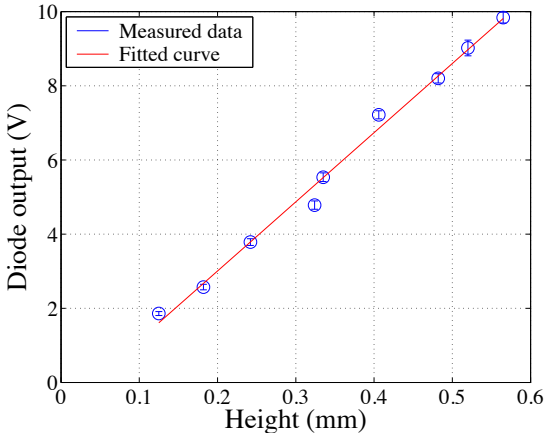

Figure 6.7: Linear relationship between the height opening of the calibration tubes and the voltage output of the photodetector

inside diameter. Different tubes had different slit height openings. Each tube was placed one at a time, and the voltage was recorded. The relationship between the slit height opening and the voltage is shown in Figure 6.7.

At the beginning of each measurement, the setup was calibrated as follows: The calibration tube with the biggest slit height opening (0.565 mm) was placed in the reed adaptor, inside the machine's cavity. The crossed polarisers were adjusted until the voltage measured from the photodetector was 9V (the photodetector saturated at 9.95 V). The calibration tube was replaced several times, and the voltage recorded. Then the calibration tube with the smallest slit height opening (0.125 mm) was placed several times, and the voltage recorded. The calibration curve was calculated from these measurements by doing a linear regression. The interquartile range of these measurements was the basis for the errors in the stiffness measurements.

After calibrating, the reed already covered was placed with its adaptor inside the machine's cavity. The pressure was increased from 0 to 7 kPa in steps of 1 kPa, and the voltage noted at each of these points. Then the pressure was decreased from 7 to 0 kPa in steps of 1 kPa, and the voltage recorded again. With this information, and with the aid of the calibration curve, the distance that each blade moved with pressure was calculated, and will be referred as δ. The stiffness was calculated as being the slope of the curve pressure vs δ. Note that there are two values of stiffness: One corresponding to the increasing pressure, and another

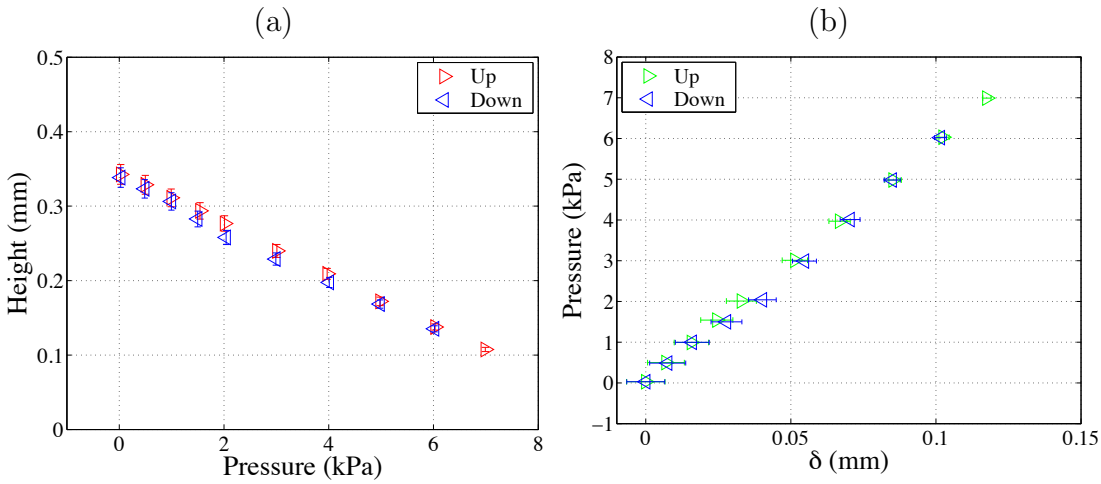

Figure 6.8: Curves of (a) height of opening of the reed vs photodetector voltage and (b) pressure vs δ observed for salt $KC_2H_3O_2$

to the decreasing pressure.

Three typical curves of height of opening of the reed vs photodetector voltage and of pressure vs δ are shown in Figures 6.8, 6.9 and 6.10. Figure 6.9 shows more deviation from a linear relationship than Figure 6.8. The latter had thus a smaller error in the stiffness measurement than the former. In some cases, for relative humidities higher than 80%, the reed approached closure, and the curve pressure vs δ showed some compression, as shown in Figure 6.10. In these cases, the stiffness was computed using only the first few samples, before the compression started to take place.

Figure 6.11 shows the measured values of stiffness vs mean relative humidity. These results suggest that there might be a decreasing trend as the humidity increases, but the uncertainties in these measurements are large, and this hypothesis needs further investigation. In particular, the results obtained with this particular experimental setup seemed to be very sensitive to the way each measurement was performed.

6.3.2 Frequency response and damping factor measurements

The equipment used for this measurements includes the PULSE system that was described in Section 5.5. The reed (uncovered) was placed in its adaptor,

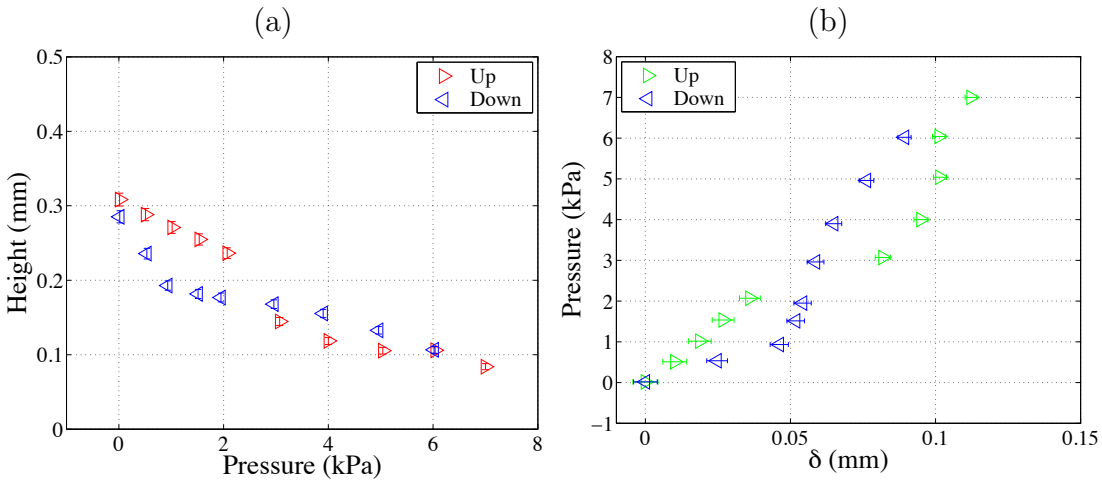

Figure 6.9: Curves of (a) height of opening of the reed vs photodetector voltage and (b) pressure vs δ observed for salt $KC_2H_3O_2$

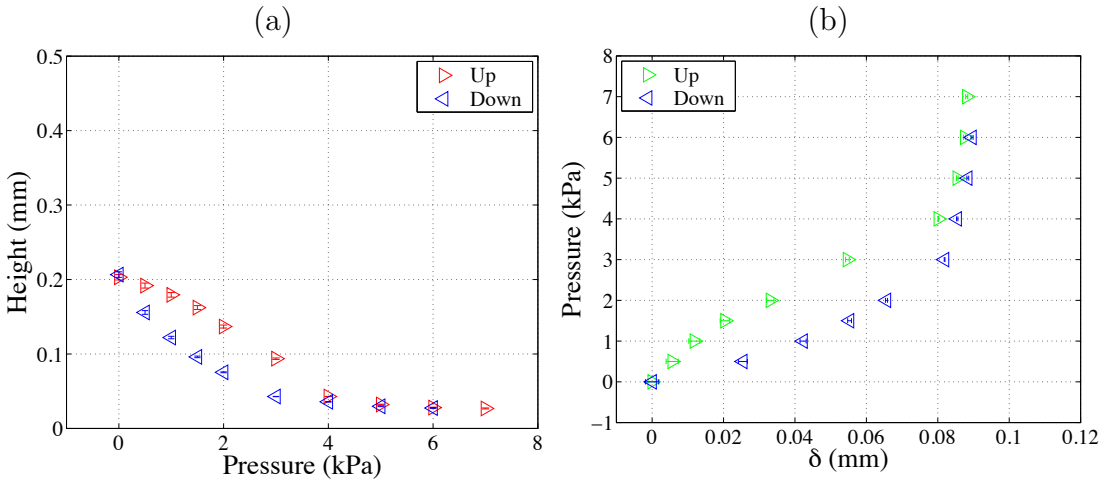

Figure 6.10: Curves of (a) height of opening of the reed vs photodetector voltage and (b) pressure vs δ observed for salt K_2SO_4

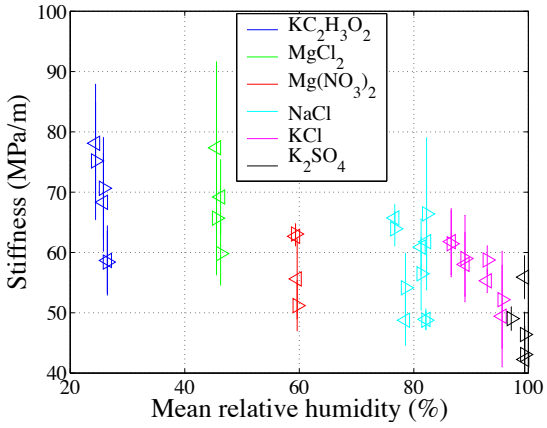

Figure 6.11: Stiffness vs mean relative humidity

attached to a Motorola loudspeaker model 42D87152HO1. A Brüel & Kjær $\frac{1}{2}$" microphone model 4133 was used to measure the pressure inside the adaptor, which served as the reference signal. A 2 mm probe was fixed to the microphone. A small hole of 2 mm diameter was drilled in the reed adaptor. This hole was placed so that when the probe was inserted, the end of the probe was at the bottom of the staple. The microphone was connected to one of the PULSE inputs. One of the PULSE outputs was connected to the loudspeaker, which generated a sinusoidal wave whose frequency varied linearly from 2 kHz to 6 kHz at a rate of 100 Hz per second. The motion of the reed was measured with a Polytec laser vibrometer that consists of a laser head model OFV 303 and a controller model OFV 3001. The controller gives a displacement output via a BNC connector, that was connected to one of the PULSE inputs. Figure 6.12 shows the experimental setup for this experiment. The PULSE software was set to calculate the cross-spectrum between the displacement of the reed and the microphone signal (reference). This cross-spectrum was later calibrated with the microphone/probe calibration data.

The resonance frequency was taken as that corresponding to a phase shift of $-90°$ between the reed displacement and the microphone signal, as this corresponds to an inward striking reed. This is in contrast to the discussion presented in Section 2.3.1, and in Figure 2.14, where the forcing pressure was set to $\Delta P = e^{j\omega t}$. But in this experiment the pressure is being applied inside the mouthpiece, and the pressure around the reed is atmospheric, so that $\Delta P = 0 - p$.

(a) (b)

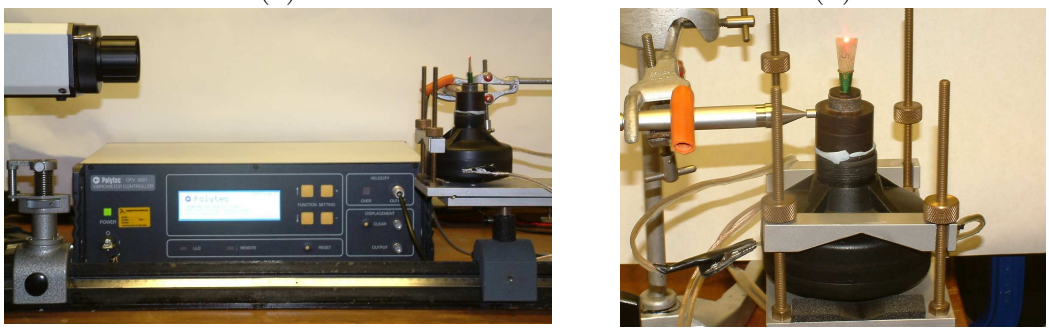

Figure 6.12: (a) Experimental setup to measure the frequency response of the reed and (b) a close up to the reed mounted in its adaptor

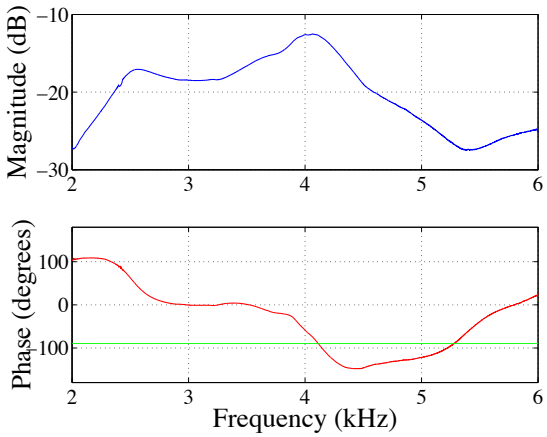

Figure 6.13: Typical frequency response of the reed under the conditions described for this experiment. In this case, the resonance frequency was taken to be 4.105 kHz, and the 3 dB bandwidth 350 Hz

In this case $p = e^{j\omega t}$, so that $\Delta P = -e^{j\omega t}$. Inserting this into equation 2.49, with the minus sign that corresponds to an inward striking reed, leads to a phase shift between the displacement and the driving force of $-90°$ at resonance. Figure 6.13 shows a typical curve resulting from this experiment.

Figure 6.14 shows the measured values of resonance frequency vs mean relative humidity. The error bars in this figure represent the 3 dB bandwidth of the resonance peak (damping factor [84]), which varied from 300 to 400 Hz in most cases, except from one measurement done at a relative humidity of 26%, which was 480 Hz. The errors of the resonance frequency were too small to be plotted. This Figure shows that the resonance frequency of the reed tends to decrease as the relative humidity increases, as predicted by Allan [1] and Carruthers [23].

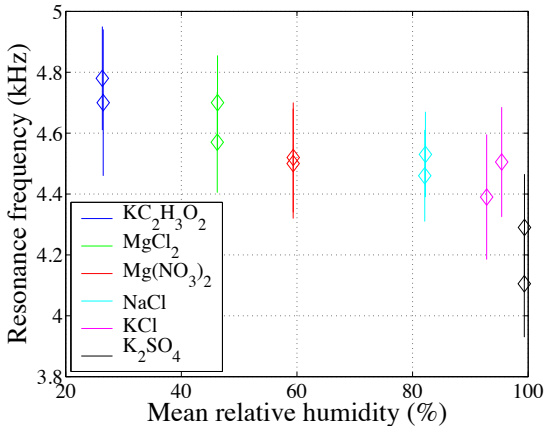

Figure 6.14: Resonance frequency vs mean relative humidity. The bars in these figure show the 3 dB bandwidth of each resonance peak

The damping factor seems to remain constant regardless of relative humidity.

6.4 Psychoacoustic attributes of the chanter sound: Pitch and timbre

The measurements of the radiated sound produced by the chanter at different blowing pressures were done using the artificial blowing machine (Section 5.3). All the sounds recorded correspond to the note D_5. The equipment used to record the radiated sound was the one described in Section 5.5. The pitch and spectral centroid measurements were calculated from the radiated sound as described in Section 5.3.2. The results of these measurements are shown in Figures 6.15 to 6.20. In all these figures, 0 cents corresponds to 586.67 Hz. The threshold pressure for each measurement is indicated in these figures by a circle. Measurements done in different days are shown in a different colour.

Let us first compare figures 6.15 and 6.20, which are the two extreme situations, corresponding to very low mean relative humidity (26%) and very high mean relative humidity (99%). The main differences between these curves can be summarised as follows:

1. The overall pitch is higher for low mean relative humidity

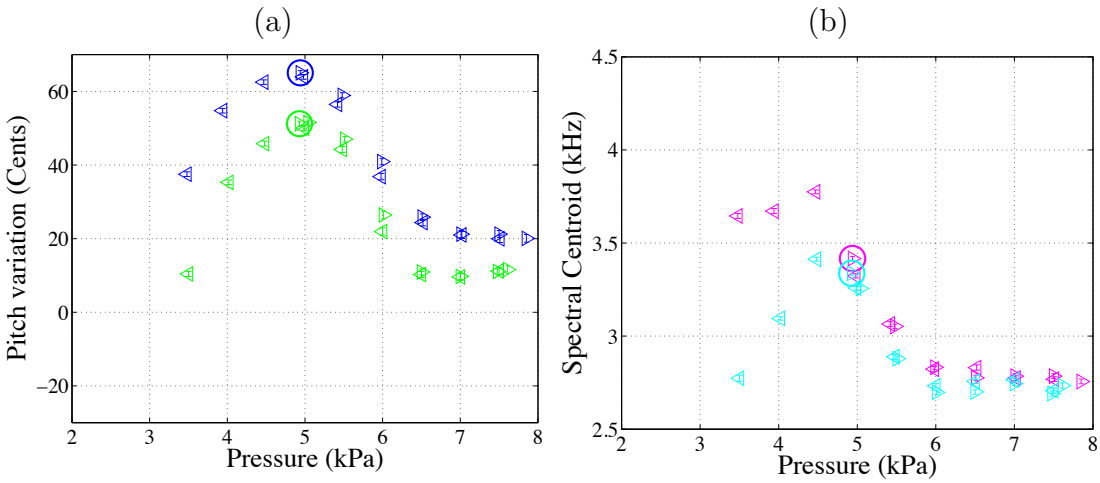

Figure 6.15: (a) Pitch and (b) spectral centroid variation of note D_5 corresponding to a mean relative humidity of 26% ($KC_2H_3O_2$)

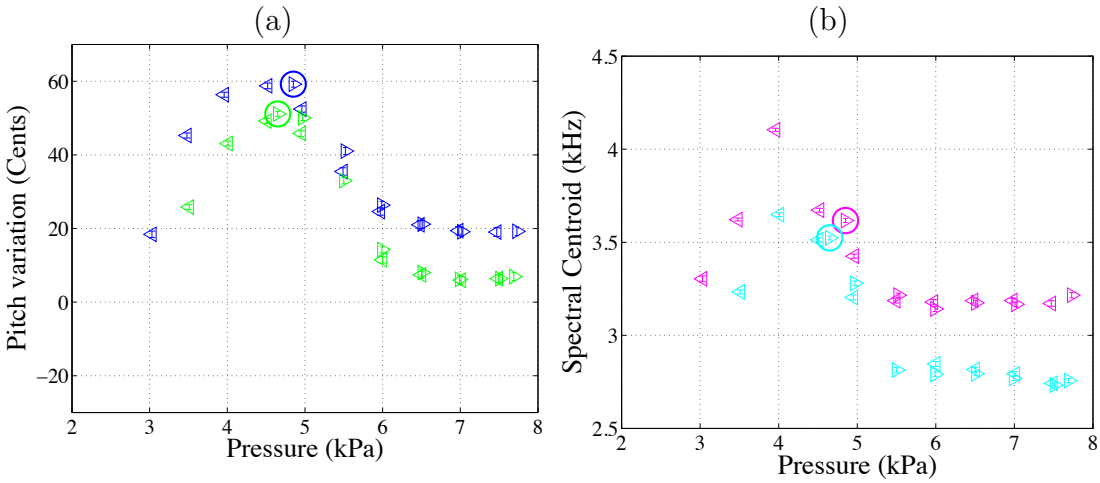

Figure 6.16: (a) Pitch and (b) spectral centroid variation of note D_5 corresponding to a mean relative humidity of 46% ($MgCl_2$)

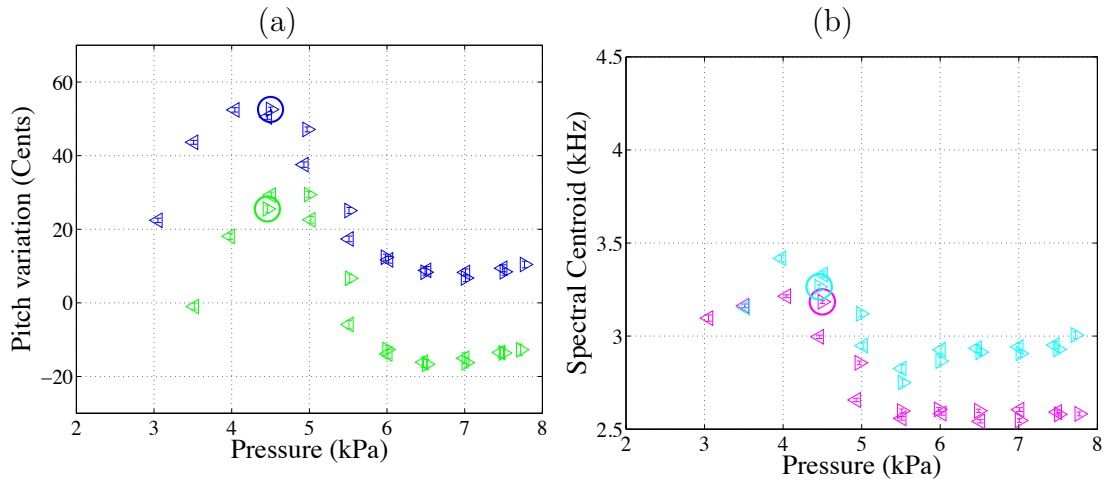

Figure 6.17: (a) Pitch and (b) spectral centroid variation of note D_5 corresponding to a mean relative humidity of 60% ($Mg(NO_3)_2$)

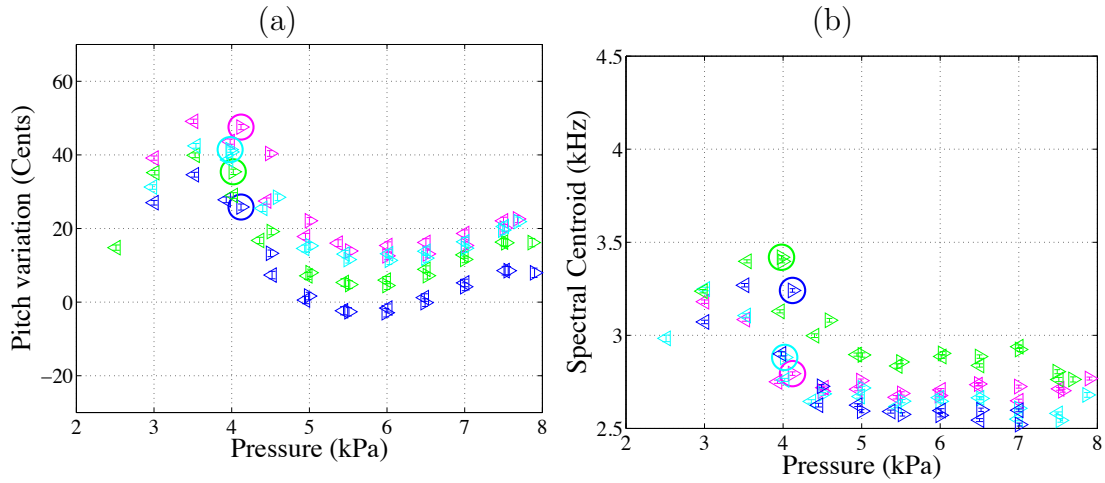

Figure 6.18: (a) Pitch and (b) spectral centroid variation of note D_5 corresponding to a mean relative humidity of 81% (NaCl)

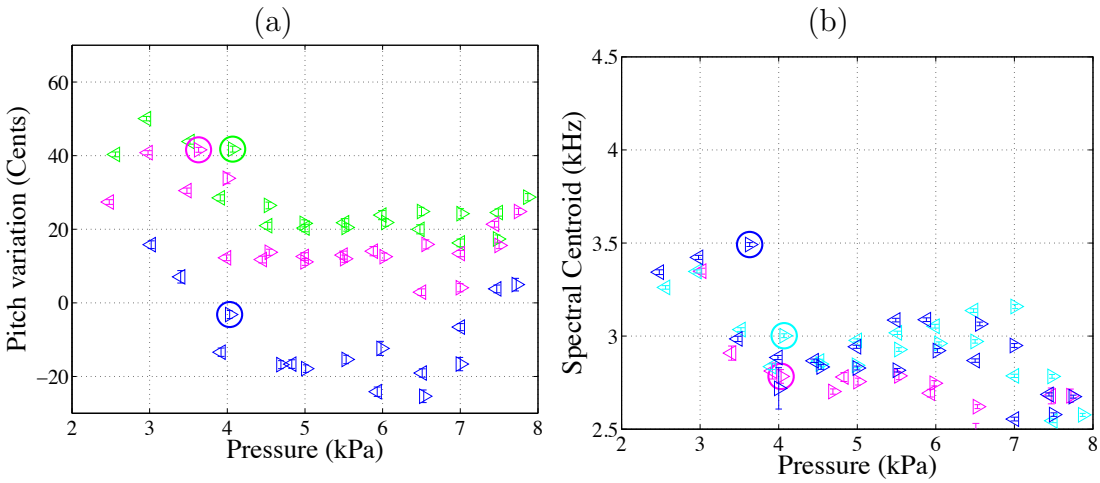

Figure 6.19: (a) Pitch and (b) spectral centroid variation of note D_5 corresponding to a mean relative humidity of 93% (KCl)

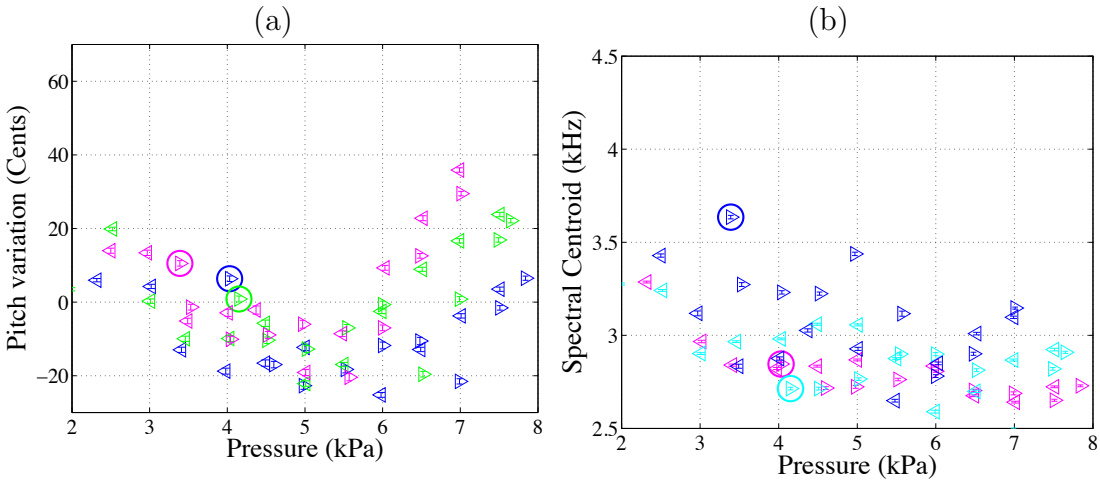

Figure 6.20: (a) Pitch and (b) spectral centroid variation of note D_5 corresponding to a mean relative humidity of 99% (K_2SO_4)

2. The pitch curve for low mean relative humidity rises with pressure up to 5 kPa; above this value it drops, stabilising at around 6.5 kPa. The pitch curve for high mean relative humidity decreases with increasing pressure, up to 5 kPa, and then it rises

3. The overall spectral centroid curve below 5 kPa is higher for low mean relative humidity

4. The spectral centroid curve for low mean relative humidity increases with pressure up to 4.5 kPa, then it decreases and stabilises at 6 kPa. The spectral centroid curve for high mean relative humidity remains almost constant with varying pressure

5. The threshold pressure at which the instrument starts to play is 4 kPa for high mean relative humidity, and 5 kPa for low mean relative humidity

A close inspection to the other results (Figures 6.16 to 6.19) reveals that these changes happen in a somewhat continuous manner, i.e. the pitch and spectral centroid curves, as well as the threshold pressure, drop gradually as the mean relative humidity increases. Moreover, the pitch variations are greater than 10 cents (just noticeable difference in pitch [75], see Section 3.2.6), and the spectral centroid variations are greater than $0.2f_a \approx 120$ Hz, which is what Kendall and Carterette [53] found to be the smallest change in spectral centroid that the human ear can perceive (see Section 3.4.5).

6.5 Conclusions

It was hypothesised that the relative humidity at which a bagpipe cane reed is stored affects its moisture content, thus its physical properties as well as the psychoacoustic attributes of pitch and timbre of the sound it produces when played with the chanter. A correlation between mean relative humidity at which the reed was stored and moisture content was found. Measurements of stiffness, resonance frequency and damping factor of the reed vs mean relative humidity were done. The stiffness measurements are at this stage inconclusive, as the measuring technique is not precise enough to show any particular trend. The measured values for resonance frequency show a definite lowering trend with

increasing mean relative humidity, as predicted by Allan [1] and Carruthers [23]. The damping factor seems to remain constant regardless of relative humidity.

It was shown that the psychoacoustic attributes were indeed affected by mean relative humidity. Measurements done after having stored the reed at certain mean relative humidities were reproducible, regardless of the fact that they were done on different days. These results suggest that the changes in pitch and spectral centroid reported in Chapter 5 and [21] were also due to variations in ambient relative humidity. A reduction of both the pitch and the threshold pressure needed to start playing the chanter was observed, as the mean relative humidity increases. The former corresponded to what Allan [1] and Carruthers [23] predicted.

Although the physical measurements done show little change with mean relative humidity, these small changes are enough to affect the psychoacoustic attributes significantly, as they are enough to be perceived by the human ear.

The question of whether the stiffness is affected by mean relative humidity remains unsolved. A different measuring technique that allows more precision and repeatability is necessary in order to answer this question.

The following Chapter presents the results of modelling the chanter and reed system using a harmonic balance technique [37]. The physical parameters measured in this Chapter serve as input parameters of the model, in an attempt to mimic the pitch and spectral centroid variation with mean relative humidity observed.

Chapter 7

Physical model and solution using the Harmonic Balance Method

7.1 Introduction

Physical modelling of woodwind instruments has been done primarily for the following purposes [85]:

- Increase of understanding of the underlying physical system
- Reconstruction of the sound through sound synthesis, which is both realistic and is able to imitate the control parameters of real instruments
- Help in design, modification and repair of existing instruments
- Aid in creation of new, possibly virtual musical instruments

The clarinet has been a popular instrument to model, as it consists of a cylindrical bore and a single reed, in contrast with the more complicated bores of brass instruments, and the double reed and lip reed mechanisms [51]. Helmholtz [45] formulated a theory on how the oscillations of wind instruments are sustained, focusing on the phase relationship between the pressure and volume flow in the mouthpiece that must be satisfied in order to maintain a self-sustained oscillation. Several models have been developed for the clarinet since Helmholtz. Backus [7]

developed a linear theory that explains some aspects of the oscillations of the clarinet. It predicted successfully the threshold pressure needed to start the oscillations of the clarinet, which depends on the stiffness of the reed, as well as the playing frequency of the instrument. Benade and Gans [16] pointed out the importance of including nonlinear effects, which explains how a wind instrument with non-harmonic air column resonances is able to produce a strictly harmonic sound. Nederveen [63] extended the work of Backus to include double reeds. Worman [89] developed what is known as Worman's theorem for the clarinet, which states that the amplitude of the N^{th} harmonic of the mouthpiece pressure p_n is related to the fundamental p_1 by $p_N \propto p_1^N$ [51]. Schumacher [77] extended Worman's model by including the fact that when the reed beats, the volume flow is blocked and can no longer provide air into the bore. Schumacher in [78] refined his model by including the possibility of calculating the transients of the oscillation. Later on, McIntyre et al. [57] extended Schumacher's work to other musical instruments, such as the violin and the flute.

Other more recent models of the clarinet include the work of Sommerfeldt and Strong [81], who modelled the reed as a non-uniform beam, and also included the effect of the vocal tract of the player; and the work of Facchineti et al. [29], who used a finite-element model for the reed and a lumped element model for the bore. Regarding more general modelling of woodwind instruments, models of bores have been developed by Benade [15] and Keefe [52], whereas finger holes have been studied by Benade [14] and Keefe [50]. More specifically into conical bores, Plitnik and Strong [69] present a method using transmission line theory to calculate the input impedance of an oboe, which includes the effect of tone holes. A model of a complete double reed conical instrument has been presented by Barjau and Agulló [11] for the "tenora".

Chapter 6 focused on measuring the physical properties (stiffness, resonance frequency and damping factor) of the chanter reed, and the psychoacoustic attributes (pitch and timbre) of the sound produced by the chanter and reed system for different relative humidity storage conditions. This Chapter presents a model of the chanter and reed system and a numerical solution through a software program `harmbal`, which predicts both the playing frequency and the spectrum of the mouthpiece pressure p of the instrument, given the reed parameters presented in Section 6.3, and the mouth pressure p_m. Section 7.2 presents the three main

equations that describe the chanter and reed system: that of the reed, air column and nonlinear coupling between the volume flow and the pressure difference across the reed. Section 7.3 describes how the equations from Section 7.2 are adapted to be used in the program `harmbal`, as well how they are solved by the program. Section 7.4 presents the characteristic curves that show the relationship between the pressure drop across the reed and the volume flow in the quasistatic regime of the reed, and indicates the theoretical minimum threshold mouth pressure $p_m = p_{th}$ to start the vibrations of the reed, as well as the minimum closing mouth pressure $p_m = p_M$ that is required to close the reed completely. This information is compared with the results obtained by `harmbal` in Section 7.5, which also describes how the model parameters were calculated, and the procedure to mimic the experiment described in Section 6.4, by doing a continuation in the mouth pressure p_m parameter. Results of the playing frequency and spectrum predicted by `harmbal` are compared to those obtained in Section 6.4.

7.2 Physical model

The chanter and reed system can be modelled as a self-sustained oscillator with a linear exciter (the reed) that is coupled nonlinearly to a linear resonator (the air column). This section presents the equations that were used to model these three components.

7.2.1 The reed

As mentioned in Section 6.3, the double reed can be modelled as a simple damped harmonic oscillator:

$$\frac{\mathrm{d}^2 y}{\mathrm{d}t^2} + g_r \frac{\mathrm{d}y}{\mathrm{d}t} + \omega_r^2 y = -\frac{1}{\mu_r} \Delta P \tag{7.1}$$

where y is the displacement of the reed, g_r its damping factor, ω_r its resonance frequency, μ_r its mass per unit area, $\Delta P = p_m - p$, p_m is the pressure inside the mouth or wind cap and p is the pressure inside the reed. The stiffness k of the reed is

$$k = \mu_r \omega_r^2 \tag{7.2}$$

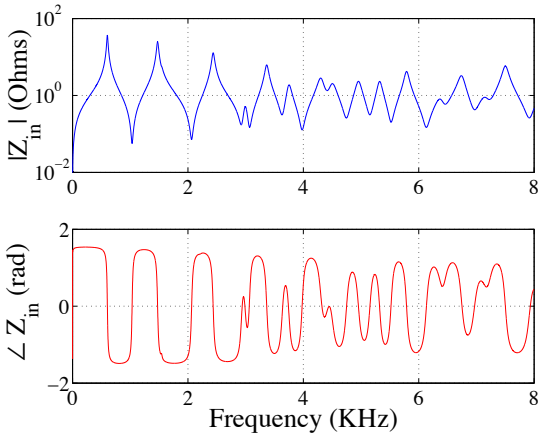

Figure 7.1: Input impedance of the air column fingered at D_5

This linear approximation only holds for non-beating reeds [36] [37].

The maximum negative value that y can take is $-h$ (see Figure 2.13 (a)), at which point the reed gap is closed and the air flow into the mouthpiece is completely blocked. This occurs when the mouth pressure p_m is equal or greater to the closing pressure p_M:

$$p_M = \mu_r \omega_r^2 h = kh \tag{7.3}$$

7.2.2 The air column

The air column is usually characterised by its input impedance, which describes the interaction between the volume velocity wave U and the pressure in the mouthpiece p. In the frequency domain:

$$P(\omega) = Z_{in}(\omega)U(\omega) \tag{7.4}$$

The input impedance of the chanter Z_{in} was calculated from the bore profile that was provided by the maker, using a transmission line model, as described in Section 2.2.5. It is shown in Figure 7.1. The first three resonances lie at: 604.1 Hz, 1475 Hz and 2437.75 Hz. The second resonance deviates from a harmonic relationship with the first by 132.9 Hz, and the third one by 207.9 Hz.

7.2.3 Nonlinear coupling

In Section 2.3.1 we derived equation 2.53, which relates the volume flow to the pressure difference across the mouthpiece in a nonlinear fashion:

$$U = w(y + h)\sqrt{\frac{2\Delta P}{\rho}} \tag{7.5}$$

where w is the width of the reed opening, and y is the displacement of the reed (see Figure 2.13 (a)).

7.3 Harmonic Balance Method

7.3.1 Introduction

Equations 7.1 (reed), 7.4 (air column) and 7.5 (nonlinear coupling) can be solved with the Harmonic Balance Method [36]. The Harmonic Balance Technique was developed initially to predict the spectrum of nonlinear forced-oscillatory systems [61]. Gilbert et al. [37] have extended its application to self-sustained oscillations.

To keep the equations as general as possible, equations 7.1, 7.4 and 7.5 are converted to dimensionless quantities, by substituting [36]:

$$\tilde{y} = \frac{y}{h} \tag{7.6}$$

$$\tilde{p} = \frac{p}{p_M} \tag{7.7}$$

$$\tilde{t} = t\omega_p \tag{7.8}$$

$$\gamma = \frac{p_m}{p_M} \tag{7.9}$$

where ω_p is the angular frequency of the first resonance peak of the air column. Similarly, equation 7.1 using dimensionless quantities becomes:

$$M\frac{\mathrm{d}^2\tilde{y}}{\mathrm{d}\tilde{t}^2} + R\frac{\mathrm{d}\tilde{y}}{\mathrm{d}\tilde{t}} + K\tilde{y} = \tilde{p} - \gamma \tag{7.10}$$

The parameters:

$$M = \left(\frac{\omega_p}{\omega_r}\right)^2 \tag{7.11}$$

$$R = \frac{\omega_p g_r}{\omega_r^2} \tag{7.12}$$

are the the dimensionless mass and damping respectively, and since the reed closes when $p_m = p_M$, $K = 1$ (dimensionless stiffness) [36].

Similarly, equation 7.5 becomes:

$$\tilde{U}(\tilde{p}, \tilde{y}) = \zeta(1 + \tilde{y})\sqrt{|\gamma - \tilde{p}|}sign(\gamma - \tilde{p}) \tag{7.13}$$

as long as $\tilde{y} > -1$, otherwise $\tilde{U}(\tilde{p}, \tilde{y}) = 0$ [36]. The "embouchure" parameter

$$\zeta = Z_0 wh\sqrt{\frac{2}{\rho p_M}} \tag{7.14}$$

is a parameter that characterises the mouthpiece [36].

Finally, the dimensionless form of the input impedance is obtained by:

$$\tilde{Z}_{in} = \frac{Z_{in}}{Z_0} \tag{7.15}$$

where

$$Z_0 = \frac{\rho c}{S} \tag{7.16}$$

S being the crosssectional area of the air column (cylindrical section) at the reed input. The dimensionless quantities in the frequency domain are:

$$\tilde{P}(\omega) = \tilde{Z}_{in}(\omega)\tilde{U}(\omega) \tag{7.17}$$

7.3.2 Principle of operation

The nonlinear problem (equations 7.10, 7.13 and 7.17) can be represented by the nonlinear function $\vec{F} = (\vec{P}, f)$, where $\vec{P}$ represents the real and imaginary parts of the mouthpiece spectrum for N harmonics, and f the playing frequency. $\vec{F}$ is solved by the Harmonic Balance Method, by treating the linear part in the frequency domain and the nonlinear part in the time domain. $\vec{P}$ is a complex vector with $2N + 2$ real components. However, the first harmonic is considered to be real, as phase shifts in the time domain do not affect the resulting signal. The total of unknowns is then $2N + 1$ for $\vec{P}$ plus the playing frequency f, giving a total of $2N + 2$ unknowns.

The iterative process followed by the Harmonic Balance Method is shown in Figure 7.2 [37]. The program starts from an initial vector $\vec{P}^0, f^0$ and after some iterations it converges to the solution $\vec{P}^\infty, f^\infty$ where:

$$\vec{P}^\infty, f^\infty = F(\vec{P}^\infty, f^\infty) \tag{7.18}$$

Solution to equation 7.18 can be found by searching for a root of:

$$\vec{G}(\vec{P}, f) = \frac{\vec{P}, f - \vec{F}(\vec{P}, f)}{P_1} \tag{7.19}$$

where the nonzero denominator avoids the trivial solution $\vec{P} = 0$. The solution of equation 7.19, if convergence is achieved, will be a periodic solution of equations 7.10, 7.13 and 7.17.

A realisation of the Harmonic Balance Method applied to self-sustained musical instruments has been developed by Snorre Farner [30] in a computer program called `harmbal`. This program uses the iterative Newton-Raphson method in order to solve equation 7.19. The results presented in the following sections of this Chapter were calculated using `harmbal` version 1.27b, provided by Snorre Farner [30], the author of the program.

7.4 Characteristic curves

In Section 2.3 the characteristic equation that shows the relationship between volume flow and pressure for low frequency regimes (quasistatic behaviour) for an inward striking reed was presented (equation 2.59):

$$U = S_r \left[1 - \frac{\Delta P}{h\mu_r\omega_r^2}\right] \sqrt{\frac{2|\Delta P|}{\rho}} sign(\Delta P) \tag{7.20}$$

where $S_r = wh$ is the area of opening of the reed at equilibrium. This equation equates to equation 7.5 as in the quasistatic regime $y = -\frac{\Delta P}{k}$ (see Section 2.3.1, equation 2.57). From the measurements presented in Section 6.3 (Figures 6.11 and 6.14), the characteristic curve of volume flow vs pressure can be calculated for each of the values of stiffness k, which correspond to each of the mean relative humidity conditions at which the reed was stored. These characteristic curves are shown in Figure 7.3.

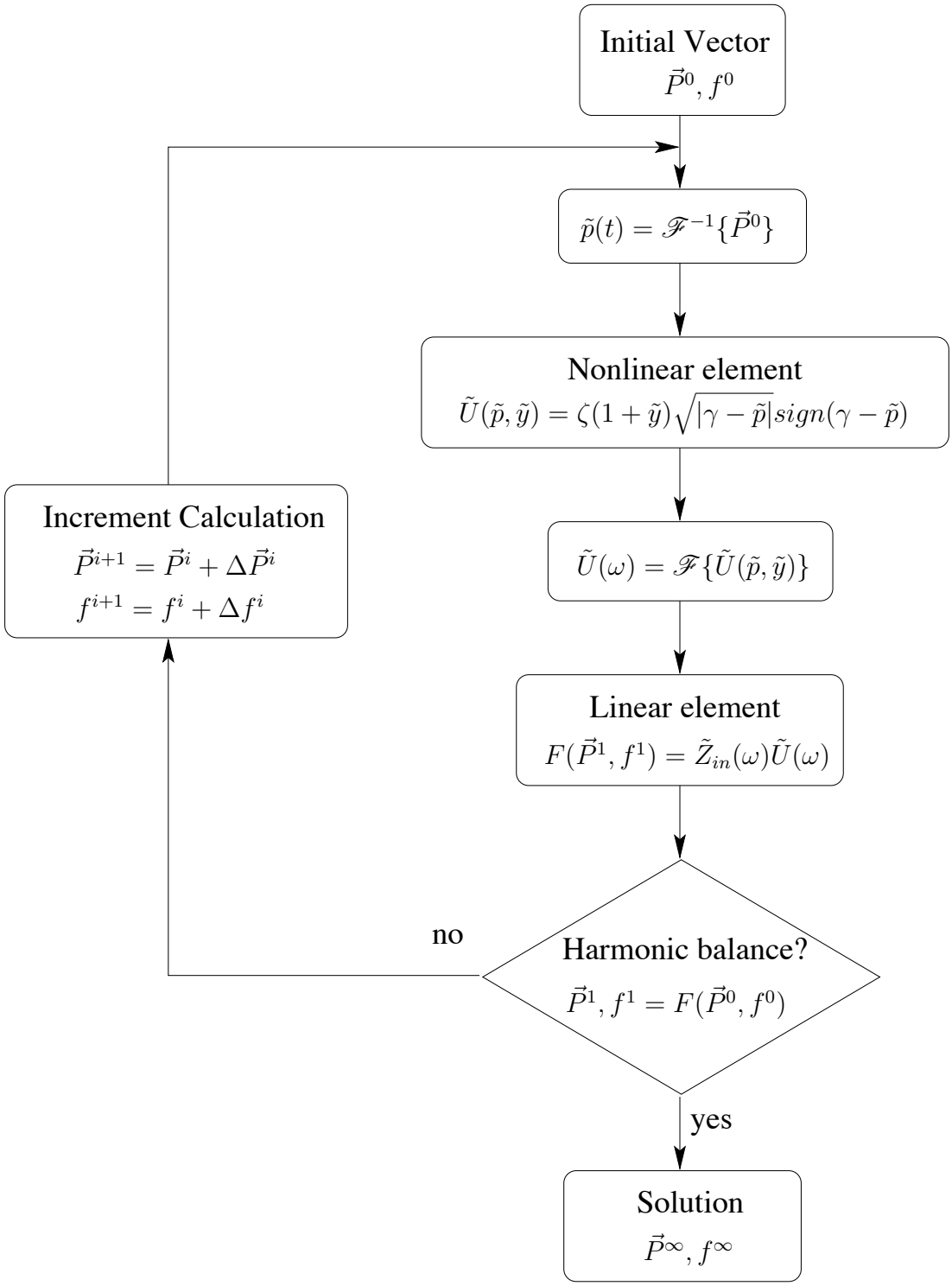

Figure 7.2: Diagram of the harmonic balance method applied to self-oscillatory systems. $\mathscr{F}\{\}$ and $\mathscr{F}^{-1}\{\}$ are the Fourier transform and inverse Fourier transform respectively. Adapted from [37]

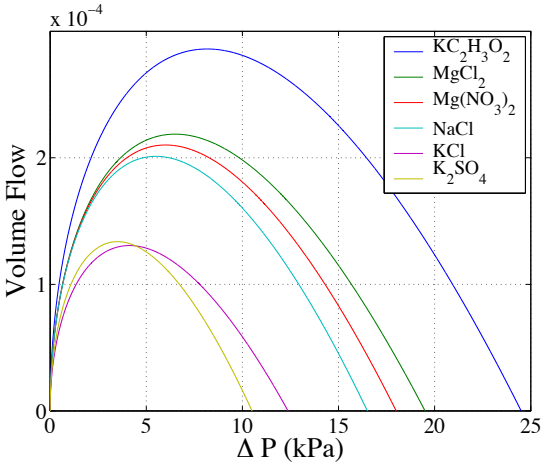

Figure 7.3: Characteristic curve of volume flow vs pressure for the values of stiffness measured in Section 6.3, which correspond to each of the humidity conditions at which the reed was stored

In Section 2.3.1 it was established that in order for the reed to act as an active generator, thus supply energy to the system, the slope of the characteristic curve must be negative. Following this, the threshold pressure p_{th} is defined as the pressure where the characteristic curve is at its maximum, and it corresponds to $p_{th} = \frac{p_M}{3}$ [66]. Table 7.1 shows the values of k and h that were used to calculate the curves in Figure 7.3 (taken from the experimental results presented in Section 6.3), as well as approximate values of threshold mouth pressure p_{th} and closing mouth pressure p_M, estimated from Figure 7.3.

Salt	k $\left(\frac{\text{MPa}}{\text{m}}\right)$	h (mm)	p_{th} (kPa)	p_M (kPa)
$KC_2H_3O_2$	70	0.35	8	25
$MgCl_2$	65	0.3	6.5	20
$Mg(NO_3)_2$	60	0.3	6	18
NaCl	55	0.3	5.5	16.5
KCl	55	0.225	4	12.5
K_2SO_4	45	0.25	3.5	10.5

Table 7.1: Approximate values of threshold pressure p_{th} and closing pressure p_M, estimated from Figure 7.3, and corresponding values for stiffness k and height of opening at rest h, taken from the experimental results presented in Section 6.3

7.5 Physical modelling using `harmbal`

The following Sections present how the program `harmbal` was used to solve the physical model presented in Section 7.2. A comparison of these results with the results obtained in Chapter 6 is also discussed.

7.5.1 Parameter calculation

In order to calculate the parameters from equations 7.11, 7.12, 7.14, and 7.16 that the program `harmbal` needs, the speed of sound and the density of air were taken to be $c = 343.37\frac{\mathrm{m}}{\mathrm{s}}$ and $\rho = 1.2\frac{\mathrm{kg}}{\mathrm{m}^3}$ respectively (values corresponding to a temperature of $T = 20°\mathrm{C}$).

Z_0 (equation 7.16) was calculated taking into account the fact that the entrance of the chanter is a cylindrical section of diameter 4.7 mm, giving $Z_0 \approx 2.4 \times 10^7 \frac{\mathrm{Pa{\cdot}s}}{\mathrm{m}}$. The first resonance of the air column ω_p was determined by close inspection of Figure 7.1 to be 3796 $\frac{\mathrm{rad}}{\mathrm{s}}$.

Table 7.2 shows the values of k, ω_r, g_r and h that were measured from the reed for each salt (see Section 6.3), and its corresponding R, M and ζ parameters calculated from equations 7.9, 7.11, 7.12 and 7.14 respectively. The units used for calculating these parameters were: $k\left[\frac{\mathrm{Pa}}{\mathrm{m}}\right]$, $\omega_r\left[\frac{\mathrm{rad}}{\mathrm{s}}\right]$, $\omega_p\left[\frac{\mathrm{rad}}{\mathrm{s}}\right]$, $g_r\left[\frac{\mathrm{rad}}{\mathrm{s}}\right]$, H [m] and p_m [Pa].

Salt	k $\left(\frac{\mathrm{MPa}}{\mathrm{m}}\right)$	ω_r $\left(\frac{\mathrm{krad}}{\mathrm{s}}\right)$	g_r $\left(\frac{\mathrm{krad}}{\mathrm{s}}\right)$	h (mm)	R ($\times 10^{-3}$)	M ($\times 10^{-2}$)	ζ ($\times 10^{-1}$)
$KC_2H_3O_2$	70	30.16	2.51	0.35	1.6693	1.5842	7.2309
$MgCl_2$	65	28.9	2.01	0.3	1.4541	1.7250	6.9472
$Mg(NO_3)_2$	60	28.27	2.26	0.3	1.7094	1.8025	7.2309
NaCl	55	28.27	1.88	0.3	1.4245	1.8025	7.5524
KCl	55	27.96	2.42	0.225	1.8694	1.8432	6.5406
K_2SO_4	45	26.39	2.2	0.25	1.9078	2.0692	7.8896

Table 7.2: Parameters R, M and ζ calculated from the measured reed parameters of k, ω_r, g_r and h for each relative humidity conditions at which the reed was stored (see Section 6.3)

With the version of `harmbal` used, the user is able to specify an input impedance through an input file to the program. This input impedance must be normalised

(i.e. as in equation 7.15). The input impedance that was input to the model is the one shown in Figure 7.1.

The program `harmbal` needs the parameters R, M and ζ presented in Table 7.2, and an initial estimate of $\vec{P}^0$ and f^0. Initially, an example file provided by Snorre Farner [30] was used, which converges for 1 harmonic. The parameters M, R and ζ from this file were changed gradually to those corresponding to each of the reed parameters for the different salts in Table 7.2 until convergence was acheived. The input impedance file was also introduced. Then the number of harmonics N was increased one by one until $N = 12$. The initial γ value for which convergence was found was 0.35. This initial file was called `0.pmt`.

7.5.2 Continuation in the parameter γ

In Section 6.4 an experiment was performed in which the blowing pressure was varied, and the radiated sound of the chanter and reed was recorded. Further analysis resulted in curves of pitch and spectral centroid vs blowing pressure.

In the program `harmbal` continuation refers to the use of one solution $\vec{P}^\infty, f^\infty$ as the initial vector $\vec{P}^0, f^0$ to calculate the next when varying a parameter [36]. We chose to vary the parameter γ, which is the dimensionless form of the mouth pressure, in order to compare the results given by the model with those presented in Section 6.4.

In order to do the continuation in γ, a MATLAB program was written. The flow chart of this program is shown in Figure 7.4. The following variables were used:

- `STEP`: This is the default amount that the parameter γ increased or decreased between solutions. It is a constant whose value is `STEP=0.001`
- `step`: This is the current step size for this iteration
- `thisgamma`: This is the current γ value, being tested for convergence. It was initialised to `thisgamma=0.35` at the start of the program, since the starting file `0.pmt` converged for this value
- `fraction`: This is an auxiliary variable that is used for varying the size of `step`, by doing `step/fraction` or `step*fraction`. Its initial value was `fraction=2`

With the following command

```
harmbal -f thisfile.pmt -i TL.imp -o (thisfile+1).pmt -c gamma
thisgamma+step
```

`harmbal` takes the file `thisfile.pmt` (initially `0.pmt`), and tries to find convergence for a γ value of `thisgamma+step` using the impedance specified in the file `TL.imp` (see Figure 7.1). If convergence is achieved, `harmbal` stores the results in the file `(thisfile+1).pmt`. If there is convergence, and it converged in more than 0 iterations, the following variables are changed:

- `thisfile=thisfile+1`
- `thisgamma=thisgamma+step`

and the process is repeated. If `harmbal` found convergence in 0 iterations, it is assumed that the step used was too small to make a difference, so the step is reset into its original value (`step=STEP`). If there is no convergence, the value `step` is reduced by dividing it over the value `fraction` (`step=step/fraction`). If `step<1x10`$^{-10}$, then step is reset to the default value (`step=STEP`), and the `fraction` value is changed to the next prime number until 101. This is to ensure that different values of γ in between `thisgamma` and `thisgamma+STEP` are tried, until convergence is achieved. After 101, it resets back to two, `step` is reset to the default value (`step=STEP`), and `step` is now calculated as `step=step*fraction` instead. This is because sometimes it is possible to jump over a region of poor convergence by setting a bigger step. The program was stopped as soon as the reed started beating, which corresponded approximately to values of $\gamma = 0.5$ [36].

We also tried to go down in γ, to that value at which the chanter started vibrating in the experiments. However, these values are well below 0.35, which approximately corresponds to the threshold of oscillation [26]. We achieved convergence only for values close to 0.35.

7.5.3 Results

Playing frequency and spectrum

Plots of playing frequency f and amplitude of the first 4 harmonics $|p_1|$ to $|p_4|$ that `harmbal` predicted for the γ values where convergence was found, are shown

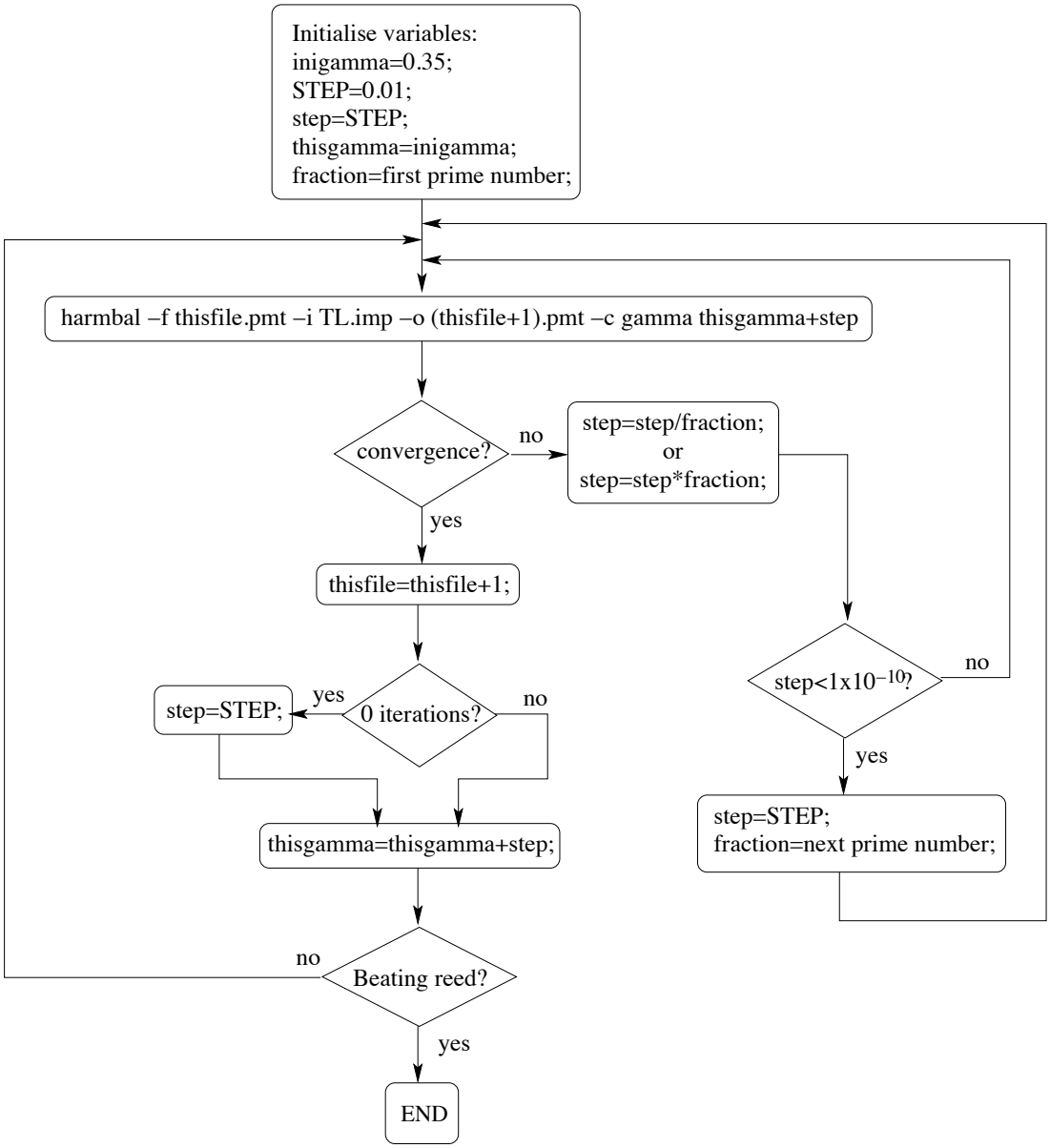

Figure 7.4: Flow chart of MATLAB program used to do the continuation of the parameter γ. This flow chart shows the case for increasing γ. For decreasing γ, `thisstep` is decreased, and the condition of "Beating reed?" changes for `thisgamma`<`mingamma`, where `mingamma` was the pressure at which the chanter started vibrating in the experiments

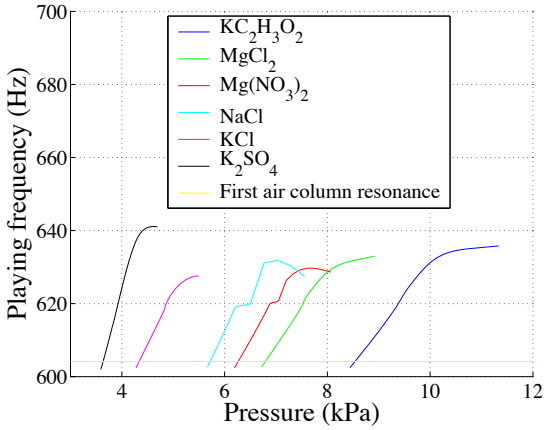

Figure 7.5: Playing frequency curves predicted by `harmbal`

in Figures 7.5 to 7.8. These plots stop at the point where the reed starts beating [36]. The frequencies that `harmbal` predicts for γ values close to the threshold pressure p_{th} are slightly below the first resonance of the air column. For increasing γ values, the nonlinearities start to have an effect on the behaviour of the chanter and reed system, and an increase in playing frequency f is observed.

The pressures where `harmbal` found convergence are well within the theoretical limits calculated with equation 2.59, and presented in Table 7.1. In fact, the lowest pressure at which `harmbal` found convergence corresponds closely to the threshold pressure p_{th} predicted by the theory (Figure 7.3 and Table 7.1).

A close inspection at the spectra shows that for pressures close to the threshold pressure p_{th}, the first harmonic dominates, and as pressure increases, higher harmonics slowly start to build up. This is because for low pressures, the nonlinearity of equation 7.13 is small, thus resulting in a purely sinusoidal response. As the pressure increases, the nonlinearity starts to build up, increasing the amplitude of higher harmonics.

Spectral centroid

As `harmbal` predicts the mouthpiece spectrum, it is possible to calculate the radiated spectrum by multiplying the latter by the transfer function of the chanter, which was measured experimentally. This was done using the artificial blowing machine with the setup described in Section 5.5. The chanter without the reed

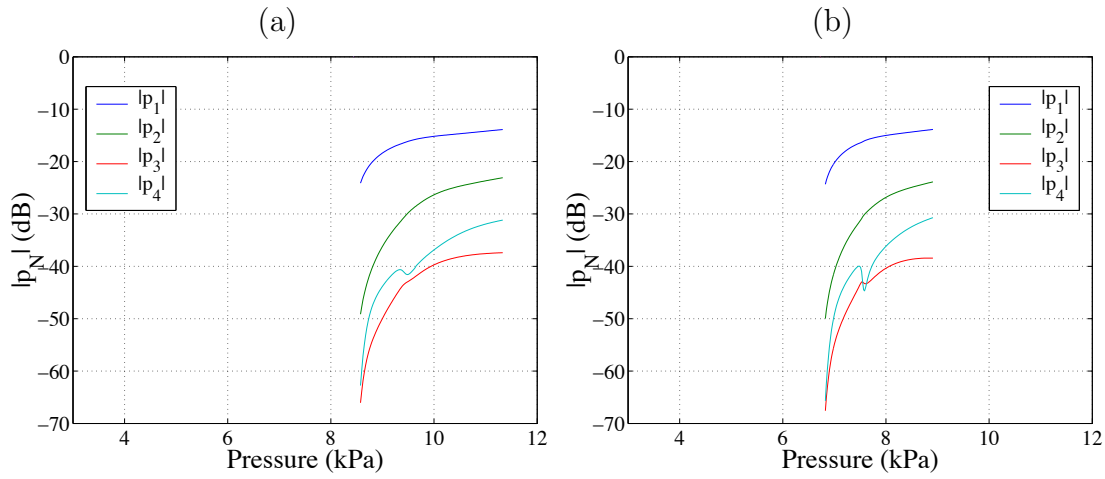

Figure 7.6: $|p_N|$ predicted by `harmbal` for salts (a) $KC_2H_3O_2$ and (b) $MgCl_2$

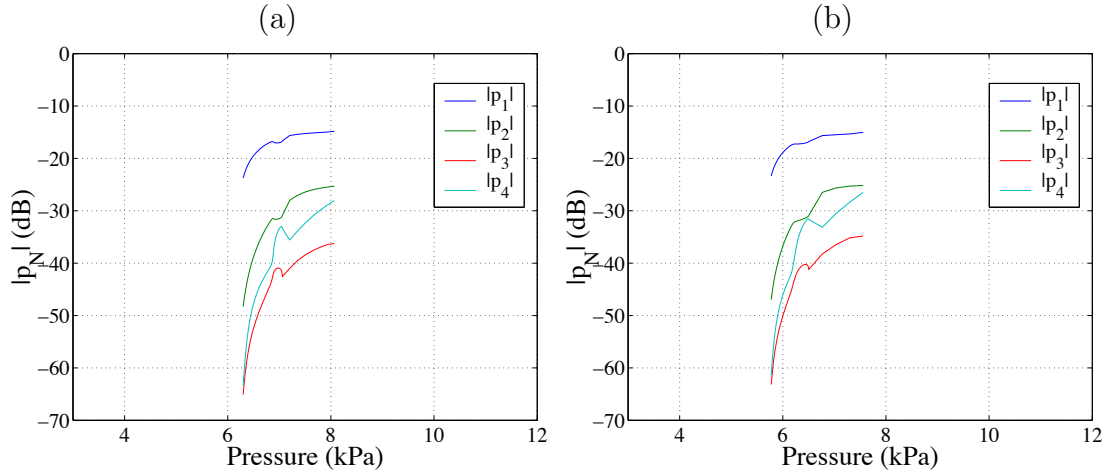

Figure 7.7: $|p_N|$ predicted by `harmbal` for salts (a) $Mg(NO_3)_2$ and (b) NaCl

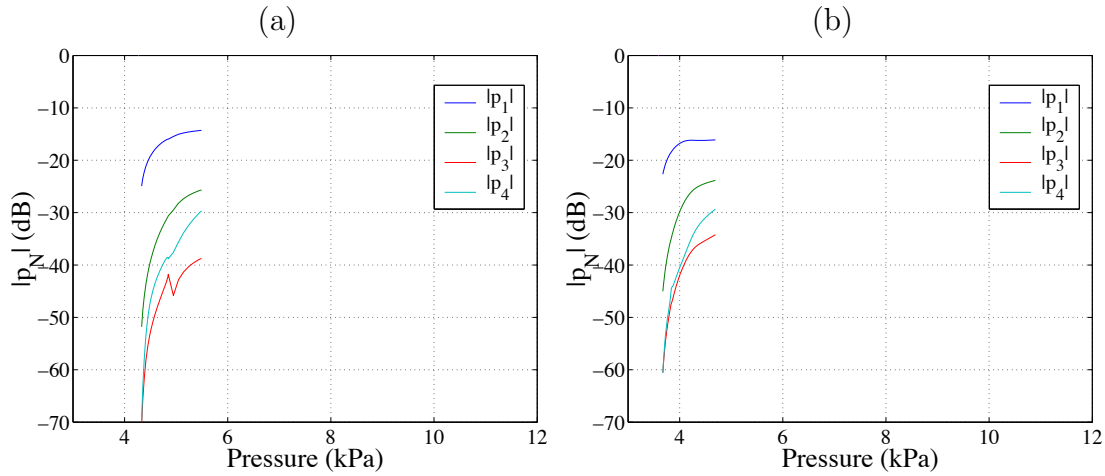

Figure 7.8: $|p_N|$ predicted by `harmbal` for salts (a) KCl and (B) K_2SO_4

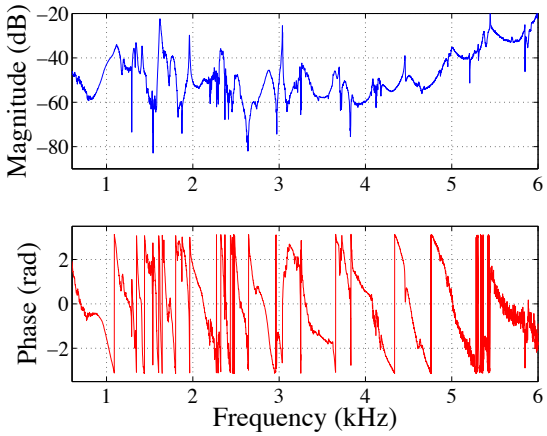

Figure 7.9: Transfer function of the chanter measured experimentally

was inserted inside the box. A loudspeaker was mounted on the box with the aid of an adapter. A 2 mm hole was drilled in the chanter, at the place where the end of the reed staple would be, so as to insert a A Brüel & Kjær $\frac{1}{2}$" microphone model 4133 with a 2 mm probe attached to it. The signal from this microphone served as reference signal. The chanter was surrounded by a cardboard tube, with a Brüel & Kjær microphone model 4938 inserted through a hole in the tube. The loudspeaker was set to generate a sinusoidal wave whose frequency varied linearly from 2 kHz to 6 kHz at a rate of 100 Hz per second. The PULSE software was set to calculate the cross-spectrum between the radiated sound and the pressure inside the mouthpiece. This cross-spectrum was later calibrated with the microphone/probe calibration data. Figure 7.9 shows the transfer function of the chanter measured under these conditions.

From the radiated spectrum, the spectral centroid at the γ values for which `harmbal` converged were calculated for each salt, following equation 3.22, and are shown in Figure 7.10. Only the first 9 harmonics were used to do this calculation, as the maximum frequency for which the transfer function was measured was 6 kHz (the frequency of the 9^{th} harmonic of a harmonic series with fundamental frequency of 635 Hz is 5.7 kHz).

As mentioned before, at pressures close to threshold p_{th} only the first harmonic dominates, making the spectral centroid low. As the pressure increases, and higher harmonics start to build up, the spectral centroid increases. These results do not show the lowering of spectral centroid with increasing relative humidity

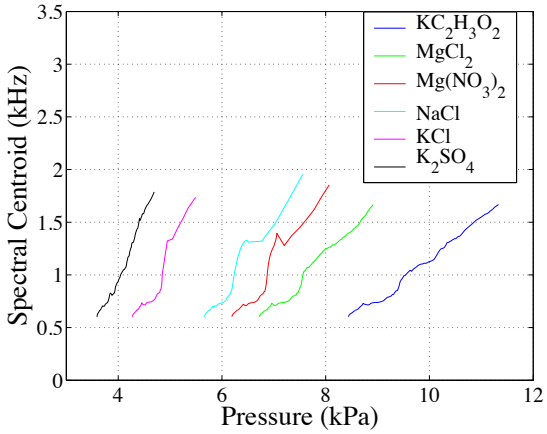

Figure 7.10: Spectral centroid curves calculated from `harmbal` results

that was found in Section 6.4.

7.5.4 Discussion

A comparison between these results and those presented in Section 6.4 show that the model was able to predict a reduction in the threshold pressure p_{th} with increasing mean relative humidity. However, there are also large discrepancies:

- The experimental results show that the chanter is able to play below the threshold pressure p_{th} once the vibrations are started (hysteresis effect due to an indirect bifurcation). The model did not predict this behaviour, but only predicted direct bifurcations without hysteresis
- the range of pressures where the chanter and reed system played in the experiments (spanning around 5 kPa) differ significantly from the `harmbal` preditcions (spanning only about 1 kPa)
- The results from the model do not show a decrease in both playing frequency and spectral centroid with increasing relative humidity
- The experimental results show a drop in pitch above the threshold pressure p_{th}, whereas `harmbal` predicts an increase of playing frequency with increasing pressure p_m in all cases, except for salt NaCl

These discrepancies might be due to the following reasons:

- The model presented here does not account for hysteresis effects that were found experimentally. This would explain why the model cannot converge for values below the threshold pressure p_{th}

- The stiffness measurements presented in Section 6.3.1 had large uncertainties, and both the k and h values used for calculating the parameters used by the model are at best very approximate. This would explain why the pressures at which the chanter and reed system played in the experiment were lower than those found by the model for 4 salts

- The reed is assumed to behave linearly, so that the model can only predict a solution for γ values where the reed does not beat. It is possible that the reed was beating in at least some of the measurements done in Section 6.4. This would explain why the chanter and reed system played whithin a wider range of pressures above p_{th} than those found with the model. It might also be that the drop in pitch observed in the experiments for pressures above p_{th} takes place when the reed starts beating. Such behaviour cannot be predicted with the current model

- The spectral centroid calculated from the mouthpiece pressure p predicted by `harmbal` took only the first 9 harmonics into account, due to the fact that the measurement of the chanter transfer function was done up to 6 kHz. This might explain why the particular shapes of the curves spectral centroid vs pressure differ from those found experimentally

7.6 Conclusions

The reed was modelled as a single reed represented by a simple harmonic oscillator according to equation 7.10. The nonlinear coupling between pressure and volume flow was modelled according to equation 7.13. The input impedance of the air column was calculated from the bore profile of the chanter using a transmission line model. The first air column resonance lay at 3796 $\frac{\text{rad}}{\text{s}}$. The dimensionless parameters of equations 7.10, 7.13 and 7.17 were calculated using the measurements of stiffness, resonance frequency and damping factor obtained experimentally, as shown in Table 7.2. The program `harmbal` was used to solve

these equations, and to do a continuation in the dimensionless mouth pressure γ to see if the experimental data presented in Chapter 6 could be mimicked.

The playing frequency predicted by `harmbal` was below the first air column resonance only for values of γ very close to 0.35 (p_{th}). This matches with what the linear theory predicts (see Section 2.4). As the pressure increases, the non-linearities start to have an effect, resulting in an increase of playing frequency.

The spectral centroid was calculated from the mouthpiece spectrum predicted by `harmbal` by multiplying it by the transfer function of the chanter. In general, an increasing spectral centroid with mouth pressure p_m was observed. This was due to the fact that more harmonics build up as the mouth pressure p_m is increased. The ranges of mouth pressures p_m where `harmbal` found convergence are well within the theoretical limits (see Table 7.1). The lowest pressure at which `harmbal` converged corresponds closely to the threshold pressure p_{th} predicted by the theory.

The similarities found between the experimental data and the results obtained by `harmbal` were:

- The threshold pressure p_{th} dropped with increasing relative humidity
- The playing frequency lay both above and below the first resonance of the air column for some values of pressure p_m

The discrepancies between the experimental data and the results obtained by `harmbal` were:

- In the experiments, the chanter plays both above and below p_{th}. `harmbal` did not converge for values of $\gamma < p_{th}$
- The results from the experiments span a larger range of pressures (around 5 kPa) than those obtained with `harmbal` (around 1 kPa)
- The results obtained with `harmbal` do not show a decreasing trend in both playing frequency and spectral centroid with increasing relative humidity found in the experiments
- The playing frequency and spectral centroid predicted by `harmbal` always increase with increasing pressure. This was not the case in the experiments

The following simplifications of the model could account for some of these discrepancies:

- The model does not take hysteresis effects into account
- The reed is modelled as a linear oscillator, which limits the results predicted by `harmbal` to pressures below the beating threshold

Other reasons that could explain the discrepancies between the experimental results and those predicted by `harmbal` are:

- The stiffness values used to calculate the input parameters for `harmbal` have large uncertainties
- The spectral centroid calculated from `harmbal` predictions only takes the first 9 harmonics into account, whereas in the experiments 36 harmonics were used

.

Chapter 8

General conclusions and future work

8.1 Introduction

The techniques by which musical instruments are made today are the result of traditions that have been developed by trial and error throughout centuries. Despite the technological advances of our era, there is hardly any scientific basis to support these techniques. Making a musical instrument is craftsman work, which is why they tend to be expensive.

Also, the quality of musical wind instruments varies widely between instrument makers, as well as between instruments of the same model. Musicians develop techniques of quality assessment that usually include parameters such as playability, responsiveness, tuning and tone quality. While most of these subjective attributes are difficult to measure objectively, the tuning and some aspects of the sound quality can be measured from the produced sound.

The aim of this work was to study how small changes in the parameters of a wind instrument (the mouthpiece, bore, size and shape of tone holes, or reed) affect the produced sound, as well as how it is perceived, by measuring the spectrum, estimating the psychoacoustic attributes of pitch and timbre, and making psychoacoustic tests, in the attempt to find a correlation between instrument quality and the way the instrument is built. Finding this correlation would help in developing a model which would mimic the behaviour of a real instrument,

aiding the instrument maker in the design of new instruments, and in the modification of an existing instrument, as it would not be necessary to develop a new prototype, or make small empirical modifications to an instrument to improve its quality. It would also be useful for instrument manufacturers and musicians themselves in the quality assessment and repair of individual instruments. This would in turn make good quality instruments cheaper and accessible to everyone.

8.2 Summary of contributions

In the course of the present work, an analysis/synthesis method was developed, which included most of the perceptual cues that aid the listener in distinguishing between two similar sounds: the relative amplitudes of the partials of the signal, the high-frequency aperiodic components, and the slow temporal variations induced by effects like vibrato. Through psychoacoustic tests in which the synthesised signals were carefully modified, it was found the threshold of distinguishability between two similar trombone sounds is between 4 and 8 dB in difference in amplitude of partials of the compared signals. In an additional test where pairs of sounds with varying degrees of difference were presented in randomised order, it was found that the 50% JND corresponds to a difference in amplitude of the partials of 2.5 dB. It was also found that some of the variations in the sound of an instrument that humans are able to perceive are due to small variations in the way the instrument is played. The player changes the timbre of the sound, even with the same instrument.

One of the parameters that change in the way a bagpipe is played is the pressure that the player exerts on the bag. An experiment was setup using an artificial blowing machine to replace the bag, where the pressure that drives the chanter was controlled by a valve, and the radiated sound of the chanter was recorded. The psychoacoustic attributes of pitch and timbre were estimated from the recorded sound. Curves of pitch and spectral centroid vs pressure were measured. It was found that this relationship is different for each played note, and also that it changes if measured on different days. A set of measurements done on a plastic reed showed no change in pitch or spectral centroid even on different days at different relative humidity conditions. It was hypothesised that this could be due to changes in geometry, age or moisture content of the reed, the

last being affected by changes in relative humidity of the air around it. Nonlinear effects such as hysteresis (the threshold mouth pressure at which the reed started vibrating was higher than the minimum pressure needed to sustain vibrations), subharmonics, beating notes, and pitch jumps were also found.

To test the hypothesis about the moisture content of the reed being responsible for the changes in pitch and timbre observed, an experiment was set up to measure how the physical attributes of the reed (stiffness, resonance frequency and damping factor), and the psychoacoustic attributes of pitch and timbre of the radiated sound of the chanter and reed system vary with moisture content. The moisture content of the reed was controlled by storing the reed in an environment with controlled relative humidity conditions for several days. After this period of time, measurements of stiffness, resonance frequency and damping factor of the reed, as well as pitch and timbre attributes of the radiated sound were done. The stiffness measurements were inconclusive, due to the fact that the results had large uncertainties. The resonance frequency showed a lowering trend with increasing relative humidity. The damping factor remained fairly constant regardless of relative humidity. The threshold mouth pressure, the pitch and spectral centroid tended to drop with increasing relative humidity. These two latter results are particularly important since they prove how small changes in the parameters of the reed affect the perceived sound of the instrument.

In order to establish whether the behaviour regarding pitch and spectral centroid found could be predicted, a physical model that models the reed as a linear simple harmonic oscillator, the bore as a linear resonator, and the coupling between them as a nonlinear relationship between the pressure and volume flow was solved using the Harmonic Balance Method with the program called `harmbal`. The parameters of the reed input to the model were taken from the results of stiffness, resonance frequency and damping factor obtained previously. The input impedance of the air column was calculated from the bore profile of the chanter using a transmission line model. The dimensionless mouth pressure parameter was varied to try to mimic the pitch and spectral variation vs mouth pressure found earlier, for the reed parameters corresponding to different relative humidity storage conditions. The threshold mouth pressure dropped with increasing relative humidity, as was found previously. For low values of mouth pressure, the linear theory was confirmed, finding a playing frequency below the

first resonance of the air column, and a spectrum with a dominant first harmonic (nearly sinusoidal response). At higher pressures, nonlinearities start having an effect, as well as the higher modes of the air column, increasing the playing frequency and the amplitude of the higher harmonics of the mouthpiece spectrum. The transfer function of the chanter was measured in order to obtain the radiated sound spectrum from the mouthpiece spectrum (predicted by `harmbal`). The spectral centroid was estimated from the radiated sound spectrum, and it showed an increasing trend with increasing mouth pressure, regardless of relative humidity. This is in agreement with having more harmonics building up when the blowing pressure increases.

8.3 Future work

An important conclusion drawn in Chapter 4 was that reducing the throat diameter of the trombone mouthpiece did not have a significant psychoacoustic effect (from the listener's point of view) in the produced sound of the instrument. However, it is possible that this small change affects the way the player feels the instrument, or even the way the instrument responds to the way the player plays it. Throughout this work, the perceptual significance of how small changes in the parameters of an instrument affect its produced sound has been stressed. Nevertheless, it is also important to study how these small changes affect how the player perceives the way the instrument responds while playing. This may affect the way he/she plays, possibly feeling more or less comfortable, and thus resulting in a better or worse performance.

The stiffness measurement presented in Chapter 6 had large uncertainties, which in turn could be responsible for some of the discrepancies presented in Chapter 6 and Chapter 7, as the model in the latter makes use of the stiffness value to calculate the threshold mouth pressure. Another technique to measure the stiffness would be to film or photograph the reed opening inside the box (through a glass window) for different mouth pressures, and measure the area of opening by means of image processing techniques. In this setup, it would also be possible to study in detail the relationship between area of opening and height of the reed. If the laser arrangement presented in Section 6.3.1 is to be reused, some modifications to the setup could be made:

- As the converging lens placed before the photodiode transfers the optical pattern into the far field, effects such as diffraction are increased, especially when the aperture of the reed is small, comparable to the laser wavelength ($\approx$ 650 nm). The current photodiode could be replaced by one of broad area, thus there would not be a need of a converging lens to focus the beam. Alternatively, a laser of smaller wavelength could be used instead

- The reed was covered by a transparent plastic film to prevent flow through it. It is possible that there were refraction effects introduced by the presence of the plastic film that affected the output voltage of the photodiode, and hence the obtained results

- The intensity of the beam was the basis for deciding what the aperture of the reed was. As the intensity of a laser beam tends not to be constant, a possible improvement would be to replace the existing laser by a more precise one, minimising these fluctuations

- Because of the highly hysteretic behaviour of the reed, a valve that allows varying the mouth pressure in a more controlled way would help to have more control during each measurement

Other studies that could improve the model presented in Chapter 7 are suggested:

- Measurements on how the geometry of the reed (more open or more closed, different reed profiles) affects the sound of the instrument

- Measurements on the flow characteristics of the reed

- Include nonlinear behaviour of the reed (beating). This could be done either by increasing the number of harmonics, or by making the characteristic curve continuous

- Include the hysteretic behaviour of the reed (indirect bifurcation)

The main objective for the future would be to develop a model that is able to predict the sound of an instrument from its physical parameters (input impedance

and characteristics of the reed). Such a model could be used as a virtual instrument, which would be useful for aiding in the design of new instruments, modification, repair and quality assessment of existing instruments. In this process, the instrument maker would not need to build the instrument in order to know how it would sound. This would in turn tend to make instruments cheaper and more accessible to everyone.

As the bore of the instrument does not change significantly over time, once a good bore design is found, the quality variations that woodwind players experience day by day would lie exclusively on the characteristics of the reed. This model would be able to find the ideal reed characteristics needed, which in turn could allow the development of synthetic reeds that mimic cane reed behaviour.

Other indirect benefits of this model would be to gain more understanding on the control parameters the instrument player uses to modify the different aspects of the instrument. This could aid new musicians in their learning process, as well as lead to the development of more effective playing techniques.

Bibliography

[1] G. E. Allan. The musical scale of the highland bagpipe. *Philosophical Magazine*, 29:154–161, 1940.

[2] André Almeida, Christophe Vergez, René Caussé, and Xavier Rodet. Physical study of double-reed instruments for application to sound-synthesis. In *Proceedings of the International Symposium on Musical Acoustics*, pages 215–220, Mexico City, Mexico, 2002.

[3] André Almeida, Christophe Vergez, René Caussé, and Xavier Rodet. Physical model of an oboe: Comparison with experiments. In *Proceedings of the International Symposium on Musical Acoustics*, pages 112–115, Nara, Japan, 2004.

[4] R. Dean Ayers, Lowel J. Eliason, and Daniel Mahgerefteh. The conical bore in musical acoustics. *The American Journal of Physics*, 53(6):528–537, 1985.

[5] John Backus. Vibrations of the reed and the air column in the clarinet. *Jounal of the Acoustical Society of America*, 33(6):806–809, 1961.

[6] John Backus. Small-vibration theory of the clarinet. *Journal of the Acoustical Society of America*, 35(3):305–313, 1963.

[7] John Backus. Multiphonic tones in the woodwind instruments. *Journal of the Acoustical Society of America*, 63(2):591–599, 1978.

[8] Kinnaird Bagpipes and Reeds Inc. Piper's pal reed protector ©.

[9] N. Bak and P. Dømler. The relation between blowing pressure and blowing frequency in clarinet playing. *Acustica*, 63:238–241, 1987.

[10] Herbert G. Baker. *Plants and civilization.* MacMillan, 2nd. edition, 1970.

[11] A. Barjau and J. Agulló. Calculation of the starting transients of a double-reed conical woodwind. *Acustica*, 69:204–210, 1989.

[12] James W. Beauchamp. Unix workstation software for analysis, graphics, modification, and synthesis of musical sounds. *Audio Engineering Society*, page Preprint 3479, 1993.

[13] A. H. Benade. On woodwind instrument bores. *Journal of the Acoustical Society of America*, 31(2):137–146, 1959.

[14] A. H. Benade. On the mathematical theory of woodwind finger holes. *Journal of the Acoustical Society of America*, 32(12):1591–1608, 1960.

[15] A. H. Benade. Equivalent circuits for conical waveguides. *Journal of the Acoustical Society of America*, 83(5):1764–1769, 1988.

[16] A. H. Benade and D. J. Gans. Sound production in wind instruments. *Annals of the New York Academy of Science*, 155:247–263, 1968.

[17] Arthur H. Benade. *Fundamentals of musical acoustics*. Oxford Univesity Press, 1976.

[18] Joseph Berkson. Application of the logistic function to bio-assay. *Journal of the American Statistical Association*, 39(227):357–365, 1944.

[19] D. M. Campbell. Nonlinear dynamics of musical reed and brass wind instruments. *Contemporary Physics*, 40(6):415–431, 1999.

[20] Murray Campbell and Clive Greated. *The musician's guide to acoustics*. Schimer Books, 1987.

[21] Sandra Carral, D. Murray Campbell, and Thomas D. Rossing. Relationship between blowing pressure, pitch, and timbre of a scottish bellows blown border bagpipe. In *Proceedings of the Stockholm Musical Acoustics Conference*, volume 1, pages 251–254, Stockholm, Sweden, 2003. KTH Speech, Music and Hearing.

[22] A. R. Carruthers. Sound radiation characteristics of the highland bagpipe in open air. *Acustica*, 38:153–156, 1977.

[23] A. R. Carruthers. Pitch changes in the sound of the highland bagpipe. *Acustica*, 41:46–50, 1978.

[24] William A. Cocks, Anthony C. Baines, and Roderick D. Cannon. Bagpipe. *Grove Music Online ed. L. Macy*, Accessed 23 September 2004.

[25] John W. Coltman. Just noticeable differences in timbre of the flute. *Catgut Acoustical Society Journal*, 3(1):26–33, 1996.

[26] Jean-Pierre Dalmont, Joël Gilbert, and Sébastien Ollivier. Nonlinear characteristics of single-reed instruments: Quasistatic volume flow and reed opening measurements. *Journal of the Acoustical Society of America*, 114(4):2253–2262, 2003.

[27] Patricio de la Cuadra, Aaron Master, and Craig Sapp. Efficient pitch detection techniques for interactive music. In *Proceedings of the International Computer Music Conference*, La Habana, Cuba, September 2001.

[28] Ward R. Drennan and Charles S. Watson. Sources of variation in profile analysis. I. Individual differences and extended training. *Journal of the Acoustical Society of America*, 110(5):2491–2497, 2001.

[29] Matteo L. Facchinetti, Xavier Boutillon, and Andrei Constantinescu. Numerical and experimental modal analysis of the reed and pipe of a clarinet. *Journal of the Acoustical Society of America*, 113(5):2874–2883, May 2003.

[30] Snorre Farner. `harmbal`. http://www.pvv.ntnu.no/~farner/pub/harmbal.

[31] I. M. Firth and H. G. Sillitto. Acoustics of the highland bagpipe chanter and reed. *Acustica*, 40:310–315, 1978.

[32] N. H. Fletcher. Excitation mechanisms in woodwind and brass instruments. *Acustica*, 43:63–72, 1979.

[33] N. H. Fletcher. The nonlinear physics of musical instruments. *Reports on Progress in Physics*, 62:723–764, 1999.

[34] Neville H. Fletcher and Thomas D. Rossing. *The physics of musical instruments*. Springer, second edition, 1998.

[35] American Society for Testing and Materials. Standard practice for maintaining constant relative humidity by means of aqueous solutions $e104 - 85$. *Anual book of ASTM standards*, 11.03:781–783, 1998.

[36] Claudia Fritz, Snorre Farner, and Jean Kergomard. Some aspects of the harmonic balance method applied to the clarinet. *Applied Acoustics*, 65:1155–1180, 2004.

[37] J. Gilbert, J. Kergomard, and E. Ngoya. Calculation of the steady-state oscillations of a clarinet using the harmonic balance technique. *Journal of the Acoustical Society of America*, 86(1):35–41, 1989.

[38] Brian R. Glasberg and Brian C. J. Moore. A model of loudness applicable to time-varying sounds. *Journal of the Audio Engineering Society*, 50(5):331–342, 2002.

[39] Stefan Glave, Jan Pallon, Chris Bornman, Lars Olof Björn, Rita Wallén, Jacob Råstam, Per Kristiansson, Mikael Elfman, and Klas Malmqvist. Quality indicators for woodwind reed material. *Nuclear Instruments and Methods in Physics Research*, B 150:673–678, 1999.

[40] Clive Greated. Beats. *Grove Music Online ed. L. Macy*, Accessed 10 December 2004.

[41] David M. Green. Discrimination changes in spectral shape: Profile analysis. *Acustica*, 82:S31–S36, 1996.

[42] John M. Grey and John W. Gordon. Perceptual effects of spectral modifications on musical timbres. *Journal of the Acoustical Society of America*, 63(5):1493–1500, 1978.

[43] John M. Grey and James A. Moorer. Perceptual evaluations of synthesized musical instrument tones. *Journal of the Acoustical Society of America*, 62(2):454–462, 1977.

[44] Cyril M. Harris, Maurice Eisenstadt, and Mark R. Weiss. Sounds of the highland bagpipe. *Journal of the Acoustical Society of America*, 35:1321–1327, 1963.

[45] Hermann L. F. Helmholtz. *On the sensations of tone: As a physiological basis for the theory of music*. Longmans, Green, and Co., 1875.

[46] A. Hirschberg. Aero-acoustics of wind instruments. In International Centre for Mechanical Sciences, editor, *Mechanics of musical instruments*, pages 291–369. Springer-Verlag, 1995.

[47] W. L. Howes. Loudness of steady sounds – a new theory. *Acustica*, 41(5):277–320, 1979.

[48] Tohru Idogawa, Tokihiko Kobata, Kouji Komuro, and Masakazu Iwaki. Nonlinear vibrations in the air column of a clarinet artificially blown. *Journal of the Acoustical Society of America*, 93(1):540–551, 1993.

[49] Walt Jesteadt, Craig C. Wier, and David M. Green. Intensity discrimination as a function of frequency and sensation level. *Journal of the Acoustical Society of America*, 61(1):169–177, 1977.

[50] Douglas H. Keefe. Theory of the single woodwind tone hole. *Journal of the Acoustical Society of America*, 72(3):676–687, 1982.

[51] Douglas H. Keefe. Tutorial on physical models of wind instruments: I. Introduction. Technical report, University of Washington, 1990.

[52] Douglas H. Keefe. Woodwind air column models. *Journal of the Acoustical Society of America*, 88(1):35–41, 1990.

[53] R. A. Kendall and E. C. Carterette. Difference threshold for timbre related to spectral centroid. In *Proceedings of the 4^{th} International Conference on Music Perception and Cognition*, pages 91–95, Montreal, Canada, 1996.

[54] Peter Kolesik, Alan Mills, and Margaret Sedgley. Anatomical characteristics affecting the musical performance of clarinet reeds made from *Arundo donax* l. (gramineae). *Annals of Botany*, 81:151–155, 1998.

[55] J. M. A. Lenihan and S. McNeill. An acoustical study of the highland bagpipe. *Acustica*, 4:231–232, 1954.

[56] F. Mammano and R. Nobili. Biophysics of the cochlea: Linear approximation. *Journal of the Acoustical Society of America*, 93(6):3320–3332, 1993.

[57] M. E. McIntyre, R. T. Schumacher, and J. Woodhouse. On the oscillations of musical instruments. *Journal of the Acoustical Society of America*, 75(5):1325–1345, 1983.

[58] B. C. J. Moore and B. R. Glasberg. A revision of Zwicker's loudness model. *Acustica*, 82:335–345, 1996.

[59] Brian C. J. Moore. *An introduction to the psychology of hearing.* Academic Press, 4^{th} edition, 2001.

[60] Brian C. J. Moore, Brian R. Glasberg, and Thomas Baer. A model for the prediction of thresholds, loudness, and partial loudness. *Journal of the Audio Engineering Society*, 45(4):224–240, 1997.

[61] Michael S. Nakhla and Jiri Vlach. A piecewise harmonic balance techinique for determination of periodic response of nonlinear systems. *IEEE Transactions on circuits and systems*, 23(2):85–91, 1976.

[62] Mark Neal. *A study of the brass instrument lip reed mechanism using artificial lips and Lattice Boltzmann flow simulations.* PhD thesis, University of Edinburgh, 2002.

[63] C. J. Nederveen. *Acoustical aspects of woodwind instruments.* Northern Illinois University Press, 1998.

[64] R. Nobili and F. Mammano. Biophysics of the cochlea II: Stationary nonlinear phenomenology. *Journal of the Acoustical Society of America*, 99(4):2244–255, 1996.

[65] Eiichi Obataya and Misato Norimoto. Acoustic porperties of a reed (*Arundo donax* l.) used for the vibrating plate of a clarinet. *Journal of the Acoustical Society of America*, 106(2):1106–1110, August 1999.

[66] S. Ollivier, J. Kergomard, and J. P. Dalmont. Idealized models of reed woodwinds. part II: On the stability of "two-step" oscillations. *Acta Acustica united with Acustica*, 91(1):166–179, 2005.

[67] Jean-François Petiot, Franck Teissiert, Joël Gilbert, and Murray Campbell. Comparative analysis of brass wind instruments with an artificial mouth: First results. *Acta Acustica united with Acustica*, 89:974–979, 2003.

[68] George R. Plitnik and Bruce A. Lawson. An investigation of correlations between geometry, acoustic variables, and psychoacoustic parameters for french horn mouthpieces. *Jounal of the Acoustical Society of America*, 106(2):1111–1125, 1999.

[69] George R. Plitnik and W. J. Strong. Numerical method for calculating input impedances of the oboe. *Journal of the Acoustical Society of America*, 65(3):816–825, 1979.

[70] Reiner Plomp. *Aspects of tone sensation: A psychophysical study.* Academic Press, 1976.

[71] H. F. Pollard. A tristimulus method for the specification of musical timbre. *Acustica*, 51:162–171, 1982.

[72] Lawrence R. Rabiner, Michael J. Chang, Aaron E. Rosenberg, and Carol A McGonegal. A comparative performance study of several pitch detection algorithms. *IEEE Transactions on Acoustics, Speech, and Signal Processing*, 24(5):399–418, 1976.

[73] Nigel Richards. Garvie bagpipes. http://www.borderpipes.co.uk/.

[74] Orlando Richards. *Investigation of the lip reed using computational modelling and experimental studies with an artificial mouth.* PhD thesis, University of Edinburgh, 2003.

[75] Juan G. Roederer. *The physics and psychophysics of Music: An introduction.* Springer-Verlag, third edition, 1995.

[76] Emery Schubert, Joe Wolfe, and Alex Tarnopolsky. Spectral centroid and timbre in complex, multiple instrumental textures. In *Proceedings of the 8th International Conference on Music Perception and Cognition*, pages 654–657, Evanston, IL, USA, 2004.

[77] R. T. Schumacher. Self-sustained oscillations of the clarinet: An integral equation approach. *Acustica*, 40:298–309, 1978.

[78] R. T. Schumacher. Ab Initio calculations of the oscillations of a clarinet. *Acustica*, 48(2):71–85, 1981.

[79] William T. Simpson. Equilibrium moisture content of wood in outdoor locations in the United States and worldwide. Technical Report FLP-RN-268, United States Department of Agriculture, Forest Service, 1998.

[80] William B. Snow. Change of pitch with loudness at low frequencies. *Journal of the Acoustical Society of America*, 8:14–19, 1936.

[81] Scott D. Sommerfeldt and William J. Strong. Simulation of a player-clarinet system. *Journal of the Acoustical Society of America*, 83(5):1908–1918, 1988.

[82] American National Standard. Acoustical terminology. *Acoustical Society of America*, ANSI S1.1-1994, 1994.

[83] Yôiti Suzuki and Hisashi Takeshima. Equal-loudness-level contours for pure tones. *Journal of the Acoustical Society of America*, 116(2):918–933, 2004.

[84] Stephen C. Thompson. The effect of the reed resonance on woodwind tone production. *Journal of the Acoustical Society of America*, 66(5):1299–1307, 1979.

[85] Maarten van Walstijn. *Discrete-time modelling of brass and woodwind instruments with application to musical sound synthesis.* PhD thesis, University of Edinburgh, 2002.

[86] H. F. Vermaas. Wood-water interaction and methods of measuring wood moisture content: Part I – Definitional aspects to NMR. *Holzforschung und Holzverwertung*, 2:30–34, 1996.

[87] G. von Bismarck. Sharpness of steady sounds. *Acustica*, 30:159–172, 1974.

[88] Wikipedia. Chromatic scale. *Wikipedia, The free enciplopedia*, 9th August 2005. http://en.wikipedia.org/wiki/Chromatic_scale.

[89] W. E. Worman. *Self-sustained nonlinear oscillations of medium amplitude in clarinet-like systems*. PhD thesis, Case Western Reserv University, 1971.

[90] H. A. K. Wright and D. M. Campbell. The influence of the mouthpiece on the timbre of cup-mouthpiece wind instruments. In *Proceedings of the International Symposium on Musical Acoustics*, pages 159–164, Leavenworth, WA, USA, 1998.

[91] E. Zwicker, G. Flottorp, and S. S. Stevens. Critical bandwidth in loudness summation. *Journal of the Acoustical Society of America*, 29(5):548–557, 1957.

[92] E. Zwicker and B. Scharf. A model of loudness summation. *Psychological Review*, 72:3–26, 1965.

[93] Eberhard Zwicker. Procedure for calculating loudness of temporally variable sounds. *Journal of the Acoustical Society of America*, 62(3):675–682, 1977.

Publications

Sandra Carral and D. Murray Campbell. The influence of the mouthpiece throat diameter on the perception of timbre of brass instruments. In *Proceedings of the International Symposium on Musical Acoustics*, pages 233–245, Mexico City, Mexico, 2002. Escuela Nacional de Música, UNAM.

Sandra Carral, D. Murray Campbell, and Thomas D. Rossing. Relationship between blowing pressure, pitch, and timbre of a scottish bellows blown border bagpipe. In *Proceedings of the Stockholm Musical Acoustics Conference*, volume 1, pages 251–254, Stockholm, Sweden, 2003. KTH Speech, Music and Hearing.

Sandra Carral and D. Murray Campbell. The influence of relative humidity on the physical characteristics of the reed, and on psychoacoustic attributes of the sound of a bellows blown scottish border bagpipe chanter and reed. In *Proceedings of the Forum Acusticum Conference*, Budapest, Hungary, 2005. Novotel Budapest Congress Centre.

Index